Measurement of Forces Between and Within Bilayers of Neutral Phospholipids

By

Michael J. McAlister

Department of Biological Sciences

(Submitted in partial fulfillment of

the requirements for the degree of

Master of Science).

BROCK UNIVERSITY

St. Catharines, Ontario,

August, 1978.

ACKNOWLEDGEMENTS

I wish to express my sincere appreciation to Dr. R. P. RAND for his assistance, encouragement and incisive discussions in all aspects of this thesis. I also acknowledge the invaluable assistance of Dr. V. A. PARSEGIAN for his derivation of several formula in this thesis as well as many helpful discussions of the results. Thanks are also due to Mrs. N. FULLER for her technical assistance and her friendly and intelligent comments on these results. Dr. L. LIS and Dr. A. COWLEY provided many helpful suggestions of which I am most grateful. I also wish to thank Dr. P. NICHOLLS for several helpful criticisms in the preparation of this manuscript.

TABLE OF CONTENTS

LIST OF TABLES

LIST OF ILLUSTRATIONS

Figure Page

LIST OF APPENDICES

ABSTRACT

Phospholipids in water form lamellar phases made up of alternating layers of water and bimolecular lipid leaflets. Three complementary methods, osmotic, mechanical, and vapour pressures, were used to measure the work of removing water from lamellar phases composed of frozen dipalmitoylphosphatidylcholine (DPPC), melted DPPC, egg phosphatidyl-ethanolamine or equimolar mixtures of DPPC and cholesterol (DPPC/CHOL). Concurrently the structural changes that resulted from this water removal were measured using X-ray diffraction. The work was divided into that which forces the bilayers together (F_R) and that which compresses the molecules together within the bilayers (F_{LP}).

A large repulsive force exists between bilayers composed of each of the lipids studied and this force increases exponentially as bilayer separation is decreased. F_R is affected by the nature of the head groups, conformation of the acyl chains and heterogeneity of these chains. In general all of the melted phosphatidylcholines (melted DPPC, egg lecithin and DPPC/CHOL) have large equilibrium separations in excess water resulting from large repulsive hydration forces between these bilayers. By comparison, egg PE has an increased attractive force, and frozen DPPC has a decreased hydration force; each results in smaller separations in water for these two lipids. The chemical potentials of the water between the bilayers for all these lipids lie on a continuum, indicating that interbilayer water cannot be characterized by two discrete states, usually referred to as "bound" or "non-bound".

For all lipids studied a maximum of 25 % of the total work done on the system goes into deforming the bilayers. The method used here

to separate repulsion from deformation, developed for us by V. A. Parsegian, provides a unique method for the measurement of lateral pressure of a bilayer and its modulus of deformability (Y). Lateral pressure is affected by the nature of the head group, conformation and heterogeneity of the acyl chains. For small changes in molecular surface area (A) near equilibrium, both melted and frozen DPPC have similar values for the deformability modulus. Thus in this regime it requires about the same force to change the angle of tilt of frozen chains as it does to compress the fluid bilayer. The introduction of cholesterol into bilayers of DPPC reduces dramatically the lateral pressure of the bilayers over a large range of molecular surface areas (A).

The variation in the magnitude of bilayer repulsion with different phospholipids provides a basis for the mechanism of lipid segregation in mixed lipid systems and suggests that interacting heterogeneous membranes may influence or modulate the composition of the opposing membrane.

The measurements of deformabilities of bilayers provides a direct comparison of them with the properties of monolayers.

GENERAL INTRODUCTION

The structure of cell membranes has been a subject of study since the late 19th century. However their thinness made the resolution of structure difficult, until the advent of modern physical and chemical techniques. The membrane is composed of lipids and proteins which vary in proportion and composition depending upon the cell type (ROUSER et al 1968).

OVERTON (1895) first demonstrated the lipid nature of cell membranes, finding that the permeability of non-electrolytes was roughly proportional to their oil-water partition coefficients. GORTER and GRENDEL (1925) extracted lipids from erythrocytes and measured the surface area of a monolayer formed by these lipids when compressed on a Langmuir trough. They discovered that this area was sufficient to cover the average area of an erythrocyte twice, and thus concluded that the cell was surrounded by a bilayer of lipid. More recent studies (BAR et al 1966) have brought these results into doubt. It can be shown that the acetone extraction used by GORTER and GRENDEL could not have contained all the membrane lipids. Also their method for calculating the average surface area of the red blood cell, and their assumption that the surface area of the lipid measured on a Langmuir balance would be the same as that in the membrane were both shown to be invalid. The work of GORTER and GRENDEL, however, laid the foundation for many of the structural models that were later presented.

MODELS FOR THE STRUCTURE OF CELL MEMBRANES

Today's ideas for the structure of cell membranes are based upon the theories presented by DAVSON and DANIELLI (1935). They proposed that the membrane was composed of a lipid bilayer with globular protein coating both sides of the membrane. The bilayer consisted of two layers of lipid in which the hydrophobic acyl chains were segregated into the middle of the membrane away from contact with water while the hydrophilic head groups

faced towards the exterior in contact with the water enviroment. The proteins were bound to the polar surfaces mainly by electrostatic attraction (Fig. 1).

ROBERTSON (1957, 1960) modified this bilayer model in his "unit membrane" hypothesis. In his model the membrane was asymmetric. The extracellular surface contained the glycoproteins while the intracellular surface was coated by proteins in the β conformation. Since most membranes appeared to have the same trilamellar appearance when fixed and stained for electron microscopy, ROBERTSON felt that his model applied to all cellular membranes (Fig. 1).

It is now thought that both these models may be too limited and non-specific to explain the variety of structure and function that is seen in membranes. SJÖSTRAND (1963) showed that the outer membrane of mitochondrion and some endoplasmic reticulum membranes appear to have a globular sub-unit structure. Membrane proteins of erythrocytes seem to be bound to the membrane in more than one way (BRETSCHER and RAFF 1975). Spectrin, which is a protein found on the cytoplasmic side of the erythrocyte membrane, can be easily removed using a low ionic strength salt solution. However glycophorin, which contains a long section of hydrophobic amino acid residues, is not released by ionic treatment and is thought to penetrate completely through the membrane. Freeze fracture electron microscopy, which cleaves the membrane through the middle of the bilayer, reveals small intramembranous particles (BRANTON 1971) which can be digested by proteases. Thus it can be seen that membrane proteins lie not only on the polar surface of the bilayer but can also penetrate into the interior. The cell membrane contains a variety of lipids which in some cells are asymmetrically distributed between the constituent monolayers. BRETSCHER (1972) found that most of the phosphatidylcholines and all of the glycolipids are found in the outer layer of the red cell membrane while most amino phospholipids are found in the inner half.

Figure 1.

Davson-Danielli model of biological membrane
(DAVSON and DANIELLI 1935)

Robertson's unit membrane model (ROBERTSON 1964)

Singer-Nicholson fluid mosaic model (SINGER and NICHOLSON 1972)

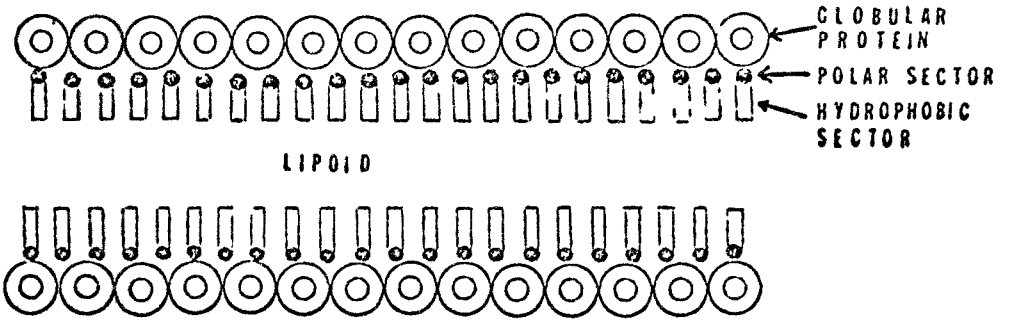
GLOBULAR PROTEIN
POLAR SECTOR
HYDROPHOBIC SECTOR
LIPOID

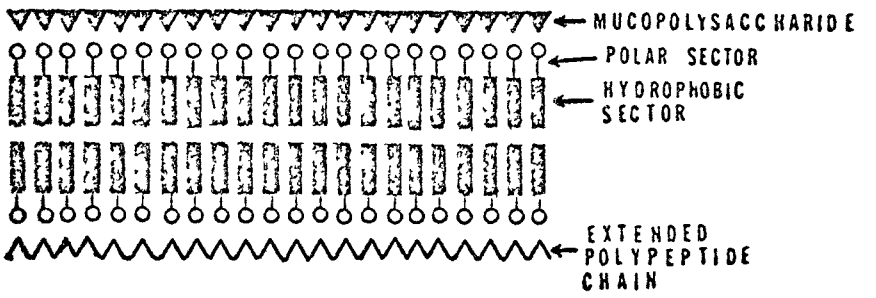
MUCOPOLYSACCHARIDE
POLAR SECTOR
HYDROPHOBIC SECTOR
EXTENDED POLYPEPTIDE CHAIN

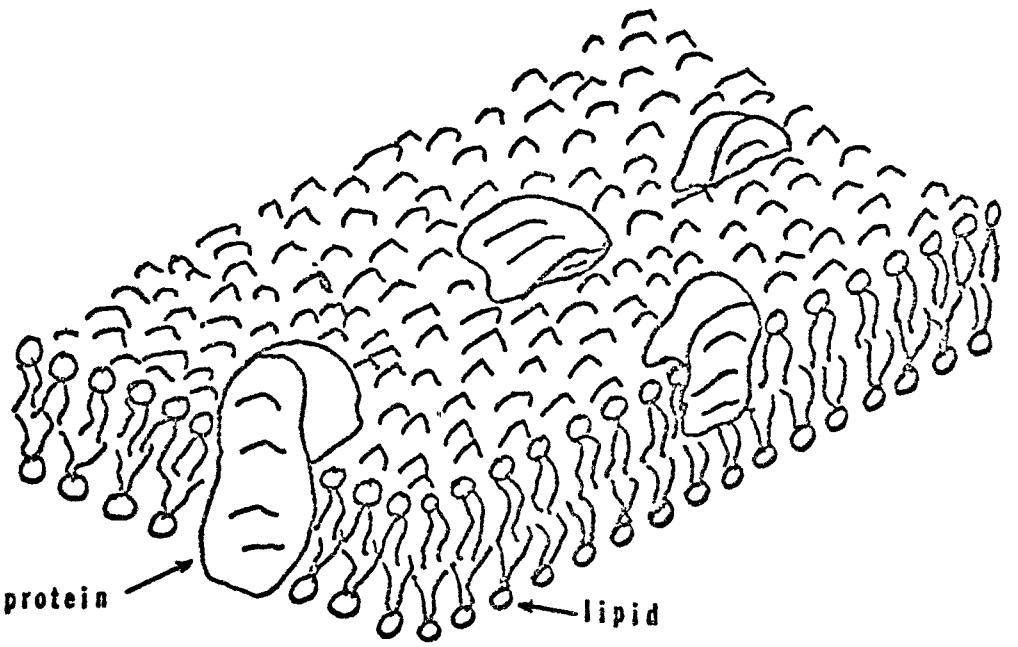
protein
lipid

This heterogeneity of composition and structure of the cell membrane led to the presentation of a general model by SINGER and NICHOLSON (1972) (Fig. 1). In their model the membrane consists of a lipid bilayer similar to that of DAVSON-DANIELLI. The lipid freely diffuses within the plane of its own monolayer (and possibly slowly "flip-flops" to the other monolayer (KORNBERG and McCONNELL 1971)). Most of the lipid is thought to be fluid or melted, but islands of frozen lipids may exist such that the viscosity of the membrane may vary in places. The proteins associated with the membrane are loosely classified as either extrinsic or intrinsic. Extrinsic proteins lie on the polar sides of the membrane bound by electrostatic attraction while intrinsic proteins penetrate into and possibly through the interior of the membrane, interacting with the acyl chains. Thus the proteins are able to make many types of interactions with other membrane components. The importance of SINGER and NICHOLSON'S model may lie in its ability to amalgamate the variety of structural and functional properties of the cell membrane. It is a very dynamic and flexible model which allows the membrane to exhibit quite different properties at various times and simultaneously in various areas of the same membrane.

MODEL MEMBRANE SYSTEMS

Support for SINGER and NICHOLSON'S structure comes mainly from studies on model membrane systems. These model systems are made from extracted or synthetic phospholipids and water, or phospholipids and proteins in aqueous solution. Model membranes are able to mimic certain of the cell membrane's structural and functional properties and have the advantage of allowing control of the type and state of the components. Such model systems are stable and easily formed and are particularly amenable to quantitative study by modern physical and chemical techniques.

Lipids can be classified into two broad groups, either simple or compound. Simple lipids are composed of glycerol and fatty acids with

the general form

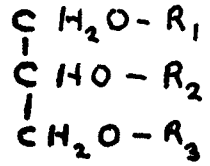

where R_1 R_2 and R_3 are fatty acids. These fatty acids may be of different lengths and have different degrees of unsaturation.

Compound lipids are esters of fatty acids containing other molecular groups in addition to glycerol. For example phosphatidylcholine (PC) is composed of glycerol, two fatty acid acyl chains, phosphate and choline while phosphatidylethanolamine (PE) contains glycerol, two fatty acid chains, phosphate and ethanolamine. Naturally occuring phospholipids from membranes usually have chains which are heterogeneous in chain length and degree of unsaturation. Synthetic phospholipids can be made which have identical acyl chains (Fig. 2).

Lipids are amphiphilic in nature, that is they contain both a hydrophilic part (eg. glycerol phosphate and choline for PC) and a hydrophobic part (the fatty acid chains). Their physical properties such as the ability for self-assembly into larger structures and the melting temperature are dependent upon both the nature of the head group and the hydrocarbon chains (TARDIEU et al 1973).

Membrane proteins are polymers of amino acids. Each protein has a different structure however, and the ease with which it can be removed from the membrane varies over a continuous spectrum, from gentle ionic treatment to total disruption of the membrane.

In model systems composed of lipid and water LUZZATI (1968) has shown that the lipids because of their amphiphilic structure will self-assemble into a variety of structures. Depending upon the lipid, the temperature and the aqueous conditions, micellar, hexagonal, cubic or lamellar structures may form. The lamellar phase is the most relevant to the study of membrane structure and consists of alternating layers of lipid and water. The lipid

Figure 2.

Molecular models of DPPC and PE.

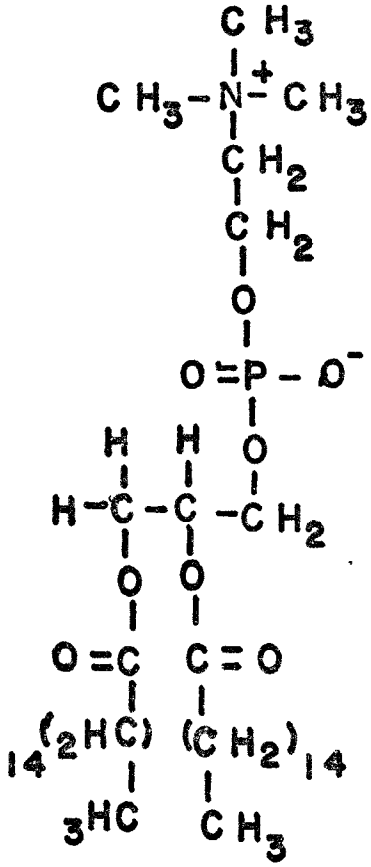

DIPALMITOYL PHOSPHATIDYL CHOLINE (DPPC)

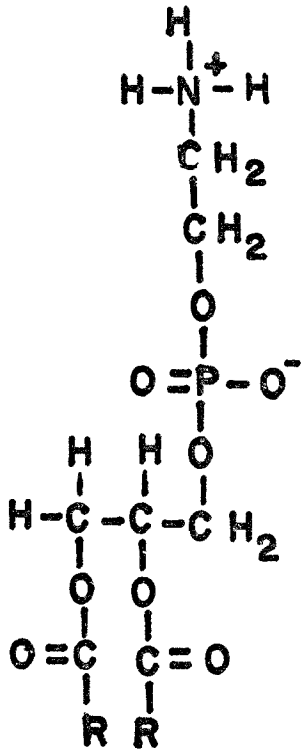

PHOSPHATIDYL ETHANOLAMINE (PE)

layer forms a bilayer structure, directly comparable to that proposed for the cell membrane, with the acyl chains segregated on the inside of the bilayer while the polar heads face into water layers. This structure is firmly established by the technique of X-ray diffraction (LUZZATI 1968).

CHAPMAN et al (1967) and others have shown, using differential scanning calorimetery and X-ray diffraction, that a sharp endothermic structural transition occurs when the acyl chains of dipalmitoly phosphatidyl choline (DPPC) (Fig. 2) are melted. This transition has been confirmed by nuclear magnetic resonance as the lipid chains show increased mobility at the melting temperature (T_c) (CHAPMAN 1967). Below the T_c the hydrocarbon chains of DPPC are stiff, fully extended and tilted with respect to the bilayer plane and are packed in an ordered fashion (hexagonal) within the bilayer. This is known as the gel phase. Above the T_c the chains are fluid or melted and show high disorder within the bilayer. The melted lipids also show rapid lateral diffusion with a diffusion constant of about 2×10^{-8} cm^2/sec (TRAUBLE and SACKMAN 1971). Above the T_c the lamellar phase formed by the lipid is described as a liquid crystal. There is little order within the bilayer, hence the liquid description, but the self-assembled structures themselves (bilayers) show high crystal-like order with respect to each other.

In artificial bilayers containing melted and frozen phospholipids there is an indication that a phase separation into clusters of gel and liquid occurs (McCONNELL 1974). In systems where many types of lipids are present, such as a natural lipid extract, no sharp transition from melted to frozen is seen (CHAPMAN 1973). Instead a broad peak in differential scanning calorimetery is produced, presumably representing a gradual change from frozen to melted as the various lipids melt at different temperatures. GULIK-KRZYWICKI et al (1969a) investigated the interactions between lipids and specific proteins with X-ray diffraction and circular dichroism in a

lipid-protein-water model system. They showed that both hydrophilic or polar and hydrophobic bonding between lipid and protein can occur and also that a variety of structural phases were formed which were dependent upon the nature of the protein, the lipid and the aqueous conditions in which they were associated.

Model systems thus provide a conv system for the study of structure and function in cell membranes and indicate that many of the polymorphic structures seen in these systems may also exist in cellular membranes.

INTERACTIONS BETWEEN MEMBRANES

The nature of cell contact phenomena is a fundamental problem for the understanding of many diverse biological processes. It has been shown (MOSCONA 1961) that dissociated cells of different tissue types will show selective cell association properties in that cells will tend to aggregate with cells of like type. Cell contact specificity also plays a critical role in cellular migration and differentiation during embryological development. For example during neuralation cells from the neural crest will break off and migrate to specific sites to form the tissues of the adrenal medulla and spinal ganglia (BERRILL 1971). Contact inhibition is also associated with the cell membrane. Normal cells, as shown in tissue culture, will cease to grow or move away upon establishing contact with other cells. Malignant cells, however, are not inhibited and continue to move over other cells (WEISS and GREEP 1977). All of the above processes involve some type of cell-cell communication.

Many of these contact phenomena are dependent upon specific molecules on opposing membranes which bind in a precise lock and key fashion (MOSCONA 1968). These short range interactions may however be influenced by more non-specific long-range forces. Theoretical studies by GINGELL (1971) and PARSEGIAN and GINGELL (1972) using a modified lyophobic colloid theory (VERWEY and OVERBEEK 1948) indicate that the non-specific forces, van der Waals

attraction and electrostatic repulsion, are significant when cell membranes approach to within 10's of angstroms of each other.

Electrostatic repulsion: Cell membranes typically contain a number of charged species which will produce an electrostatic surface potential. PARSEGIAN and GINGELL (1972) have calculated the magnitude of this electrostatic repulsion at various distances as two membranes approach each other, using charge densities and ionic concentrations which are close to those found in biological systems (Fig. 4).

Van der Waals attraction: Approaching membranes will experience attraction caused by van der Waals interactions between them. Estimates of these energies in membrane systems have been more difficult primarily because of the limited knowledge of spontaneous charge fluctuations which are the basis of van der Waals or electrodynamic forces (see below). However for a hydrocarbon membrane-water model system attractive electrodynamic energy as a function of membrane separation has been constructed (Fig. 3). The total energy of interaction (V_T) as a function of membrane separation is the sum of the attractive and repulsive energies (Fig. 5).

Force is defined as the negative rate of change of energy with distance, so the total force is $-dV_T/dX$ where V_T represents energy of interaction and X is separation distance (GINGELL 1971). The gradient $-dV_T/dX$ is zero at maximal and minimal values of V_T and thus the force is also zero at these points. Figure 5 shows the relationship between force and energy.

It can be seen from Figure 5 that an energy "well" can be produced by a combination of these attractive and repulsive energies. The lowest point in this well represents a minima of the energy of the system and hence membranes will tend to remain at the separation distance which corresponds to this energy minimum. The depth of the well is an indication of the stability of the minimum. The corresponding force vs. separation curve shows that the total force is zero at the bottom of this energy well; thus

Figure 3.

Curve illustrating electrodynamic energy versus membrane separation (PARSEGIAN and GINGELL 1972).

Figure 4.

Curve illustrating electrostatic interaction energy versus membrane separation (PARSEGIAN and GINGELL 1972).

Figure 3

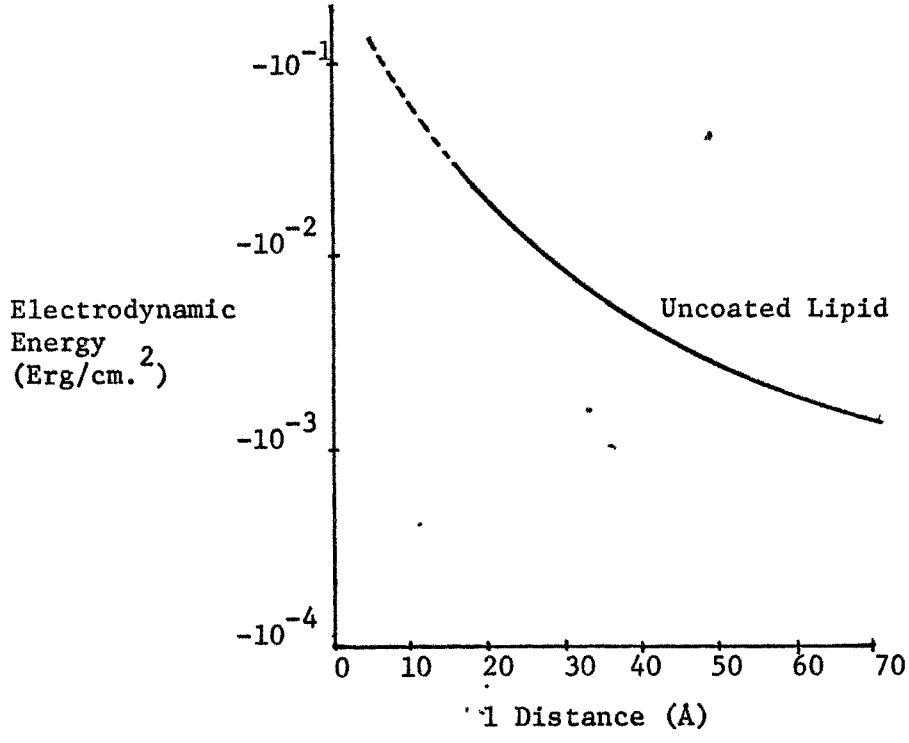

Figure 4

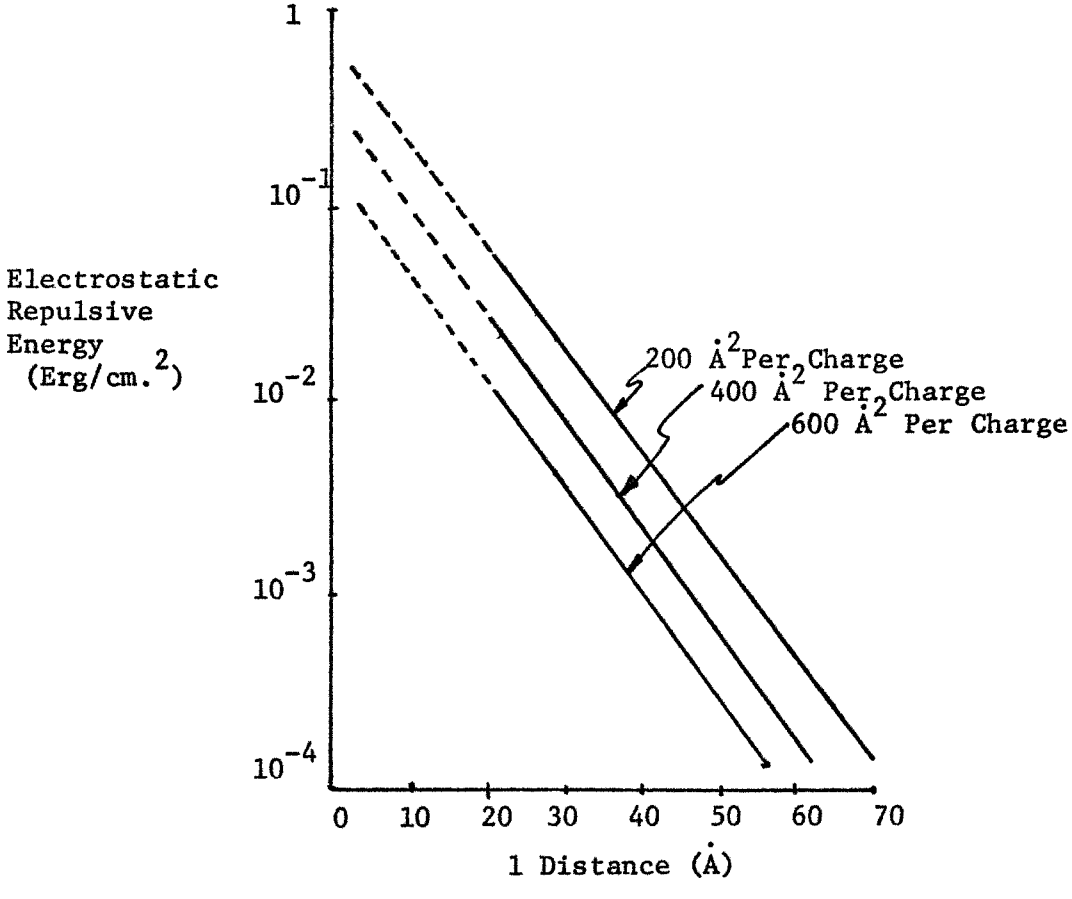

Figure 5.

Curve illustrating total potential energy and force of interaction between plane parallel double layers representing biological membranes (GINGELL 1971).

Figure 5

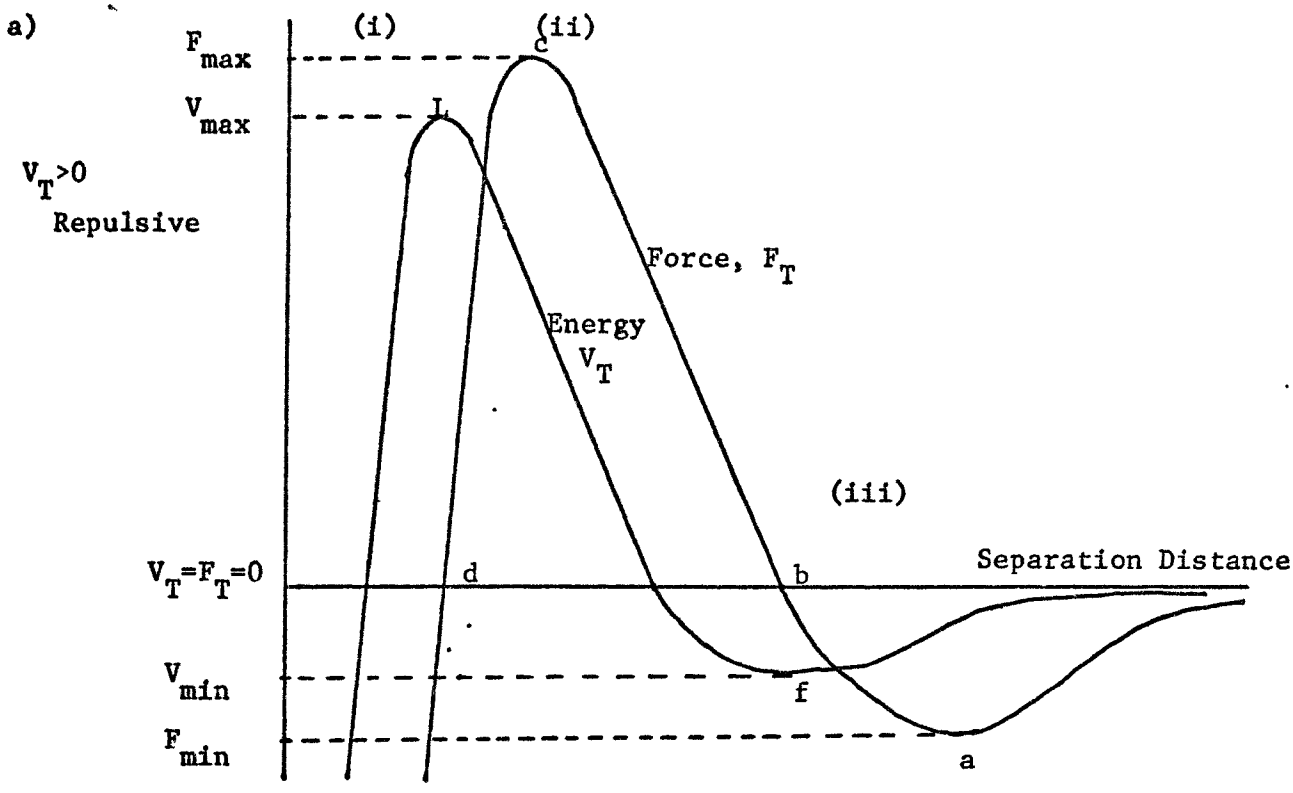

(i) Primary Minimum
(ii) Energy Barrier
(iii) Secondary Minimum

(From Gingell 1971)

a force would be required to move the membranes away from this point in either direction. The membranes are therefore stabilized at this separation by a balance between the repulsive electrostatic force and the attractive van der Waals force.

This theory of a balance of forces has been used to explain the equilibrium spacing seen in the lamellar phase formed by egg lecithin in water (LENEVEU 1976). If water is added to lecithin the bilayers will move apart until a separation of 27.5 Å is reached (SMALL 1966). Water added after this will not enter between the bilayers but will form a separate phase. Thus it is at this equilibrium separation that the balance between attractive and repulsive forces is reached. If this balance is upset, for example by adding charge to the bilayers, which increases the repulsive force, the bilayers will move further apart (GULIK-KRZYWICKI 1969b). In the case of lecithin and the other lipids which were used for the experiments in this thesis, no net charge exists on them. The balance that is struck for these lipids is between an attractive van der Waals force and what we call a repulsive hydration force.

THE ATTRACTIVE FORCE

Van der Waals attraction between particles arises from transient electrical polarization of these particles. This polarization is due to charge displacements arising from molecular or electron cloud distortions or molecular orientation. Estimates of van der Waals energies were originally calculated using pairwise additivity of the interactions between individual atoms and molecules (VERWEY and OVERBEEK 1948). This however proved unsatisfactory for solids or liquids in which molecules felt simultaneous interactions between many bodies. LIFSHITZ (1956) developed a theory in which the material is treated as a continuum. Using this theory PARSEGIAN (1975) has derived an expression (Equ'n 1) to evalute the energy (G) required to bring two parallel semi-infinite planar bodies from infinite separation to separation X, where X is small compared to the extent of the

opposing faces.

$$G \propto -\frac{kT}{12\pi X^2} \sum_{n=0}^{\infty} \left(\frac{\epsilon_l - \epsilon_w}{\epsilon_l + \epsilon_w} \right)^2 \qquad (1)$$

Where k=Boltzman's Constant
T= Absolute Temperature
X=Distance Between Bodies
ϵ =Dielectric of Lipid or Water Evaluated at all Frequencies

It may be noted that the energy is related to the difference in the dielectric permitivities or polarizabilities between the bodies and the suspending medium. This has been confirmed experimentally by LENEVEU (1977). On increasing the concentration of a sucrose solution between egg lecithin bilayers from 0-40 %, the difference in polarizabilities between the lipid bilayers and the interbilayer space first decreases, then reaches a minimum, and finally increases. It was observed that the change in separation between bilayers, reflect the changes in attractive forces between them, and follow the predicted pattern.

Traditionally van der Waals interactions have been described in terms of a Hamaker constant (H) such that

$$G=-H/12\pi X^2 \qquad (2)$$

Where H= Hamaker Constant
X= Distance Between the Bilayers (d_w)

Here H is a function involving atomic densities and individual atomic or molecular polarizabilities of the interacting bodies and the suspending medium. The coresponding attractive force between planar bodies is

$$F_A=-H/6\pi X^3 \qquad (3)$$

THE REPULSIVE FORCE

The nature of the repulsive force between lecithin bilayers, which opposes the van der Waals attraction, is less clearly understood. PARSEGIAN (1967) developed a theory in which the lecithin bilayer surface is described

as a diffuse double layer. Electrostatic repulsion will exist between negatively charged phosphates on the head groups. The positive charge on the choline group acts as an independent counterion whose distance from the phosphate group may vary because of a very flexible $-CH_2-CH_2-$ linkage. The magnitude calculated for this force, however, was not great enough to balance theoretical attractive forces. Another theory is that the repulsive force stems from the solvation or hydration of the head groups. In order for the bilayers to approach, force must be applied to remove the water that hydrates or is "bound" to the hydrophilic head groups. This force has been measured for colloidal clay particles (BARCLAY and OTTEWILL 1970, 1972) and for egg lecithin bilayers (LENEVEU 1976, 1977).

How the water is actually associated with the head groups is rather poorly understood. CHAPMAN and LADBROOKE (1967) have shown with differential scanning calorimetry that for egg lecithin, of the 33 waters per head group at maximum hydration, there are ten to tweleve that are "tightly bound" and do not show an endothermic transition (ie. freeze). This "bound" water will also exclude small sugars such as sucrose and glucose (LENEVEU 1977). It had been thought that the rest of the 21-23 waters have the energy of bulk water, however electron spin resonance studies by SANSON et al (1976) have shown that there is a change in the distribution of the water when the lipid is only half hydrated. It has also been found that small-chain fatty acids have three different diffusion rates through lecithin multilayers of different water contents (RIGAUD and GARY-BOBO 1977) which supports the theory that there exist three different and discrete classes of water between the bilayers.

By exposing egg lecithin multilayers to an osmotic pressure LENEVEU et al (1976) measured the force required to push these neutral bilayers together. They found that the magnitude of this repulsive hydration force was very large when bilayers were < 25 Å apart and they also showed that the force decayed exponentially with bilayer separation (d_w) and could be

described by the equation

$$\text{Force} = 1.0 \times 10^{11} (\text{ dynes/cm}^2) \exp^{-(d_w/1.93 \text{ Å})} \qquad (4)$$

These hydration forces preclude close approach by unperturbed egg lecithin bilayers.

The purpose of the work described in this thesis was to measure the hydration forces between neutral phospholipid bilayers of egg PE, DPPC (both melted and frozen) and DPPC/Cholesterol 1:1 and to examine the effect of head group, nature of the chain population and state of the chains upon these forces.

MATERIALS

Egg phosphatidylethanolamine (PE) was purchased from NUTFIELD LIPID PRODUCTS (South Nutfield, Redhill SY. Great Britain) and used without further purification. Cholesterol was purchased from CALBIOCHEM (Los Angeles, California 90094) and used without further purification. Three sources of dipalmitoyl phosphatidylcholine (DPPC) were used. Some was purchased from SERDARY RESEARCH LABORATORIES (London, Ont.) and used without further purification. Another batch from the same source was chromatographed through Al_2O_3 using the method of ROBLES and VAN DEN BERG (1969). Thirdly DPPC was synthesized in this laboratory using the method of ROBLES and VAN DEN BERG (1969). O-SN-Glycero-3-phosphorylcholine was obtained from egg lecithin (CHADHA 1970) and the fatty acid anhydride was prepared using the method of SELINGER (1966). DPPC from each of the above sources produced the same equilibrium spacing in excess water as determined by X-ray diffraction. Lipids were checked periodically for purity using thin layer chromatography and showed $\leq$ 1% contamination. All Lipids were stored under nitrogen at -18 °C until used. Dextran (MW 2,000,000) was purchased from PHARMACIA (Sweden). Water, double-distilled in glass was used for all lipid and dextran samples.

METHODS

The method of X-ray diffraction was used to measure structural parameters of the lamellar phase made up of alternating layers of lipid and water. The X-ray camera used was of the Guinier type operating in vacuo. The CuK_1 line (λ =1.540 A) was isolated using a bent quartz crystal monochrometer. Diffraction patterns were recorded photographically. The samples were sealed between mica windows $\simeq$ 1mm apart. Samples requiring temperatures higher than room temperature were controlled to $\pm$ 0.2°C with thermoelectric elements. All samples contained powdered teflon mixed directly with the sample which acted as an internal standard to calculate the diffraction spacings. The photographs of the diffraction spacings were measured using a travelling microscope. Repetitive measurements of the same sample showed that the maximum error in the d spacing was $\pm$ 0.5 Å.

Diffracted X-rays will form constructive interference patterns according to the conditions set by the BRAGG equation.

$$n\lambda = 2d \sin\theta \qquad (5)$$

where λ = Wavelength of the X-rays
d = Distance between the Planes
θ = Angle of Incidence of the Beam on the Plane
(Fig. 6)

The repeat spacing of the unit cell or total d spacing is measured in the lamellar phase. If we assume that the lipid and water form separate layers, that is the water does not penetrate into the lipid layer plane, then the thickness of bilayer (d_1) and the distance between bilayers (d_w) can be calculated. Within the total d spacing the lipid and water are packed according to their volume concentrations. Thus

$$d_1 = \phi d \qquad \text{and} \qquad d_w = d - d_1 \qquad (6)$$

where ϕ is the volume fraction of the lipid in the sample.

$$\phi = [1 + [(1-C)/C]\ \bar{V}_w/\bar{V}_p]^{-1} \qquad (7)$$

C = Weight fraction of lipid in sample
$\bar{V}_w$, $\bar{V}_p$ = Partial specific volumes of water and phospholipid respectively

Figure 6.

Diagram of diffraction of X-rays by parallel planes and lipid bilayers.

Θ = Angle of incidence of the beam on the planes.

d = Distance between planes

d_l = Thickness of bilayer

d_w = Distance between bilayers

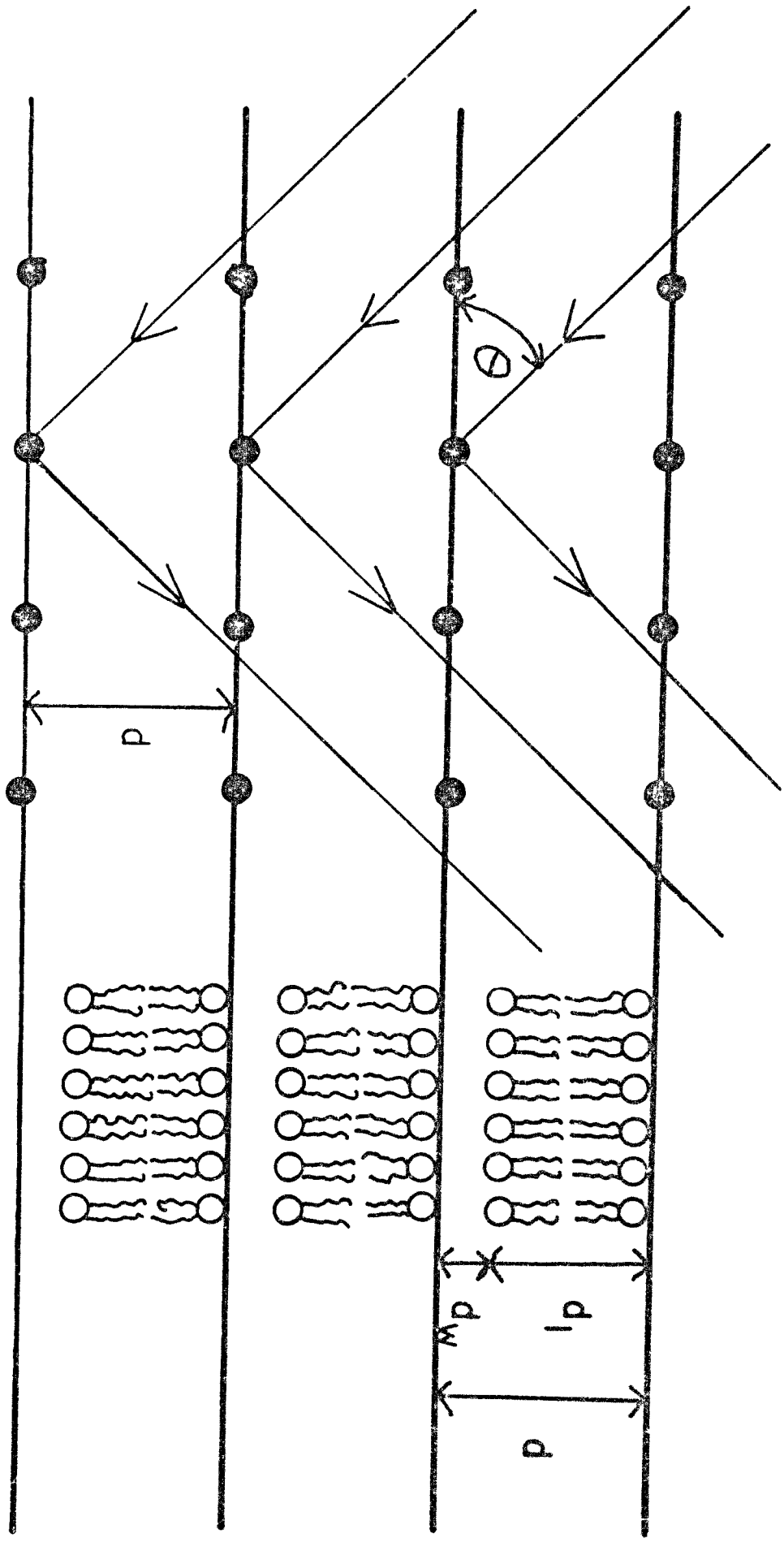
θ
d
d
d

Since the partial specific volumes of the lipids and of water are within approximately 3 % of each other (LUZZATI 1968) we have assumed that $\bar{V}_w = \bar{V}_p = 1.00\ cm^3 gm^{-1}$.

The cross-sectional area (A) available to one phospholipid on the surface of the bilayer is

$$A = 2\ (\ MW \cdot \bar{V}_p / d_1 \cdot N \cdot 10^{-24}\ ) \qquad (8)$$

where MW = Molecular Weight of the Lipid
N = Avogadro's Number

The volume of water associated with each lipid molecule is

$$V_w = (d_w/2) \cdot A \qquad (9)$$

With the assumption that the lipids are packed hexagonally in the bilayer the parameter d_{pp} can be defined as the center to center distance between head groups within the bilayer and is

$$d_{pp} = \sqrt{2A/\sqrt{3}} \qquad (10)$$

The area available to one phospholipid plus one cholesterol molecule was calculated according to the methos of RAND and LUZZATI (1968).

$$A = 2\ (\ MW_p \cdot \bar{V}_p + f \cdot MW_c \cdot \bar{V}_c / d_1 \cdot N \cdot 10^{-24}\ ) \qquad (11)$$

where MW_p, MW_c = Molecular Weight of phospholipid and cholesterol
$\bar{V}_p$, $\bar{V}_c$ = Partial Specific Volumes for phospholipid and cholesterol
f = Mole ratio of cholesterol to phospholipid

Phase diagrams for DPPC (50°C), DPPC (25°C), egg PE (25°C) and DPPC/CHOL 1:1 (25°C) were constructed in which the structural parameters d, d_1, d_w and A were measured for various lipid concentrations in water. To do this the lipid and water were mixed by weight in small weighing bottles. After a period of about 48 hours, in order to ensure equilibrium, the samples were transferred to the X-ray sample holder. The samples were mounted at the temperature at which the diffraction was to be performed. For DPPC the same sample was used for both frozen and melted diffractions and the sample was not moved between runs. This was done in order that the teflon calibration line at room temperature could be used to calculate the diffraction

Figure 7.

Diagram of structural parameters measured in the multi-lamellar lipid-water system.

d = Total repeat spacing.

d_l = Thickness of the bilayers.

d_w = Distance between bilayers.

A = Area available to 1 phospholipid on the surface of the bilayer.

V_w = Volume of water associated with a lipid molecule.

d_{pp} = Center to center distance between head groups within a bilayer.

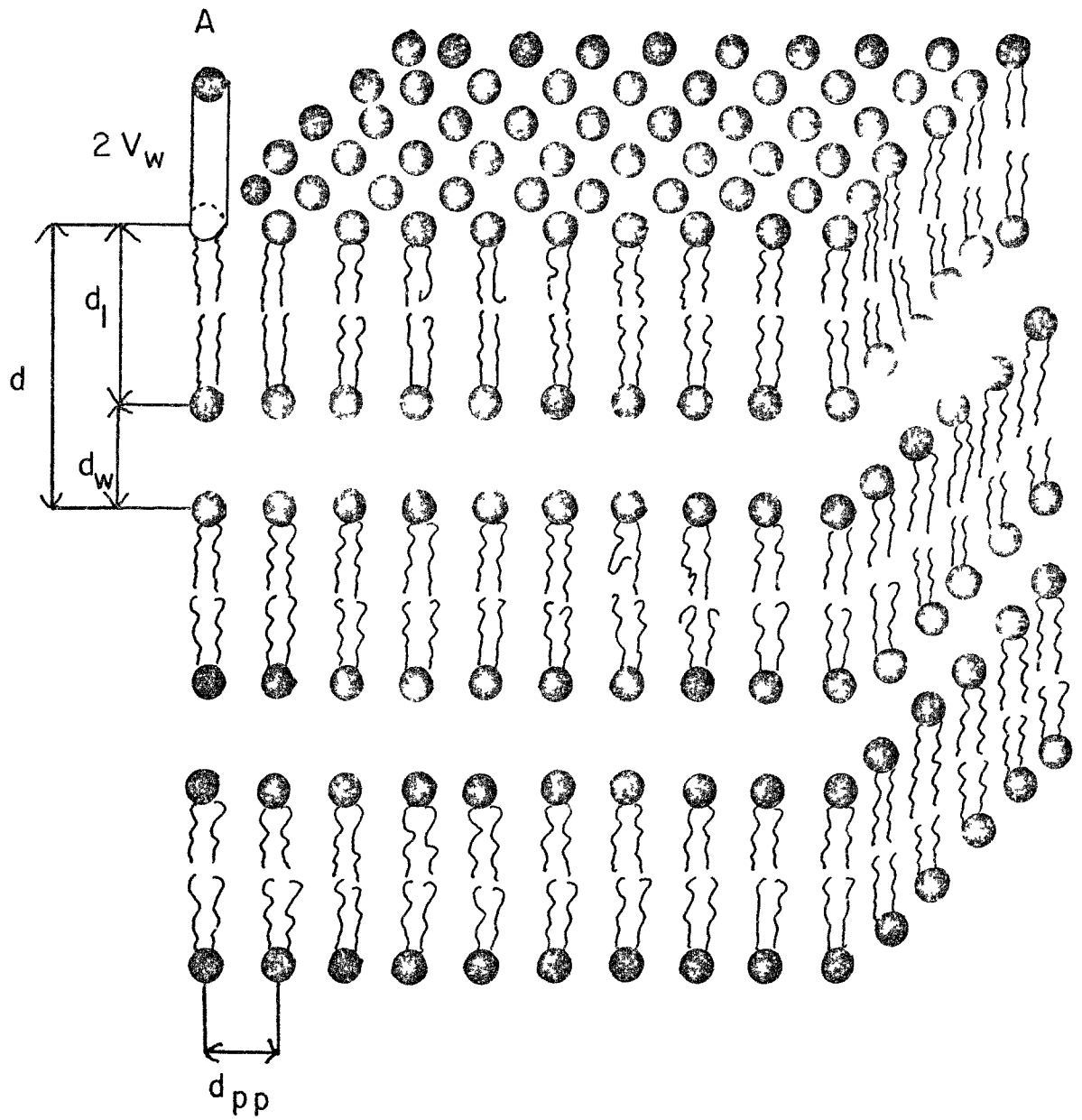
A
2 V_w
d_l
d
d_w
d_{pp}

spacings for the same sample when the temperature was raised. At the temperature selected for melted DPPC (50°C) the chains were clearly fluid as shown by the disappearance of the sharp 4.2 Å line and the appearance of a diffuse 4.5 Å band.

DPPC/CHOL 1:1 was prepared by dissolving equimolar amounts of DPPC and cholesterol in chloroform. The solutions were combined and the solvent removed by rotary evaporation with final drying under vacuum.

FORCE MEASUREMENT

Three techniques were used to measure the work required to remove water from the multilayer system and X-ray diffraction was used to measure the structural changes that resulted. This was done for each of frozen DPPC, melted DPPC, egg PE and DPPC/CHOL 1:1. In each technique the chemical potential (μ_w) of the water with which the multilayer must come into equilibrium is established. In the first method the lipid is immersed in a high molecular weight dextran solution of known concentration (Fig. 8). Since the dextran molecule is large (LENEVEU 1977) it cannot enter into the lattice structure. Thus the lipid must compete for the water against the osmotic pressure exerted by the dextran solution. The concentration of the dextran solution was determined from its refractive index using an ABBÉ refractometer. The osmotic pressure was determined from the relationship between osmotic pressure and dextran concentration which had previously been measured experimentally (LENEVEU 1976). The dextran solution-lipid samples were mixed in weighing bottles, allowed to equilibrate for two days, and then transferred to the X-ray sample holders for diffraction. From the phase diagram for DPPC it was seen that more water was taken up by melted DPPC than by frozen DPPC. This difference in uptake of water would change the concentration of the dextran solution and hence its osmotic pressure. To correct for this change, the lipid was thoroughly dispersed in the dextran solution at room temperature such that the ratio of lipid

Figure 8.

Diagram of the three techniques used to apply pressure to the lipid-water lamellar lattice.

$\mu_w = -\pi \overline{V}_w$

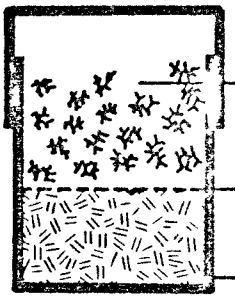

$\mu_w = -P \overline{V}_w$

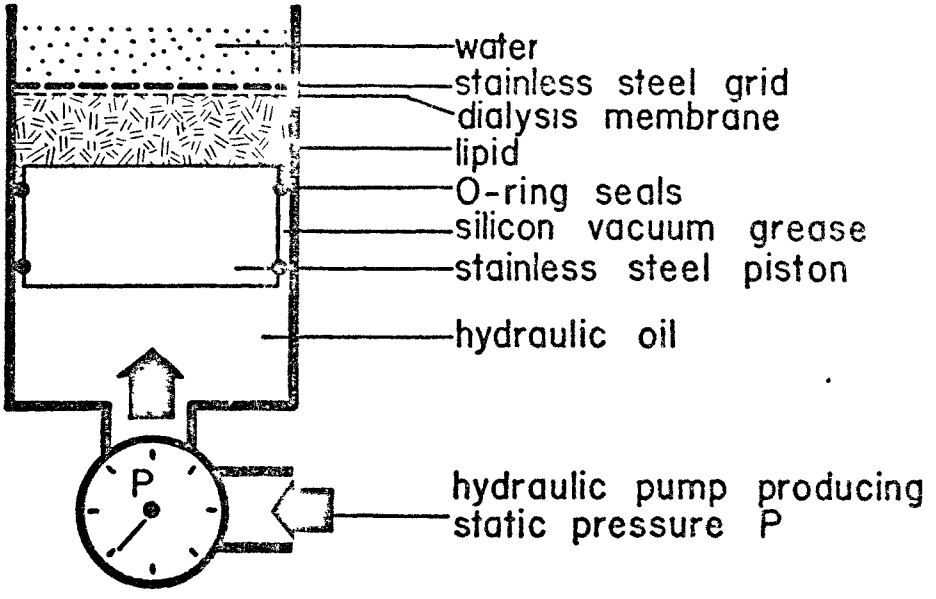

$\mu_w = RT \ln \frac{p}{p_o}$

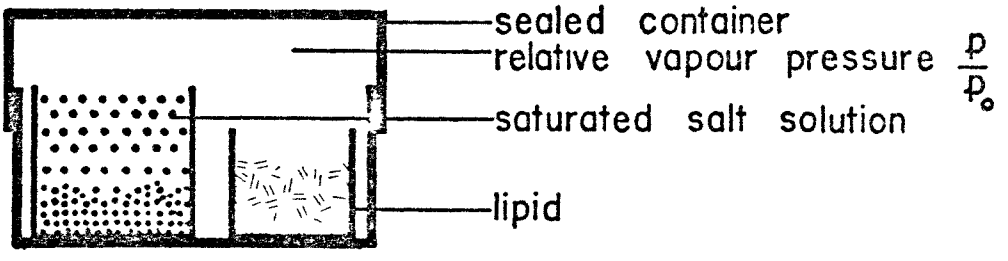

to dextran was uniform throughout the sample. By knowing the weight ratio of the lipid to dextran and the amount of water taken up by the lipid in going from the frozen to the melted state (from the phase diagram) it is possible to calculate the percent change in dextran concentration and hence the osmotic pressure at both temperatures.

The second method for limiting the amount of water in the multilamellar system involved the use of a hydraulic pressure cell (Fig. 8). With this apparatus a mechanical pressure is exerted by a hydraulic piston on the lipid sample. The sample was restrained by a dialysis membrane which allowed passage of water but not lipid. The pressure was measured directly by Marsh pressure gauges. The lipid was added dry and allowed to imbibe water against the mechanical pressure. The sample was left three to four days on the pressure cell at room temperature in order to equilibrate, then transfered to the X-ray sample holder.

In the third method the lipid was put into contact with a vapour pressure of known relative humidity (Fig. 8). The vapour pressure was generated by various saturated salt solutions. At equilibrium the chemical potential (μ) between the bilayers is equal to that of the vapour. The μ of the vapour can be calculated from the known relative humidities of the salt solutions and is the work of moving water from the interbilayer space to bulk water. By dividing the work per mole by the molar volume of water the force per unit area between bilayers is calculated. The lipid was added dry and allowed to equilibrate for three to four days. The sample was weighed both dry and at equilibrium with the vapour and thus the final concentration of the lipid was determined.

In each of these three methods the lipid is competing for the water against an external pressure. At equilibrium the total internal pressure between bilayers is equal to the external pressure applied to the bilayers.

$$P_{ext} = P_{rep} - P_{att} \qquad (12)$$

where P_{ext} = External Pressure
P_{rep} = Repulsive Pressure between Bilayers
P_{att} = Attractive Pressure between Bilayers

The external pressure is produced by either the osmotic pressure of a dextran solution (π);

$$\pi = P_{ext} = -\mu_w / V_w = \quad (\text{dynes} / \text{cm}^2) \qquad (13)$$

the mechanical pressure exerted by a hydraulic piston (P);

$$P = P_{ext} = -\mu_w / V_w \ (\text{dynes} / \text{cm}^2) \qquad (14)$$

or the vapour pressure generated by a saturated salt solution (ρ);

$$(RT \ln \rho/\rho_o)/V_w = P_{ext} = -\mu_w / V_w \ (\text{dynes} / \text{cm}^2) \qquad (15)$$

where μ_w = Chemical potential of water between bilayers relative to bulk water
P_{ext} = External pressure compressing the system
V_w = Molar volume of water

Using these three techniques we have been able to relate the total spacing (d) to the applied external pressure for frozen DPPC, melted DPPC, egg PE and DPPC/CHOL 1:1. Experiments using the dextran and the hydraulic pressure techniques did not allow for the direct measurement of the weight of lipid in the sample holder. Therefore in order to determine the parameters d_l and d_w for these samples it is assumed that the measured d spacing is the sum of the same d_l and d_w as the corresponding d value from the phase diagram; in other words that denying water to the lipid either gravimetrically or by the pressure techniques will result in the same structural changes. Thus by combining the phase diagram, the external pressure and the d spacings for each lipid we can determine the relation between external pressure and the structural parameters d_w, d_l, A, d_{pp} and V_w.

ANALYSIS

Removal of water from the fully swelled multilayer system has two major structural consequences. The lipid head groups will come closer together in a direction normal to the plane of the membrane (a decrease in d_w) and will also pack closer within each bilayer (a decrease in A). In order to separate the energies required to effect each of these changes, a method derived by Dr. V. Parsegian was used (FULLER 1978) as described below.

METHOD I.

The volume of water per phospholipid molecule is

$$V_w = A \left(d_w / 2 \right) \qquad (16)$$

At any equilibrium value, V_w will take on values for A and d_w which minimize the free energy of the system. That is

$$\delta G = 0 = \frac{\partial G}{\partial (d_w/2)} \delta (d_w/2) + \frac{\partial G}{\partial A} \delta A$$

$$= \left(\frac{\partial G}{\partial (d_w/2)} - \frac{A}{d_w/2} \frac{\partial G}{\partial A} \right) \delta (d_w/2) \qquad (17)$$

For this minimization of the energy to occur the parenthesized quantity in equation 17 must be zero;

$$\frac{\partial G}{\partial (d_w/2)} - \frac{A}{(d_w/2)} \frac{\partial G}{\partial A} = 0 \qquad (18)$$

and thus

$$\frac{\partial G}{\partial A} = \frac{(d_w/2)}{A} \frac{\partial G}{\partial (d_w/2)} \qquad (19)$$

The work of changing the water volume (ΔV_w) goes into changes in area (ΔA) and separation ($\Delta d_w / 2$). The total work done is

$$\Delta G = \frac{\partial G}{\partial A} \Delta A + \frac{\partial G}{\partial (d_w/2)} \Delta (d_w/2) \qquad (20)$$

The ratio of the work going to change $d_w / 2$ and A is

$$\frac{\frac{\partial G}{\partial d_w/2} \Delta d_w}{\frac{\partial G}{\partial A} \Delta A} = \frac{\Delta (d_w/2)/(d_w/2)}{\Delta A / A} = \frac{\Delta (\ln (d_w/2))}{\Delta (\ln A)} = X \qquad (21)$$

Now since

$$\Delta G = -P \Delta V_w \qquad (22)$$

the change in energy as $d_w / 2$ is changed is

$$\frac{\partial G}{\partial (d_w/2)} = -P \frac{\Delta V}{\Delta (d_w/2)} \left(\frac{X}{1+X} \right) = F_R \qquad (23)$$

This is the force between phospholipids in opposite bilayers acting across the inter-bilayer space d_w.

The change in energy as A is changed is

$$\frac{\partial G}{\partial A} = \frac{P \Delta V}{\Delta A} \left(\frac{1}{1+X} \right) = F_{LP} \qquad (24)$$

This is the compressive force (lateral pressure) acting on a phospholipid molecule within a bilayer.

We may also calculate the change of energy as d_1 is changed

Since $V_l = A\, d_l / 2$ (where V_l = volume of lipid molecule) therefore

$$\frac{\partial G}{\partial d_l} = \frac{\partial G}{\partial A} \cdot \frac{\partial A}{\partial d_l} = \frac{\partial G}{\partial A} \cdot -\frac{A}{d_l} = F_{d_l} \qquad (25)$$

This is the force acting on a phospholipid molecule within a bilayer in a direction perpendicular to the bilayer plane.

The change of energy as d_{pp} is changed is

$$\frac{\partial G}{\partial d_{pp}} = \frac{\partial G}{\partial A} \cdot \frac{\partial A}{\partial d_{pp}} = \frac{\partial G}{\partial A} \cdot \sqrt{3}\, d_{pp} = F_{d_{pp}} \qquad (26)$$

This is the force acting on a phospholipid molecule within a bilayer in a direction parallel to the bilayer plane.

In order to solve these equations least squares quadratic fits were obtained for A vs V_w, $d_w / 2$ vs V_w and $\ln (d_w / 2)$ vs $\ln A$ for each lipid. These quadratic equations and their derivatives were used as analytical functions to evaluate F_R, F_{LP}, F_{d_l}, and $F_{d_{pp}}$ for each lipid.

Alternatively these inter- and intra-bilayer forces can be separated by a simpler method described below.

METHOD III

$$\Delta G = -P \Delta V_w \qquad (27)$$

Choosing A and d_w as descriptive variables, we divide the change in the water volume (ΔV_w) into

$$\Delta V_A = (d_w / 2) \Delta A \qquad (28)$$

and

$$\Delta V_{d_w} = A \Delta d_w / 2 \qquad (29)$$

where, by geometry, $V_w = A (d_w / 2)$.

The applied pressure P times each of these volume changes gives the change in molecular free energy with deformation and with separation;

$$\frac{\partial G}{\partial A} = -P\, d_w / 2 = F_{LP} \qquad (30)$$

and

$$\frac{\partial G}{\partial d_{w/2}} = -P\, A = F_R \qquad (31)$$

Since $d_1 A = 2V_1$, with V_1 the molecular volume of a phospholipid molecule, we have

$$\frac{\partial G}{\partial d_1} = P(dw / 2)\ A / d_1 = P\ V_w / d_1 = F_{d_1} \qquad (32)$$

for the rate of change of molecular free energy with bilayer thickness d_1. Assuming hexagonal packing of the phospholipids (LUZZATI 1968), we may write $A = \sqrt{3} / 2\ d_{pp}^2$ and the rate of change of molecular free energy with distance between polar groups on one bilayer becomes

$$\frac{\partial G}{\partial d_{pp}} = -P\sqrt{3}\ (\ d_w / 2\ )\ d_{pp} = F_{d_{pp}} \qquad (33)$$

The repulsive force (F_R) measured here is a net force composed of a repulsive hydration (F_H) and an attractive van der Waals force (F_A). That is $F_R = F_H - F_A$. F_H was fit to the form $F_H = F_0 \exp^{-d_w/\lambda}$. It was assumed that van der Waals attraction followed the form $F_A = -H/6\pi d_w^3$ (PARSEGIAN 1975). An estimate of the attractive force (F_A) at the equilibrium separation in water may be made by extrapolating F_H to this equilibrium spacing (LENEVEU 1976) since at this point F_A and F_H are equal. Since we can estimate a value of F_A at the equilibrium separation in water, we may also calculate a value for the London-Hamaker constant (H).

To obtain energies of repulsion F_H minus the attractive force (F_A) was integrated (that is $\int_0^{d_w'} F_0 \exp^{-d_w/\lambda} - (H/d_w^3)\ d\ d_w$). To obtain the energies of deformation the areas under the curves F_{LP} vs A were measured graphically.

Young's modulus is used as a measure of bilayer elasticity. It is defined as Y = Stress / Strain. In this system an anal gous modulus may be defined as

$$Y = (2 / d_1)\frac{\partial G}{\partial A} A^0 - A / A^0 \qquad (34)$$

where A^0 = Cross-sectional area available to a phospholipid at fully swelled equilibrium

RESULTS AND DISCUSSION

The dependence of the structural parameters d, d_l, d_w and A upon the concentration of lipid in water for frozen DPPC, melted DPPC, egg PE and the DPPC/Cholesterol 1:1 mixture are illustrated in figure 9. Tabulated values for all figures in the results are found in Appendix I. The phase diagrams for frozen DPPC, PE and DPPC/CHOL agree with previous work (CHAPMAN et al 1967, RAND et al 1971, RAND and LUZZATI 1968). The phase diagram for melted DPPC is in agreement with RAND, CHAPMAN and LARSSON (1975) but varies from the results published by JANIAK et al (1976). Our findings were checked using lipid from three sources (see MATERIALS) as well as several samples prepared from lipid supplied by Dr. D. Papahdjopoulos and all gave identical results.

As water is added to each lipid the total d spacing increases, the result of a decrease in d_l accompanied by an increase in d_w. The final equilibrium d_w represents the interbilayer separation at which the repulsive hydration force and the attractive van der Waals force balance.

The relationship between total d spacing and external pressure (combining the three techniques shown in Fig. 8) is shown in figures 10-13. The equilibrium spacing in bulk water for each lipid is indicated by an arrow.

Figure 9.

Variation of d, d_l, d_w and A with weight percent lipid in water for frozen DPPC (25°C), melted DPPC (50°C), egg PE (25°C) and DPPC/Cholesterol 1:1 (25°C).
Equilibrium values in excess water given in figure.
Data from Tables I-IV.

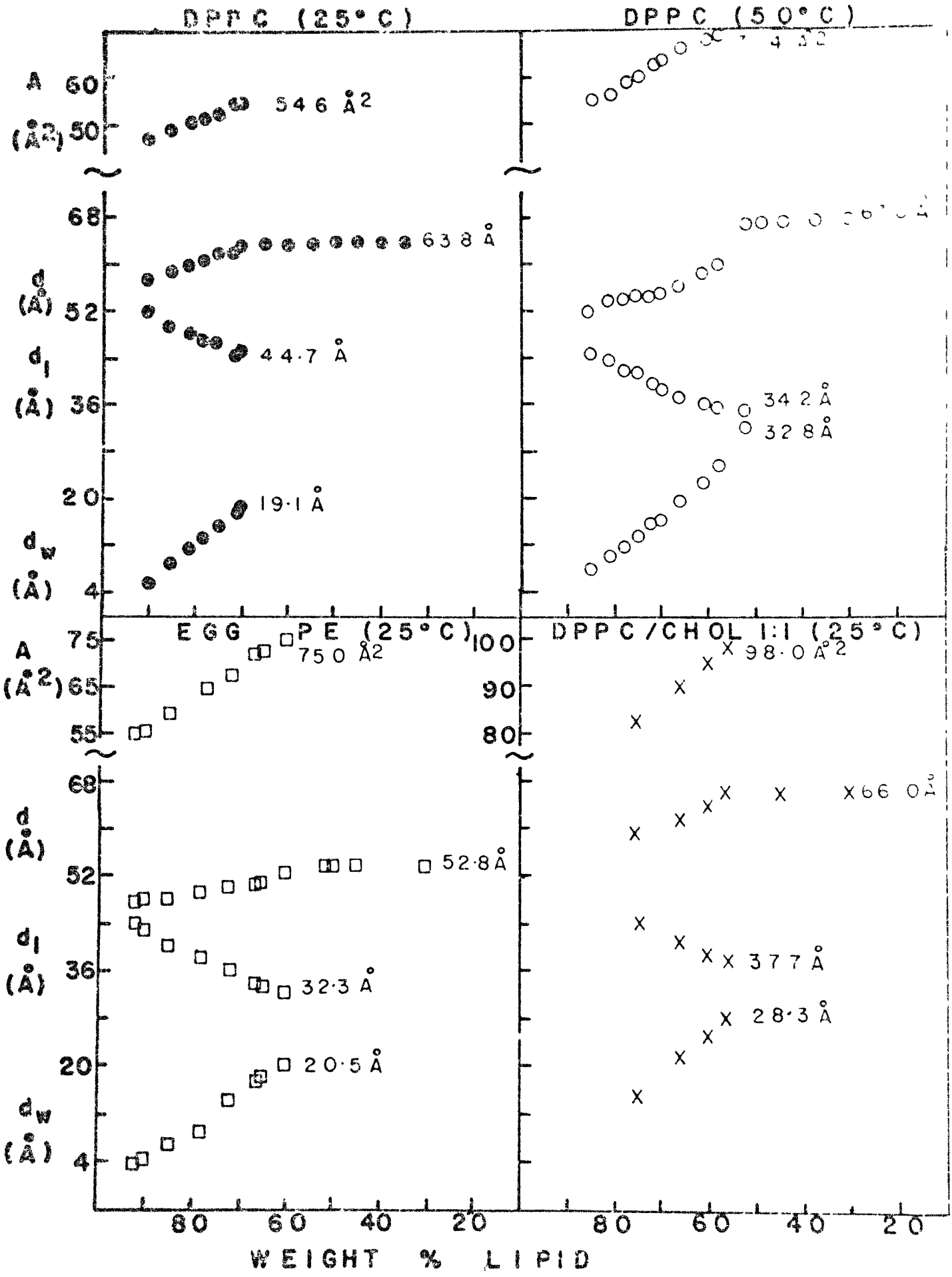
DPPC (25° C)
DPPC (50° C)
A (Å²)
546 Å²
d (Å)
d₁ (Å)
63·8 Å
44·7 Å
19·1 Å
d_w (Å)
34·2 Å
32·8 Å
EGG PE (25° C)
DPPC/CHOL 1:1 (25° C)
75·0 Å²
98·0 Å²
66·0 Å²
52·8 Å
32·3 Å
20·5 Å
37·7 Å
28·3 Å
WEIGHT % LIPID

Figure 10.

Applied pressure P (dynes / cm^2) versus total d spacing (Å) for frozen DPPC (25°C).

Arrow indicates the equilibrium separation in water.

Data from Table V.

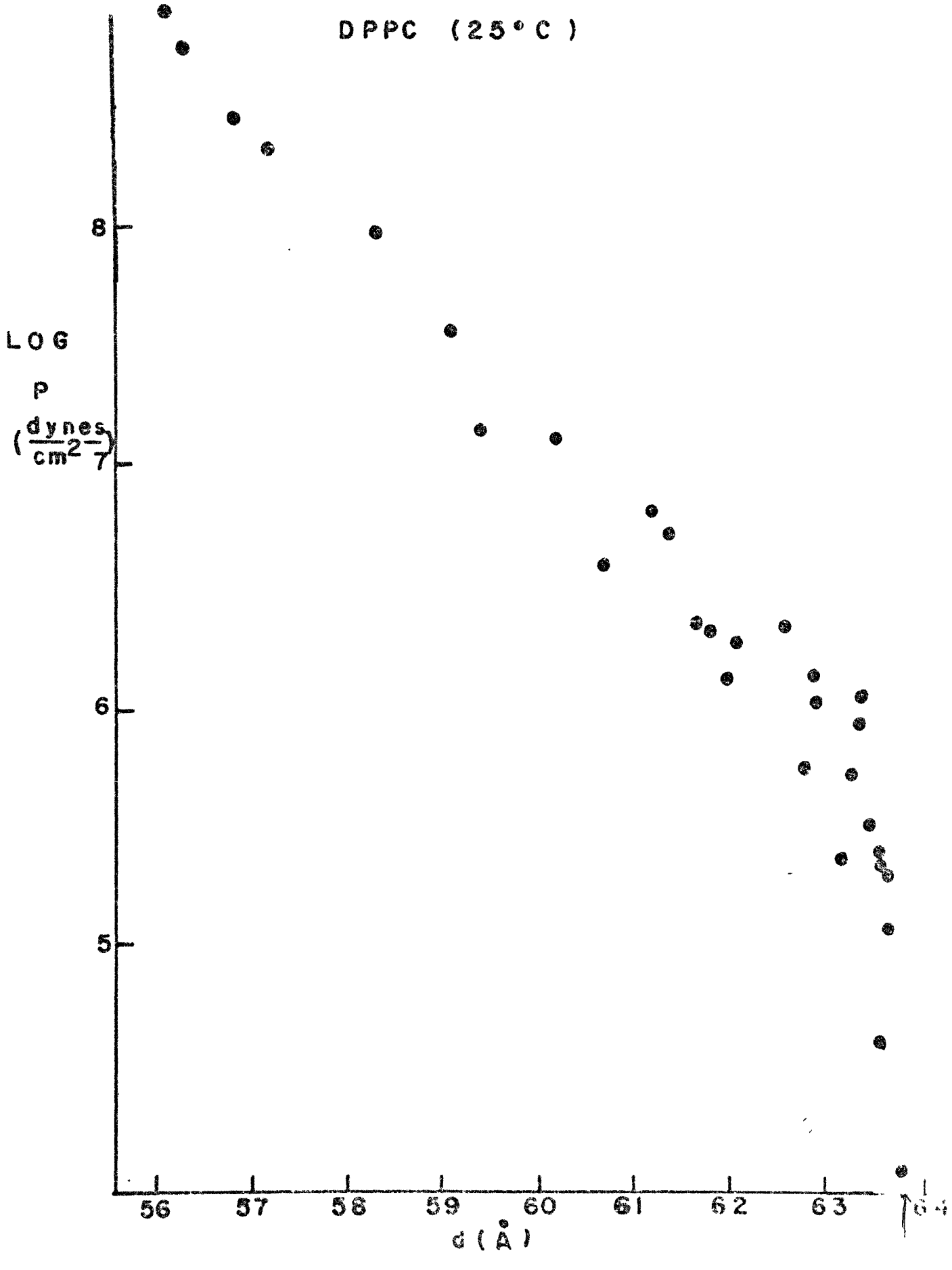
DPPC (25° C)
LOG P (dynes/cm2)
8
7
6
5
56
57
58
59
60
61
62
63
64
d (Å)

Figure 11.

Applied pressure P_e (dynes / cm^2) versus total d spacing (Å) for melted DPPC (50°C).

Arrow indicates the equilibrium separation in water.

Data from Table VI.

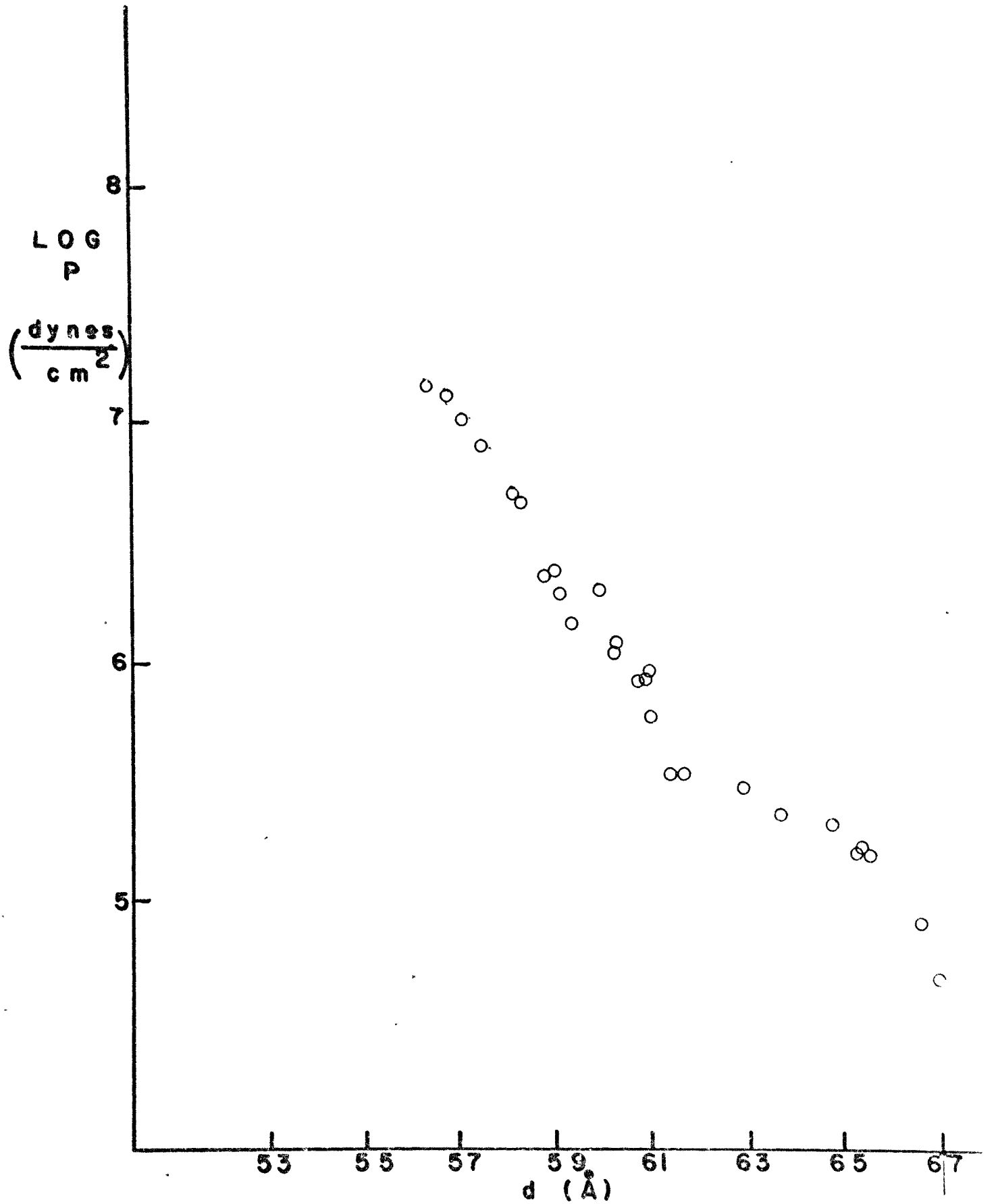
DPPC (50° C)
LOG P
(dynes / cm²)
8
7
6
5
53
55
57
59
61
63
65
67
d (Å)

Figure 12.

Applied pressure P_o (dynes / cm^2) versus total d spacing (Å) for egg PE.

Arrow indicates the equilibrium separation in water.

Data from Table VII

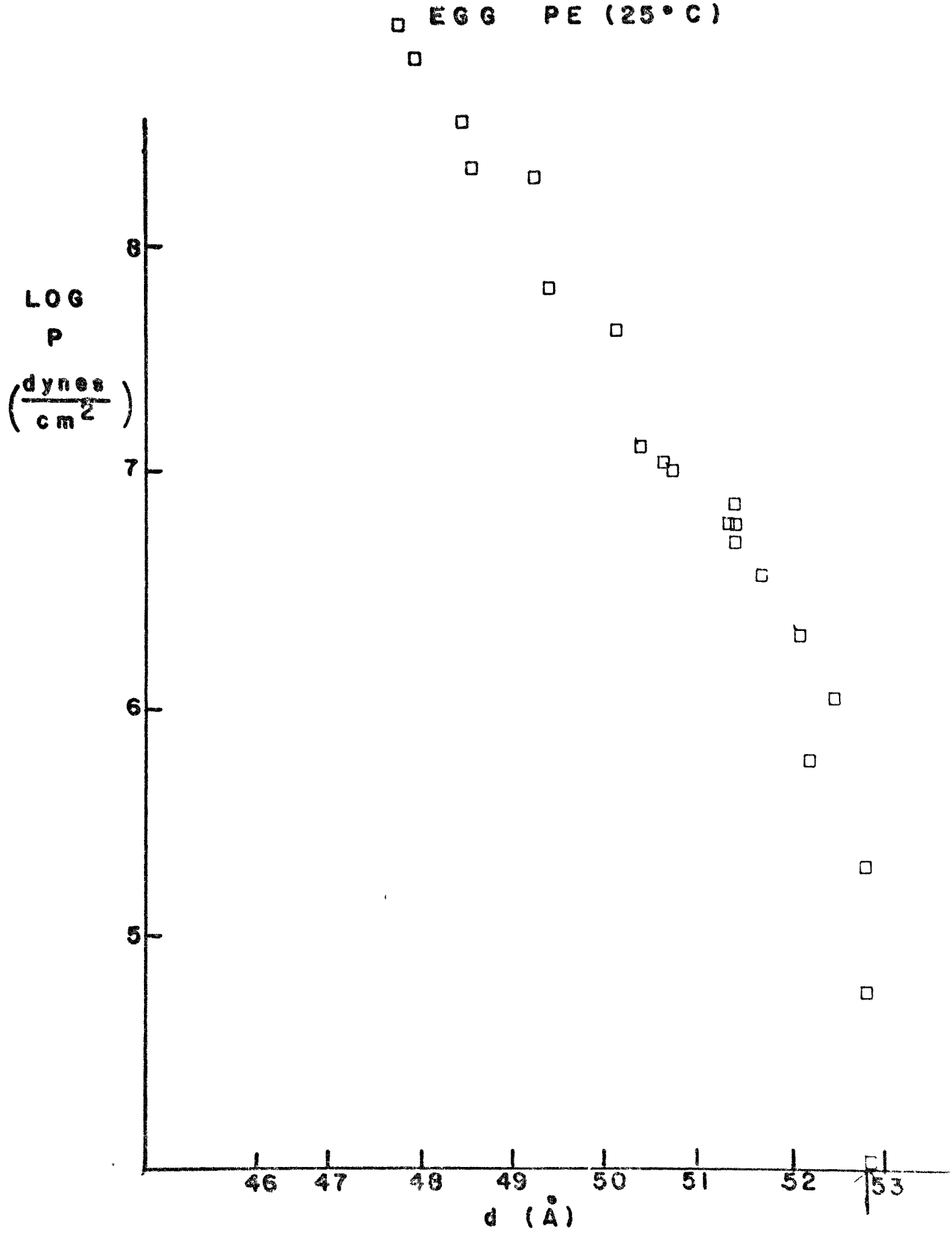
EGG PE (25° C)
LOG P
(dynes/cm²)
8
7
6
5
46
47
48
49
50
51
52
53
d (Å)

Figure 13.

Applied pressure P (dynes / cm^2) versus total d spacing (A) for DPPC/Cholesterol 1:1 (25 C).

Arrow indicates the equilibrium separation in water.

Data from Table VII

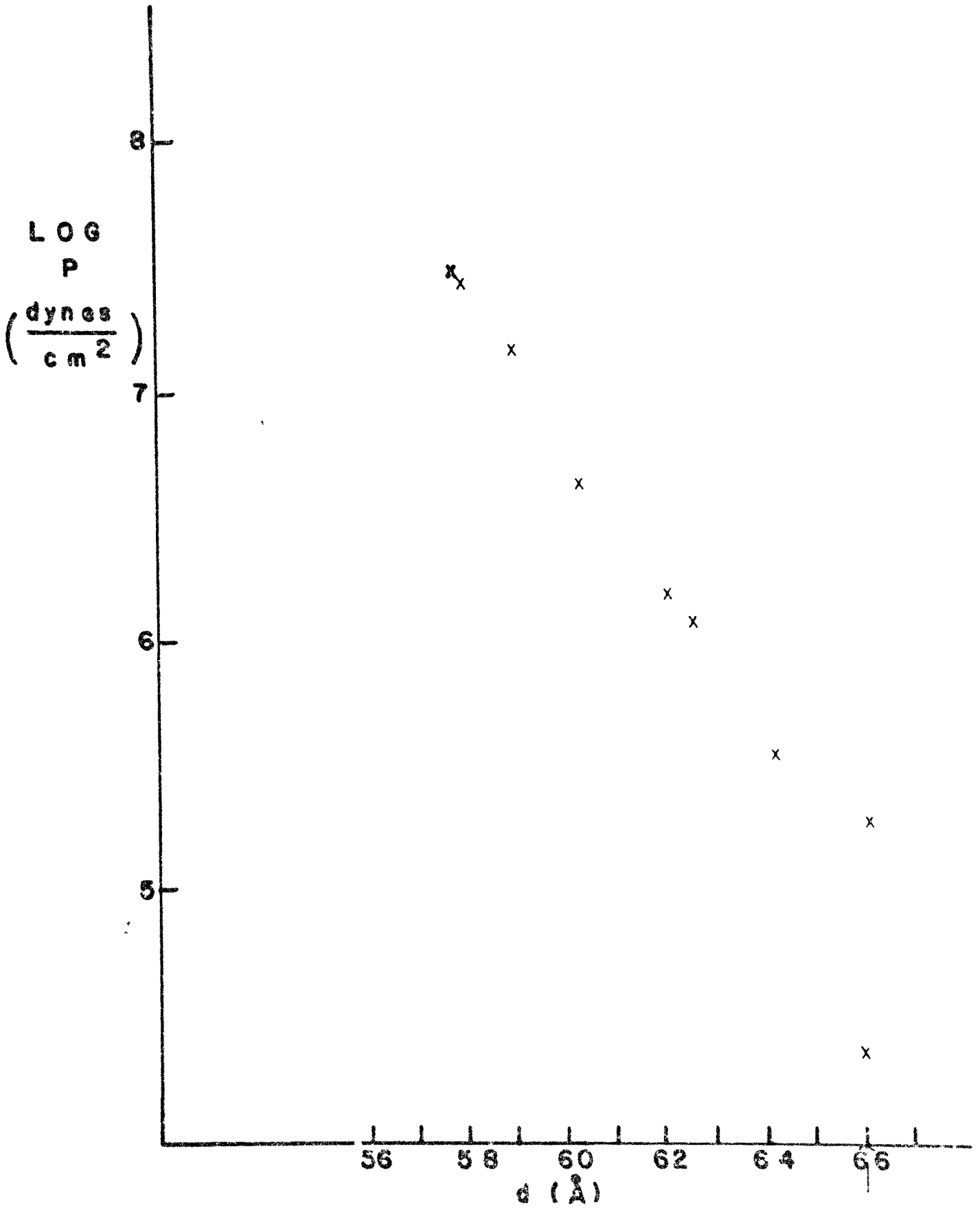
DPPC/CHOLESTEROL 1:1 (25° C)
LOG P (dynes/cm²)
8
7
6
5
56
58
60
62
64
66
d (Å)

The relationship between the net repulsive force (F_R) between bilayers and their separation (d_w), as well as the lateral pressure (F_{LP}) as it is related to the molecular surface area (A) were determined from these data for each lipid using METHOD II described earlier.

HYDRATION FORCE

Figures 14 and 15 show the relationship between the repulsive force F_R and bilayer separation for the four lipids studied. The three techniques combined allow measurement of this force over a large range of bilayer separations. For frozen DPPC all but the last four waters per phospholipid have been removed. All the lamellar phases will show some type of structural transition if more than the lowest indicated amount of water is removed.

Specifically, frozen DPPC and egg PE will change into non-lamellar phases if sufficient water is removed, the chains of melted DPPC will crystallize and cholesterol will crystallize out from the DPPC/CHOL mixture.

The large repulsive forces reported for egg lecithin (LENEVEU et al 1976, 1977) persist for all of the neutral lipids studied here. These hydration forces become very large, exceeding 10 atmospheres ($10^{7.5}$ dynes/cm^2) at distances less than 10 Å for frozen DPPC.

It may be seen, for each lipid, that the total repulsive force F_R near equilibrium d_w in excess water deviates from the exponential decay that describes most of the curve. This is due to the influence of the attractive van der Waals force which becomes significant in magnitude relative to the hydration force near this equilibrium separation in water. At this equilibrium separation the attractive and repulsive forces must be equal, therefore an estimate of the attractive force (F_A) can be made by extrapolation of the exponential repulsive force to this spacing (Figs. 14, 15) (LENEVEU et al 1976). If we assume that van der Waals attraction follows the form $F_A = -H/6\pi d_w^3$ and is equal to F_H at the equilibrium separation in water, then we may calculate the London-Hamaker constant "H" for each of the lipids (Table 1). These constants are of the order of magnitude expected for lipid-water multilayers (PARSEGIAN and NINHAM 1971).

Since F_A varies inversly with the cube of bilayer separation (PARSEGIAN 1975), it can be seen that the larger hydration forces (F_H) will far out-weigh F_A at separation only a few angstroms closer than the equilibrium spacing in water. For example F_A for all lipids composes less than 9 % of the net repulsive forces at a separation 10 Å closer than the equilibrium separation in water. Therefore an equation of the type $F = F_0 \exp^{-d_w/\lambda}$ which empirically describes the net repulsive force (F_R) for most of the curve (Fig. 15) (excluding forces which are near equilibrium) is composed primarily

Table 1

Calculated London-Hamaker constants (H)

LIPID	F_A (dynes / molecule) (a)	H (ergs)
DPPC 25°C	2.63×10^{-9}	$5.0\text{-}7.5 \times 10^{-14}$
DPPC 50°C	4.67×10^{-10}	$3.7\text{-}5.0 \times 10^{-14}$
Egg PE	2.04×10^{-8}	$3.8\text{-}5.2 \times 10^{-13}$
DPPC/CHOL	2.23×10^{-9}	$8.8\text{-}11 \times 10^{-14}$
Decane (b)	-	$0.9\text{-}5.5 \times 10^{-14}$

(a) Measured at the equilibrium separation in water.
(b) (PARSEGIAN and NINHAM 1971)

of the the hydration (F_H), since F_A will be insignificant in comparison.

The "length constant" λ in the exponential description of F_H, for each lipid, indicates how quickly the hydration force will increase as the separation between bilayers is decreased; the smaller it is the greater the rate of increase of the force as d_w is decreased. The length constants were tested for significant differences by the method of BLISS (1967) and increase in the order frozen DPPC < egg PE < melted DPPC < DPPC/Cholesterol.

The difference in chemical potential between the water between the bilayers with that of bulk water (μ_w) is plotted along the right-hand axis of figures 14 and 15. These differences are very small, most being less than 1 Kcal / mole. Thus although these small chemical potentials result in large hydration forces and must be very important from a structural point of view, they probably have an insignificant effect on chemically dependent processes, such as diffusion barriers, near the membrane.

The curves of figures 14 and 15 have no detectible discontinuities. All the chemical potentials calculated for the water between the bilayers fall on a continuum and each is lower than that of pure water. To remove the first waters between the bilayers requires work and therefore even these first waters have a chemical potential below that of bulk water. This indicates that the water cannot be classified as either bound or non-bound but rather varies continuously between these two extremes.

The energy required to reduce the interbilayer spacing (d_w) from its equilibrium in water may be obtained by integrating the net repulsive force F_R.

$$\text{Since } F_R = F_H - F_A \qquad (35)$$

$$\text{then } \int F_R = \int F_H - \int F_A \qquad (36)$$

$$\text{and } \int F_R = \int F_0 \exp\left(-d_w/\lambda \right) - H/6\pi d_w^{\,3}\, d\, d_w \qquad (37)$$

These repulsive energies are plotted in figures 16 and 17. Figure 16 is the energy per molecule required to bring the bilayers to a certain separation, figure 17 is the energy per molecule required to bring bilayers

to a given change in d_w from their equilibrium separation in water. The energies are small for close approach by individual molecules; however for single molecules to approach they must leave the bilayer structure, a highly unlikely event (the critical micelle concentration for DPPC is $0.5\text{-}4.6 \times 10^{-10}$ M SMITH and TANFORD 1972). However the energy required for small patches of bilayer containing many molecules to approach each other can be obtained simply by multiplying the values in figures 16 and 17 by the number of molecules. For even small patches of area similar to those expected for cellular contact, a large barrier must be overcome. In the case of frozen DPPC it would require 15 kT units to bring two planar membranes of 0.5 μ^2 to within 10 Å of each other (assuming no deformation of the membranes). The probability of this would be negligable ($e^{-15} = 3 \times 10^{-7}$) and thus it is likely that membranes must be deformed or modified in some major way before close approach can occur.

Figure 14.

Interbilayer force F_R per lipid molecule (dynes) versus bilayer separation d_w (Å) for frozen DPPC (25°C).

The right hand axis is the difference in the chemical potential of the water between the bilayers μ_w (cal / mole) relative to pure water.

The top axis is the number of waters per phospholipid molecule.

Dotted line indicates the magnitude of attractive force F_A at equilibrium separation in water.

Equation is an exponential fit to the repulsive hydration force F_H.

Data from Table V.

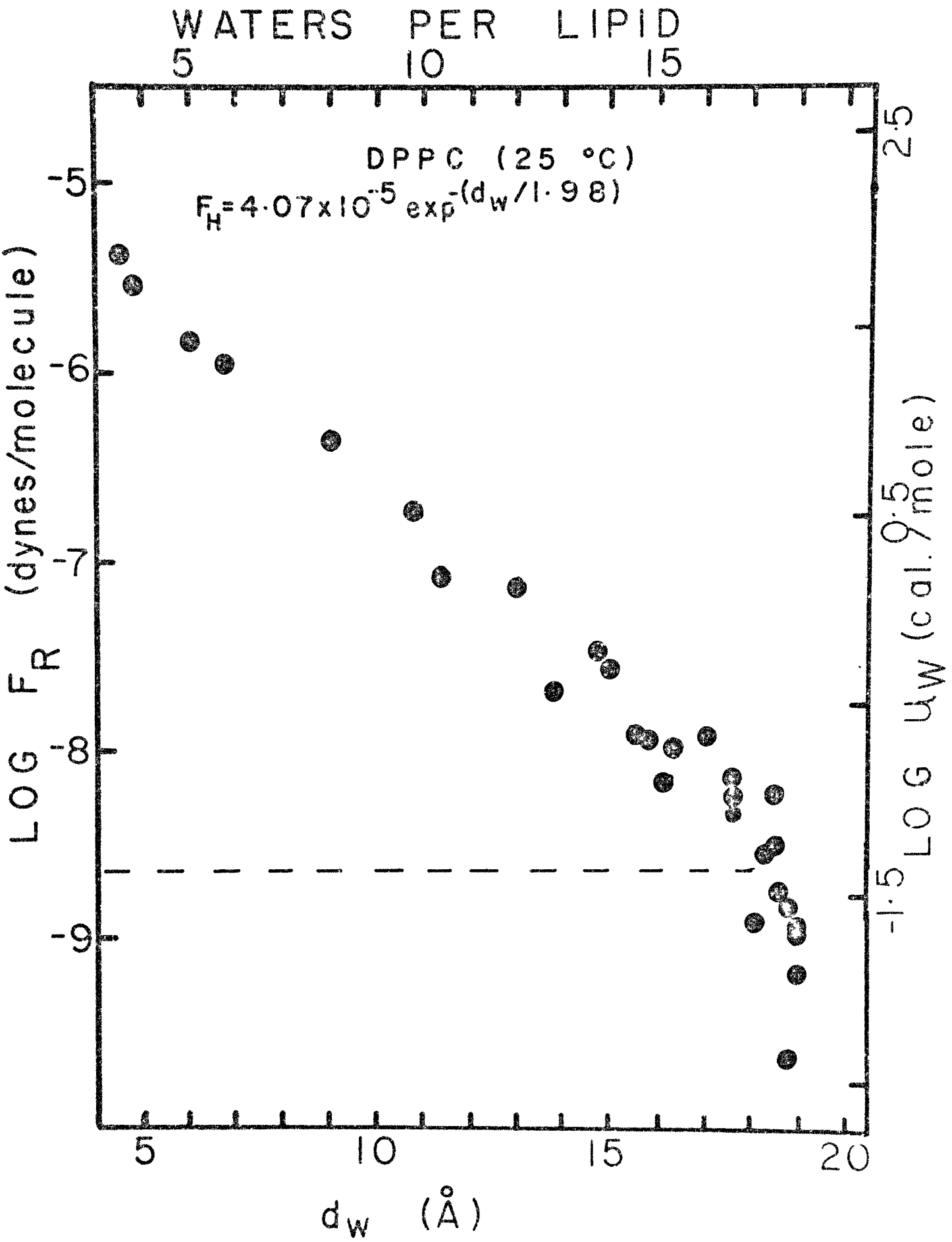
WATERS PER LIPID
5
10
15
DPPC (25 °C)
$F_H = 4.07 \times 10^{-5} \exp^{-(d_w/1.98)}$
LOG F_R (dynes/molecule)
-5
-6
-7
-8
-9
-1.5 LOG u_w (cal./mole)
2.5
9.5
5
10
15
20
d_w (Å)

Figure 15.

Interbilayer force F_R per lipid molecule (dynes) versus bilayer separation d_W (Å) for DPPC (25°C), DPPC (50°C), egg PE (25°C) and DPPC/Cholesterol 1:1 (25°C).

Other axis labelled as shown in legend of figure 14.

Data from Tables V-VIII.

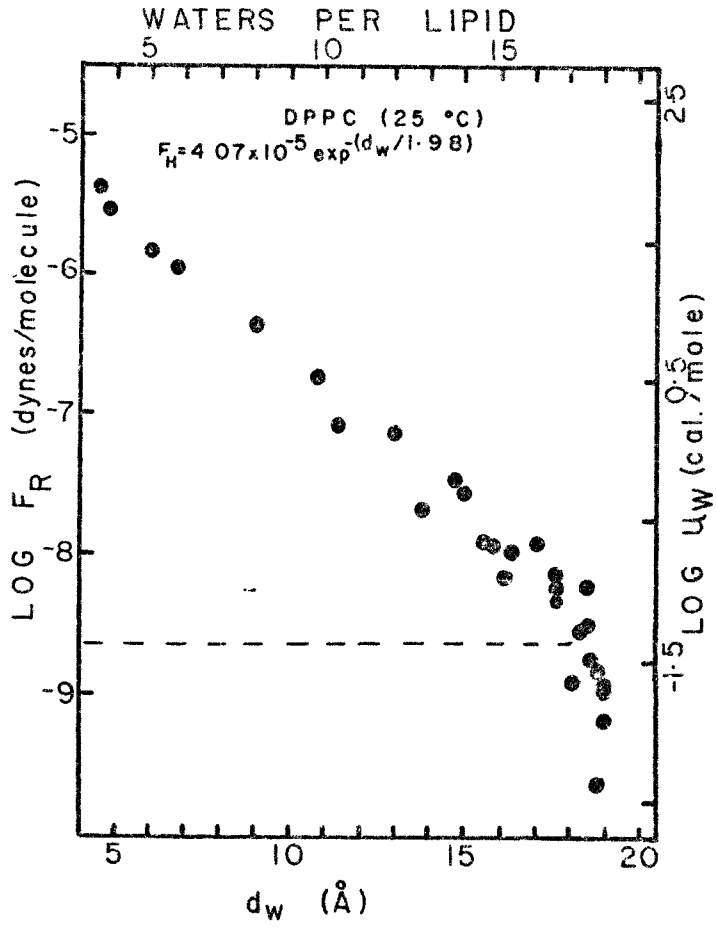
WATERS PER LIPID
5
10
15
DPPC (25 °C)
$F_H = 4.07 \times 10^{-5} \exp^{-(d_w/1.98)}$
LOG F_R (dynes/molecule)
-5
-6
-7
-8
-9
LOG U_W (cal./$^{0.5}$mole)
2.5
-1.5
5
10
15
20
d_W (Å)

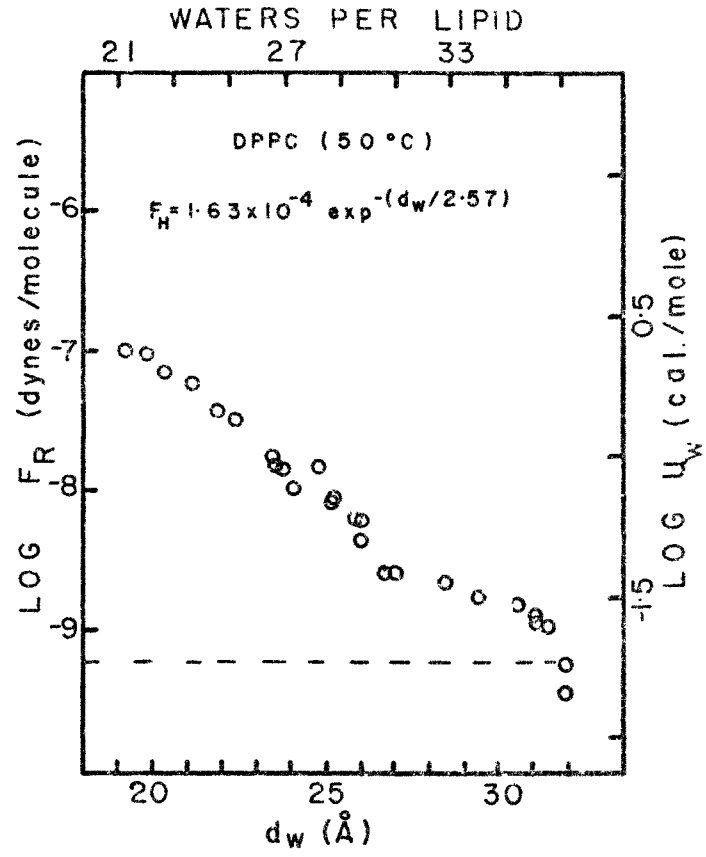
WATERS PER LIPID
21
27
33
DPPC (50 °C)
$F_H = 1.63 \times 10^{-4} \exp^{-(d_w/2.57)}$
LOG F_R (dynes/molecule)
-6
-7
-8
-9
LOG U_W (cal./mole)
0.5
-1.5
20
25
30
d_W (Å)

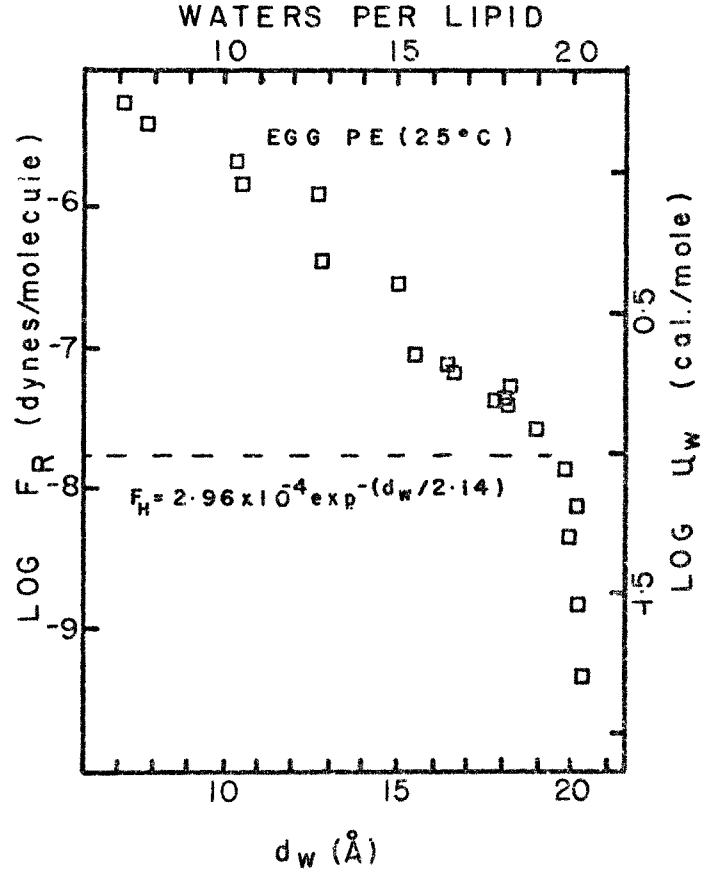
WATERS PER LIPID
10
15
20
EGG PE (25°C)
$F_H = 2.96 \times 10^{-4} \exp^{-(d_w/2.14)}$
LOG F_R (dynes/molecule)
-6
-7
-8
-9
LOG U_W (cal./mole)
0.5
-1.5
10
15
20
d_W (Å)

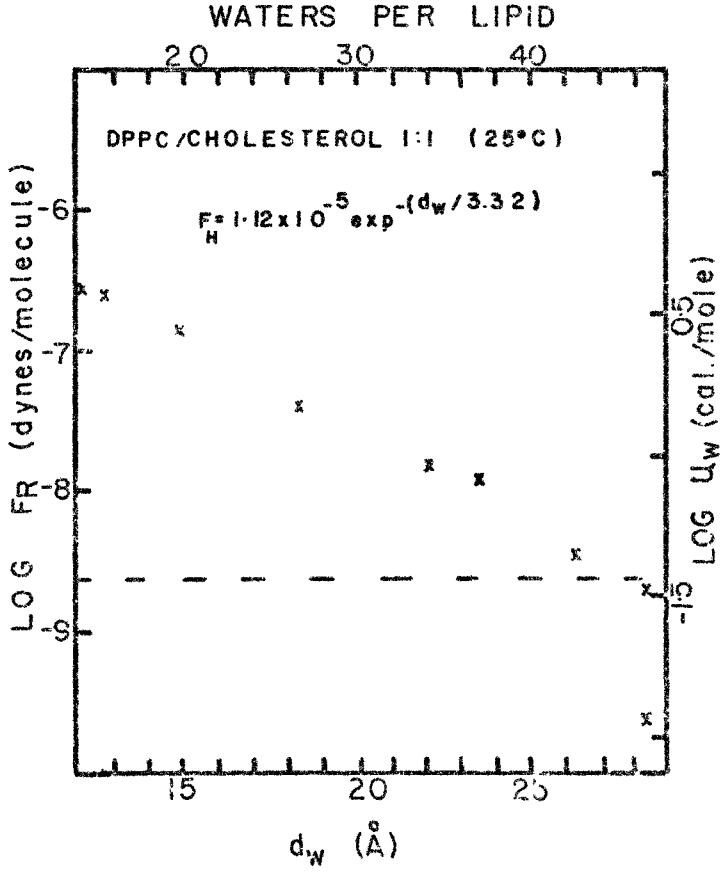
WATERS PER LIPID
20
30
40
DPPC/CHOLESTEROL 1:1 (25°C)
$F_H = 1.12 \times 10^{-5} \exp^{-(d_w/3.32)}$
LOG FR (dynes/molecule)
-6
-7
-8
-9
LOG U_W (cal./mole)
0.5
-1.5
15
20
25
d_W (Å)

Figure 16.

Energy per molecule (kT) required to change d_w versus bilayer separation d_w (Å) for DPPC (25°C), DPPC (50°C), egg PE (25°C) and DPPC/Cholesterol 1:1 (25°C).

Arrows indicate equilibrium bilayer separations in water.

Data from Table IX.

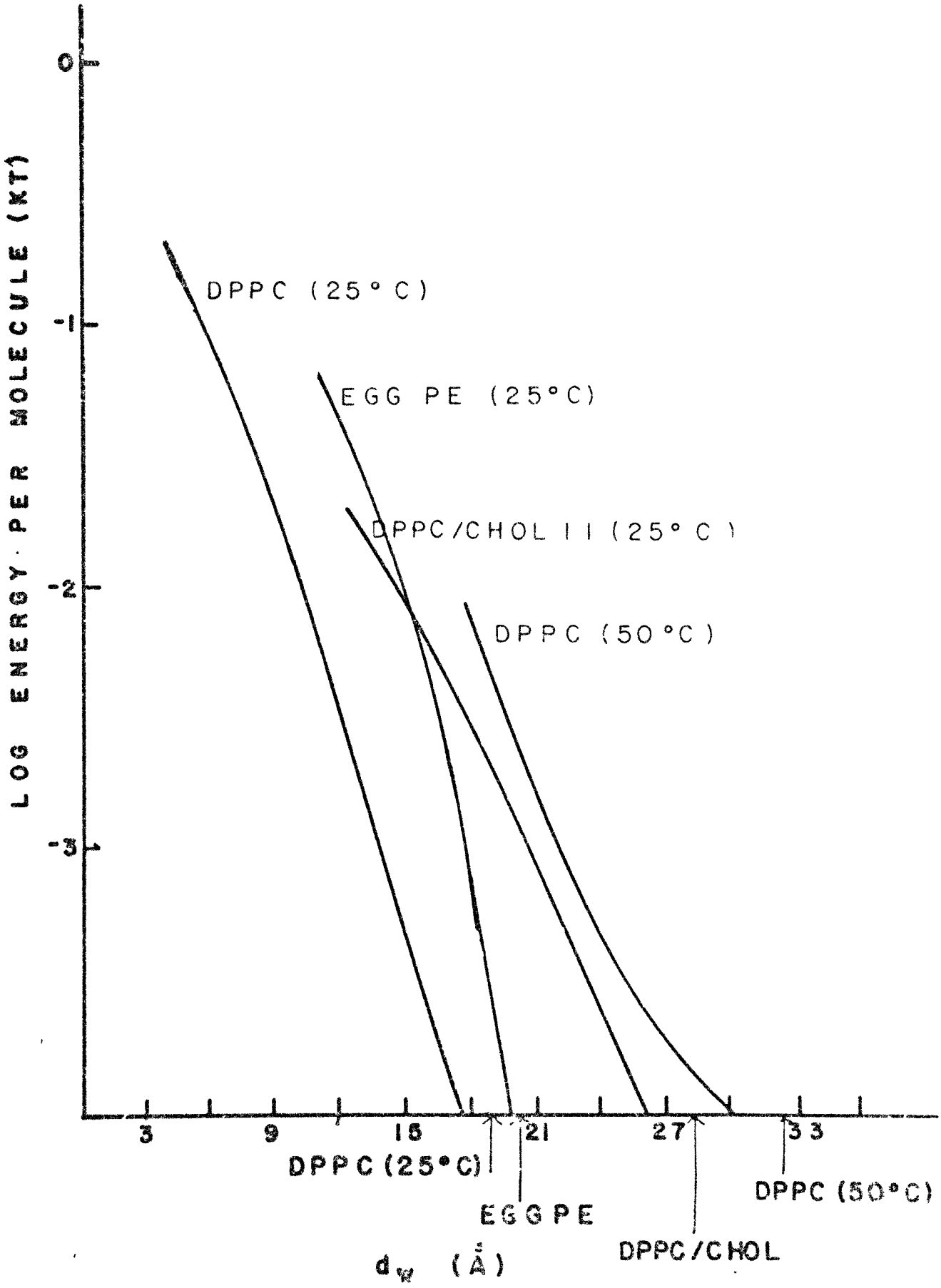
LOG ENERGY PER MOLECULE (KT)
0
-1
-2
-3
DPPC (25° C)
EGG PE (25°C)
DPPC/CHOL II (25° C)
DPPC (50°C)
3
9
15
21
27
33
DPPC (25°C)
EGG PE
DPPC/CHOL
DPPC (50°C)
d_w (Å)

Figure 17.

Energy per molecule (kT) required to change d_w versus the change in bilayer separation from equilibrium d_w in water (Δd_w) for DPPC (25°C), DPPC (50°C), egg PE (25°C) and DPPC/Cholesterol 1:1 (25°C).

Data from Table IX.

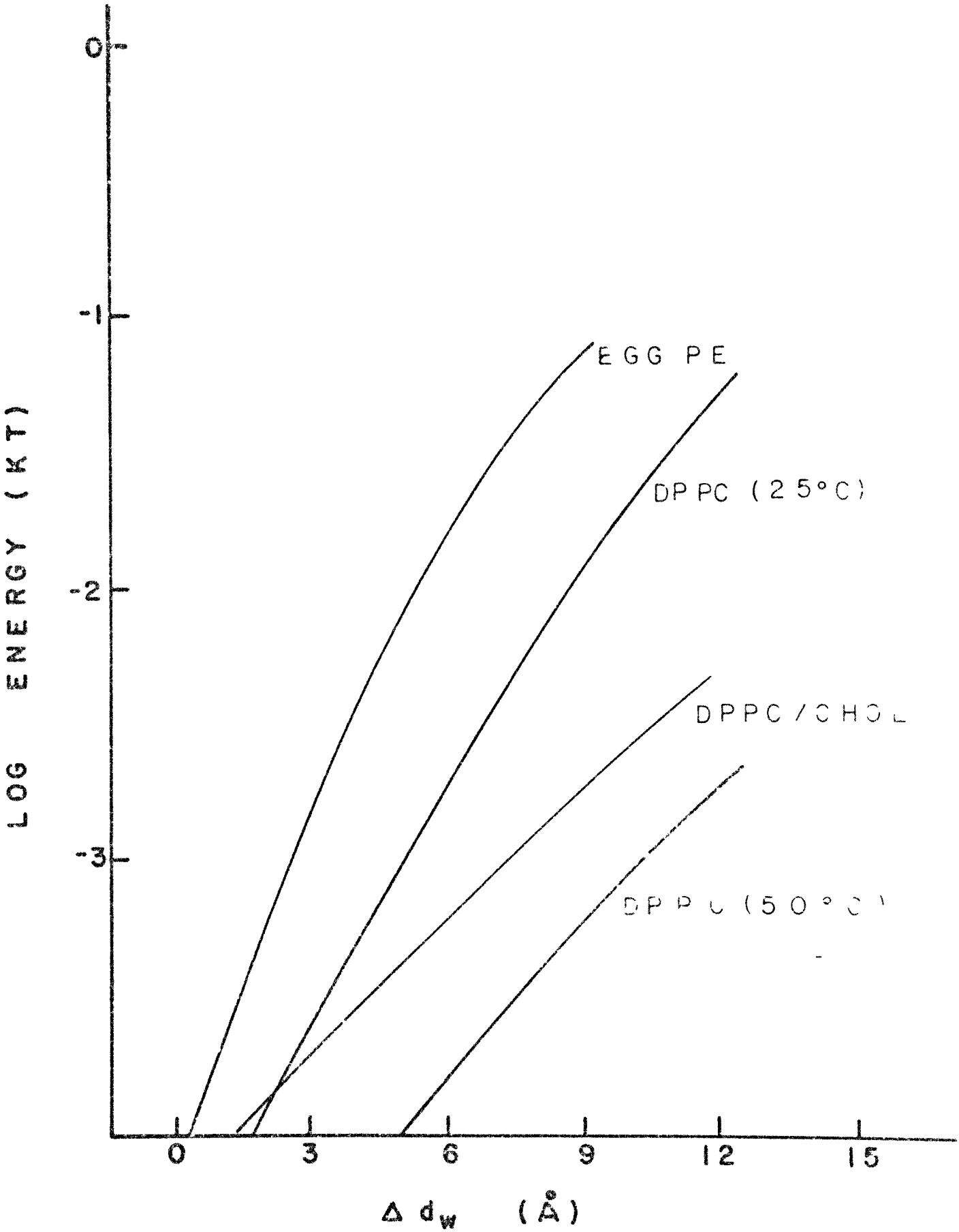
LOG ENERGY (KT)
0
-1
-2
-3
EGG PE
DPPC (25°C)
DPPC/CHOL
DPPC (50°C)
0
3
6
9
12
15
Δ d_w (Å)

DEFORMATION FORCE

In addition to bringing the bilayers closer together (a decrease in d_w) the isotropic pressure applied to the system will also deform the bilayers by reducing the cross-sectional area per phospholipid (A).

Figure 18 shows the percent of the total work done on the system that goes into this deformation. This proportion was calculated using METHOD I described earlier. It can be seen that for all lipids less than 25 % of the total work done goes into deformation and as more water is removed, this proportion decreases.

Figure 19 is a comparison of F_R, the repulsion between molecules on adjacent bilayers, and $F_{d_{pp}}$, the repulsion between molecules in the same bilayer, for frozen DPPC. $F_{d_{pp}}$ increases much more rapidly for a reduction in polar group separation within the bilayer (d_{pp}) than does F_R for the same reduction in polar group separation between bilayers (d_w). This relationship holds true for the other lipids studied as well (Appendix I). Thus phospholipids in bilayers are already closely packed even in excess water, making deformation difficult. It is easier to push bilayers together (decrease d_w) than to deform them (decrease A). This deformation "stiffness" explains why most of the work goes into overcoming hydration forces (Fig. 18).

Lateral pressure (F_{LP}) as a function of area is shown in figures 20-23. For all these lipids the cross-sectional areas have been significantly changed (for frozen DPPC $\Delta A = 7$ $\mathring{A}^2$). This is the first measurement of the lateral pressure of a bilayer and is analogous to monolayer studies where the pressure produced by a monolayer is measured as a function of molecular area. However unlike a monolayer (TAYLOR et al 1973, YUE et al 1976), the lateral pressure of a bilayer is zero at equilibrium area in excess water. Thus a bilayer will stop swelling in excess water when a

certain equilibrium molecular area is reached, while a monolayer will continue to expand untill it is in essence a two-dimensional gas. We assume that the net force (F_{LP}) is composed of attractive and repulsive components as was F_R, however as the equilibrium area in water is approached, F_{LP} gradually decreases and their is no sudden drop in force as there is when F_R approaches equilibrium d_w. We are therefore unable to calculate the value of the attractive component or "surface tension" (EVANS and WAUGH 1977) at equilibrium and it may be that this surface tension cannot be described by an equation as relatively simple in form as F_A.

Since A and d_1 are geometrically linked by the volume of the lipid molecule ($d_1A = 2V_1$) which remains constant, we can express deformation in terms of bilayer thickness (Fig. 24). This is the force acting perpendicular to the bilayer acting to increase its thickness.

We can also describe the mechanical properties of the bilayer in terms of a quantity analagous to Young's Modulus "Y" (see METHODS) (Figs. 25, 26). The scatter in Y is due to an estimated error of about 2 % in bilayer dimensions. It can be seen that as the area (A) increases, Y decreases. The values of Y at equilibrium areas for these lipids will give an idea of membrane stiffness. The values for Y at equilibrium lie between estimates for corresponding moduli found in isolated bilayers that contain hydrocarbon solvent (WHITE 1976, REQUENA et al 1975) (Table 2).

F_{LP} versus area is not easily fit to either an exponential or an inverse power law, and hence energies cannot be obtained by integration as was done for F_R. Therefore to obtain deformation energies we have measured the areas under the curves by graphical methods. These energies are plotted in figures 27 and 28. Figure 27 shows the energy needed to bring a phospholipid to a given molecular area, while 28 shows the energy required to change A a given amount from its equilibrium value in excess water. To change

the area of a molecule by 7 $\mathring{A}^2$ requires considerably less than 1 kT unit for frozen DPPC. Indeed for all these lipids we can expect relatively large fluctuations in area due to thermal energy.

Table 2

Young's modulus (Y) at equilibrium area

LIPID	Y (dynes / cm^2) (a)
DPPC 25°C	2.5×10^7
DPPC 50°C	2.0×10^7
Egg PE	1×10^8
DPPC/CHOL	9×10^6
Lecithin (b)	3.4×10^5
Lecithin (c)	10^9

(a) Average value at equilibrium area.
(b) (WHITE 1976)
(c) (REQUENA et al 1975)

Figure 18.

Percentage of work done on the system that goes into bilayer deformation versus area ($\AA^2$) for DPPC (25°C), DPPC (50°C), egg PE (25°C) and DPPC/Cholesterol 1:1 (25°C).

Data from equations in Appendix VIII.

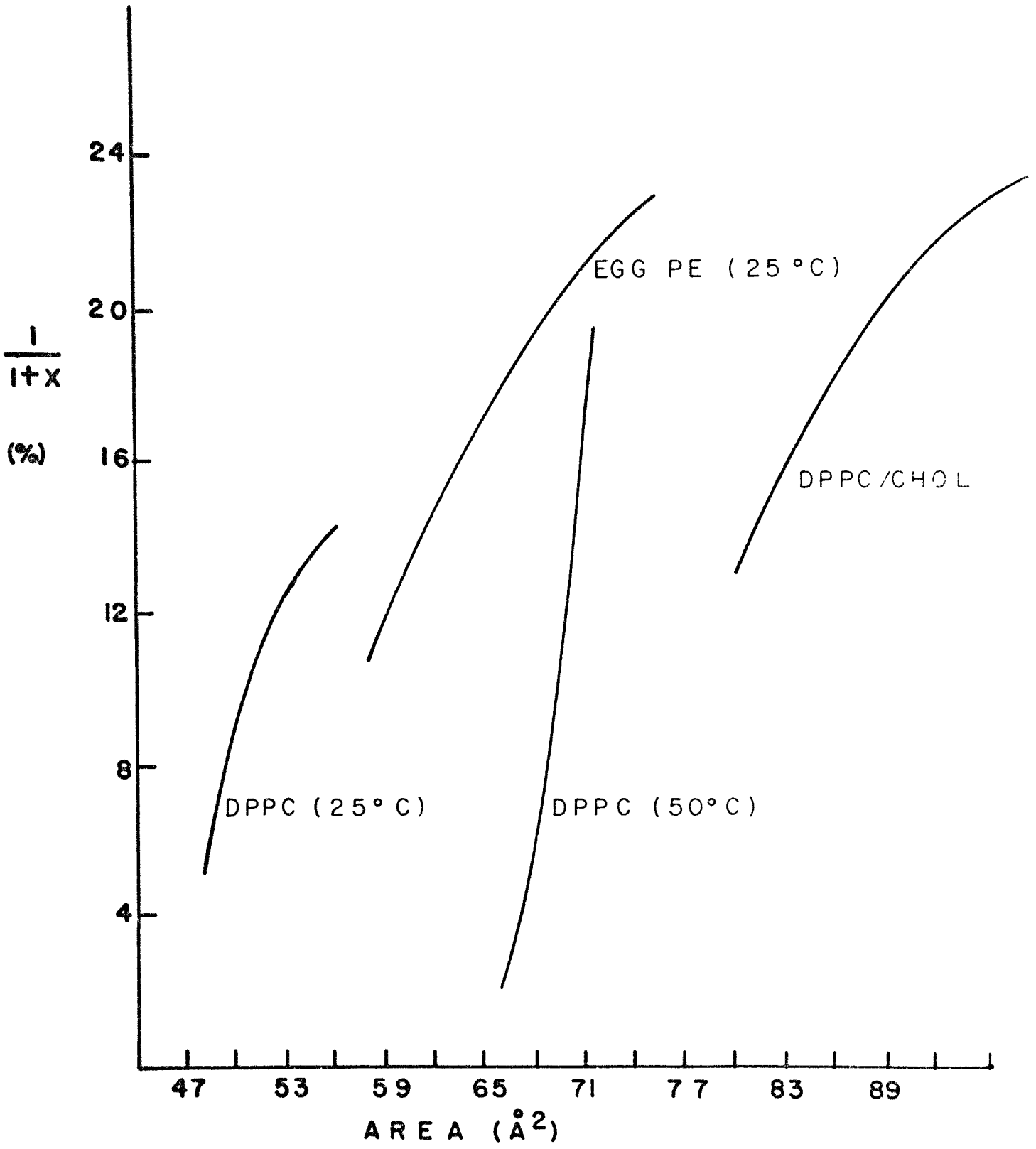
24
20
16
12
8
4
1/1+X
(%)
EGG PE (25°C)
DPPC/CHOL
DPPC (25°C)
DPPC (50°C)
47
53
59
65
71
77
83
89
AREA (Å²)

Figure 19.

Comparison of interbilayer force per molecule F_R (dynes) versus bilayer separation d_w (Å) and intrabilayer force per molecule $F_{d_{pp}}$ (dynes) versus center to center distance between head groups within the bilayer d_{pp} (Å) for DPPC (25°C).

Data from Table V.

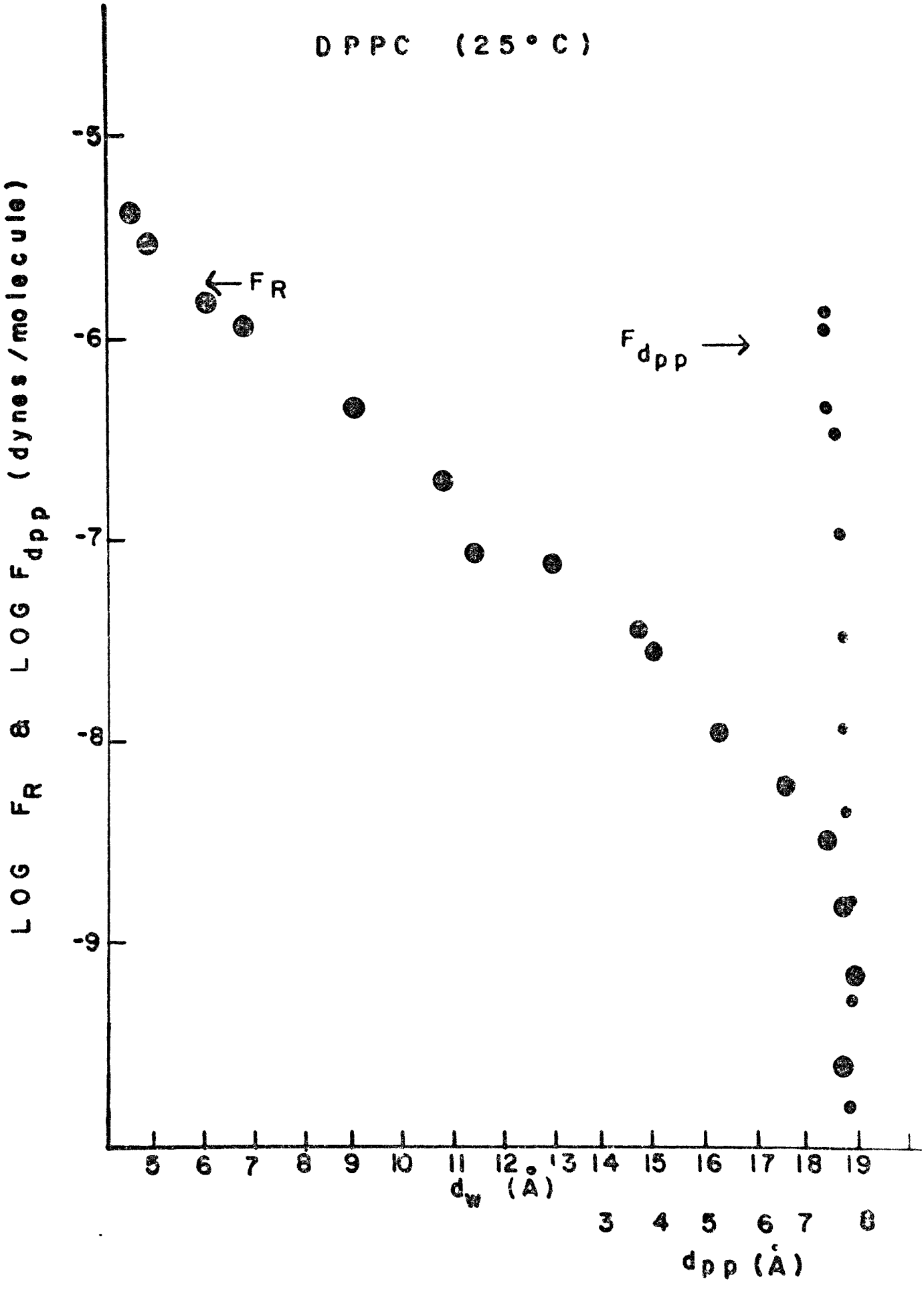
DPPC (25° C)
LOG F_R & LOG F_{dpp} (dynes/molecule)
-5
-6
-7
-8
-9
$\leftarrow F_R$
$F_{dpp} \rightarrow$
5 6 7 8 9 10 11 12 13 14 15 16 17 18 19
d_w (Å)
3 4 5 6 7 8
dpp (Å)

Figure 20.

Lateral pressure F_{LP_2} (dynes / cm) versus cross-sectional area A ($Å^2$) for DPPC (25°C).

Data from Table V.

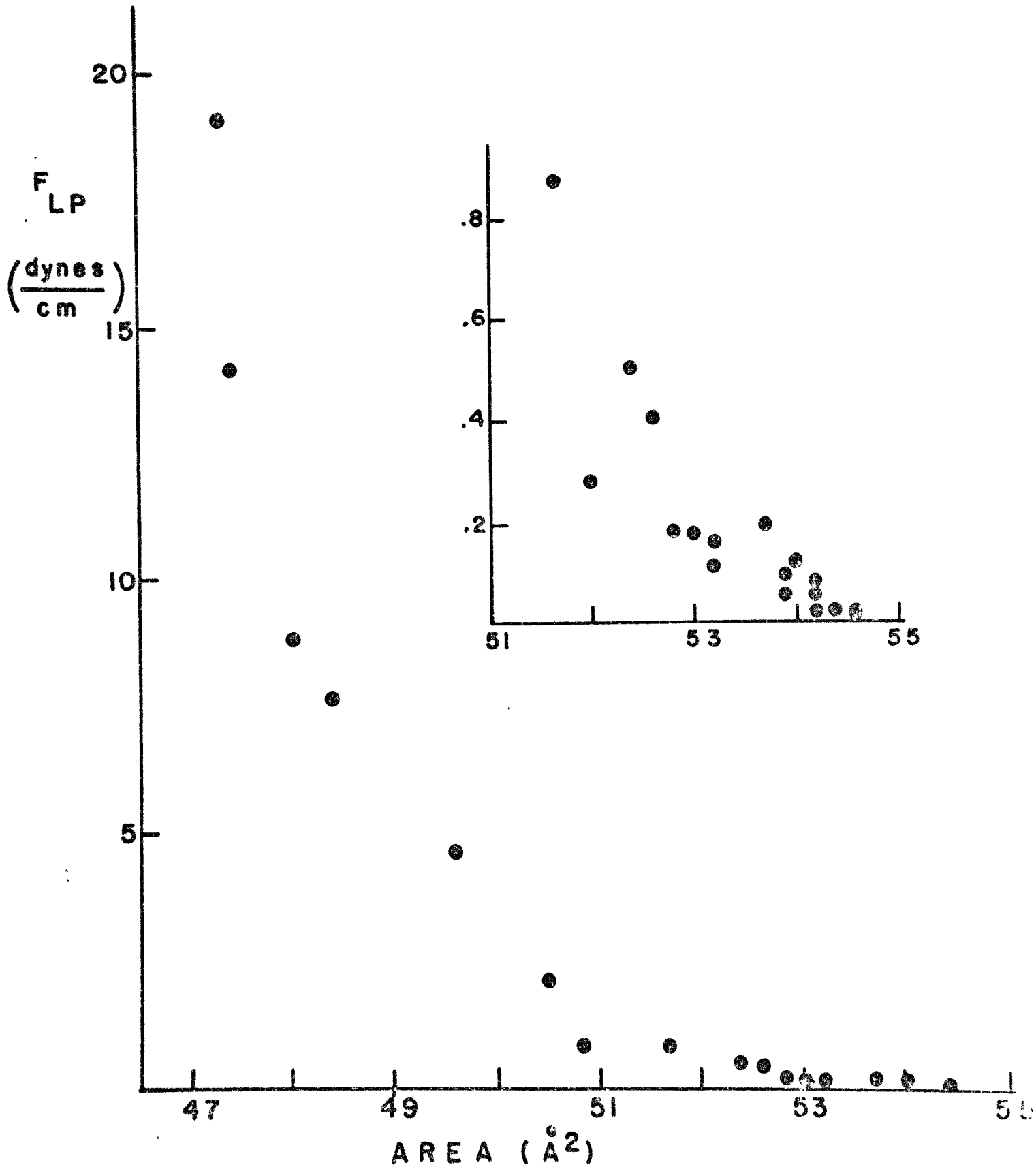
DPPC (25°C)
F LP
(dynes/cm)
20
15
10
5
.8
.6
.4
.2
51
53
55
47
49
51
53
AREA (Å2)

Figure 21.

Lateral pressure F_{LP} (dynes / cm) versus cross-sectional area A ($Å^2$) for DPPC (50°C).

Data from VI.

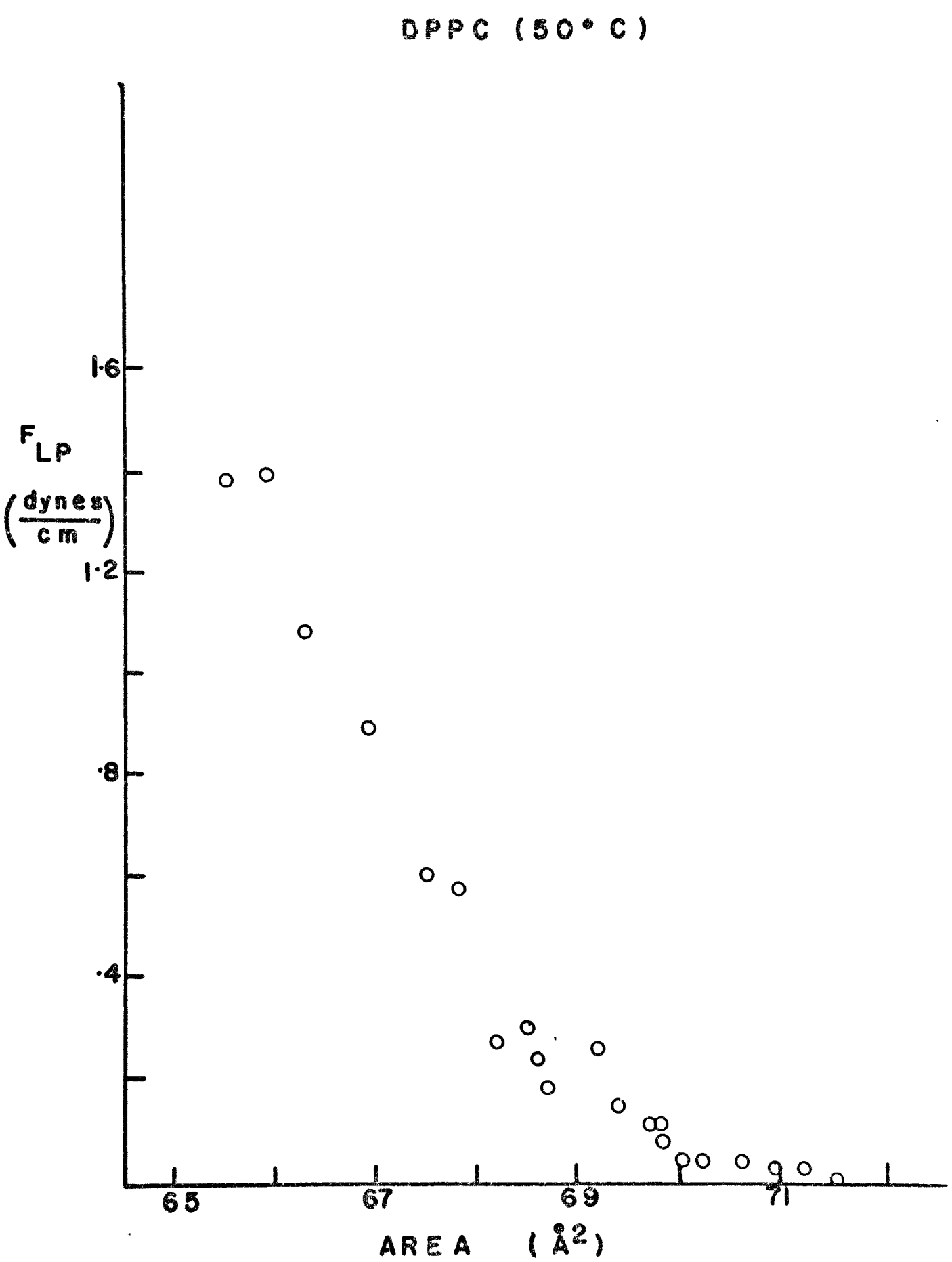
DPPC (50° C)
1·6
1·2
·8
·4
F_{LP}
$\left(\frac{dynes}{cm}\right)$
65
67
69
71
AREA ($Å^2$)

Figure 22.

Lateral pressure F_{LP} (dynes / cm_{ρ})
versus cross-sectional area A ($\AA^2$)
for egg PE (25°C).

Data from Table VII.

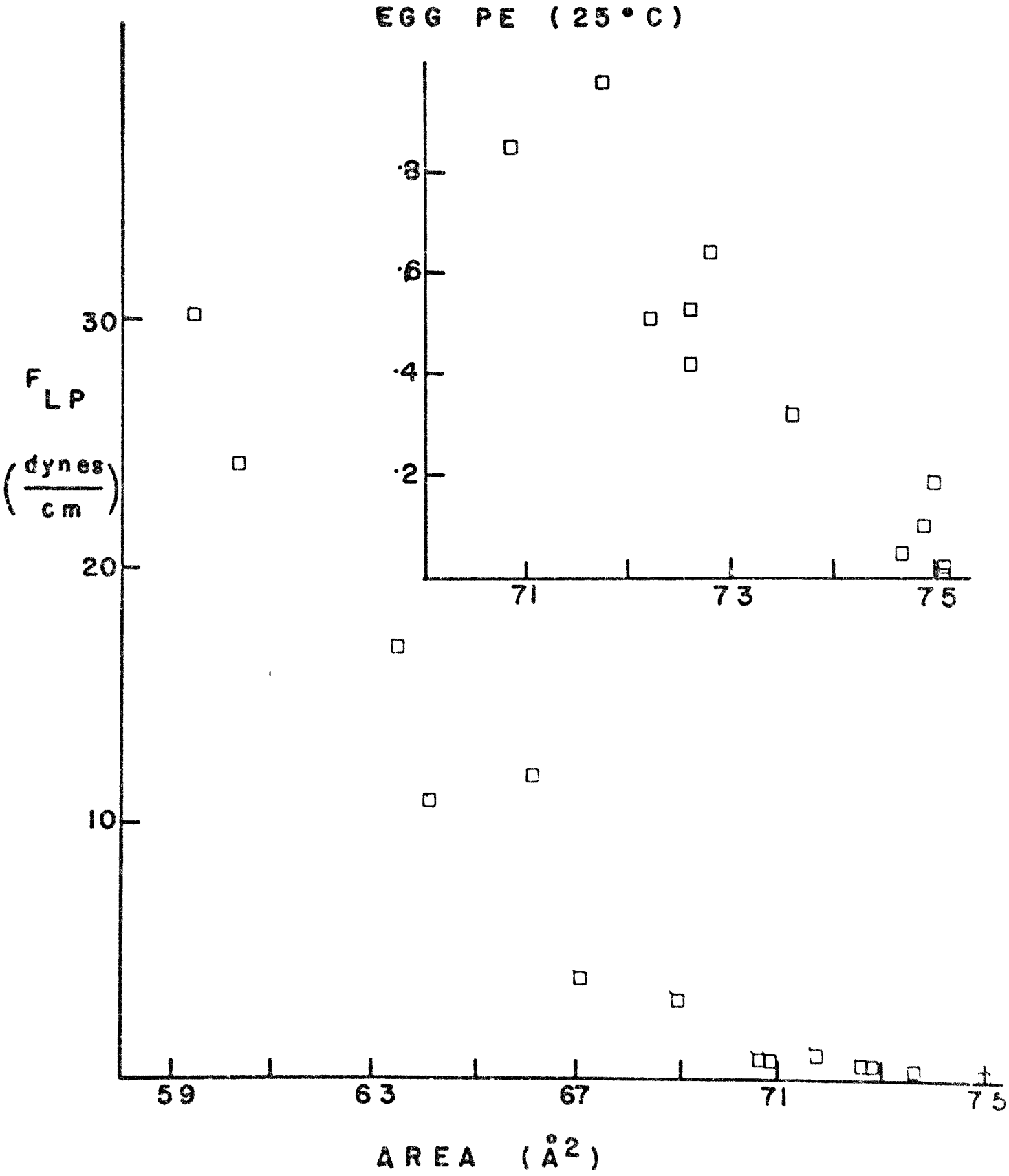
EGG PE (25°C)
F LP
(dynes/cm)
30
20
10
59
63
67
71
75
AREA (Å2)
·8
·6
·4
·2
71
73
75

Figure 23.

Lateral pressure F_{LP} (dynes / cm) versus cross-sectional area A ($Å^2$) for DPPC/Cholesterol 1:1 (25°C).

Data from Table VIII.

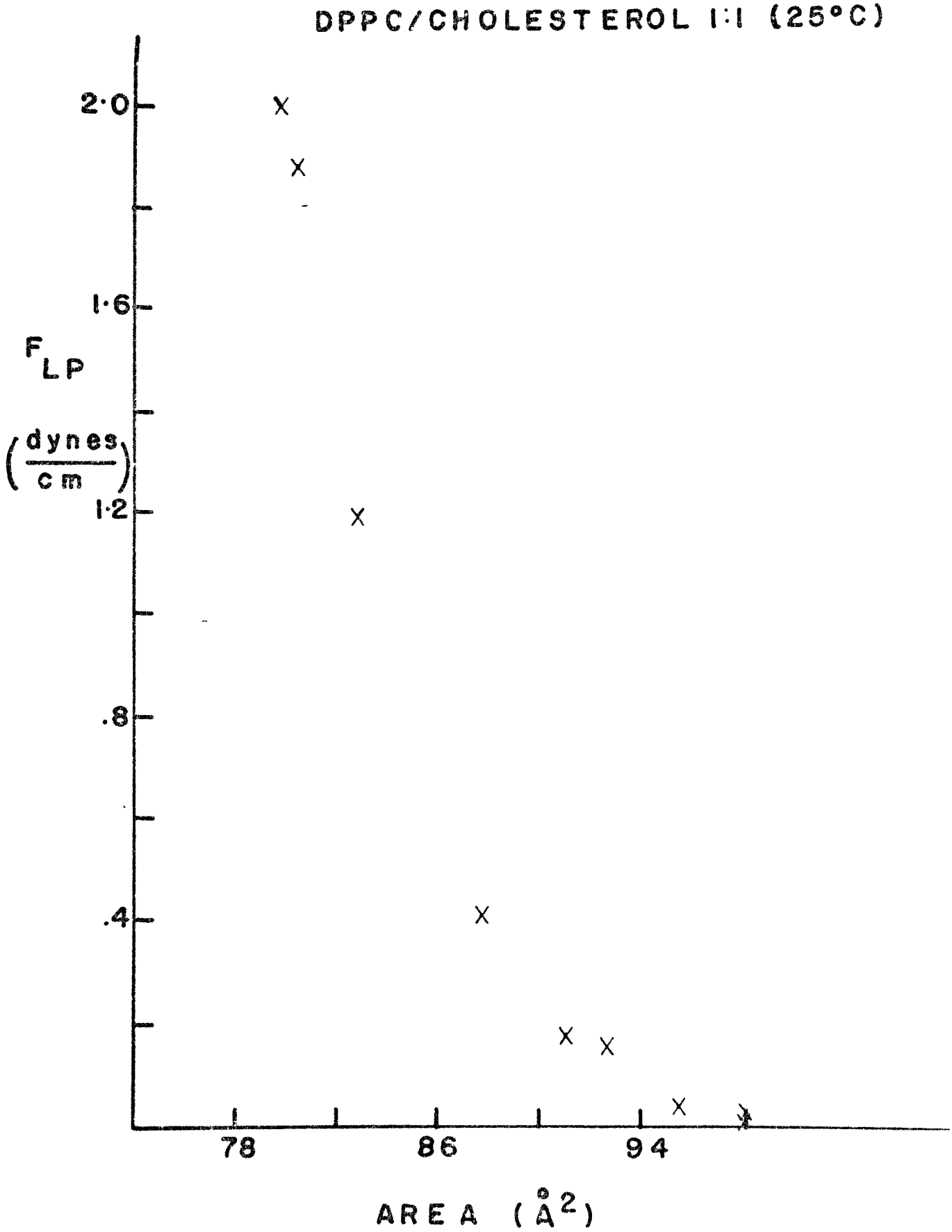
DPPC/CHOLESTEROL 1:1 (25°C)
2·0
1·6
1·2
.8
.4
F_{LP}
$\left(\frac{dynes}{cm}\right)$
78
86
94
AREA ($Å^2$)

Figure 24.

Force per molecule F_{d_1} (dynes) required to change d_1 versus thickness of the bilayer d_1 (Å) for DPPC (25°C).

Data from Table V.

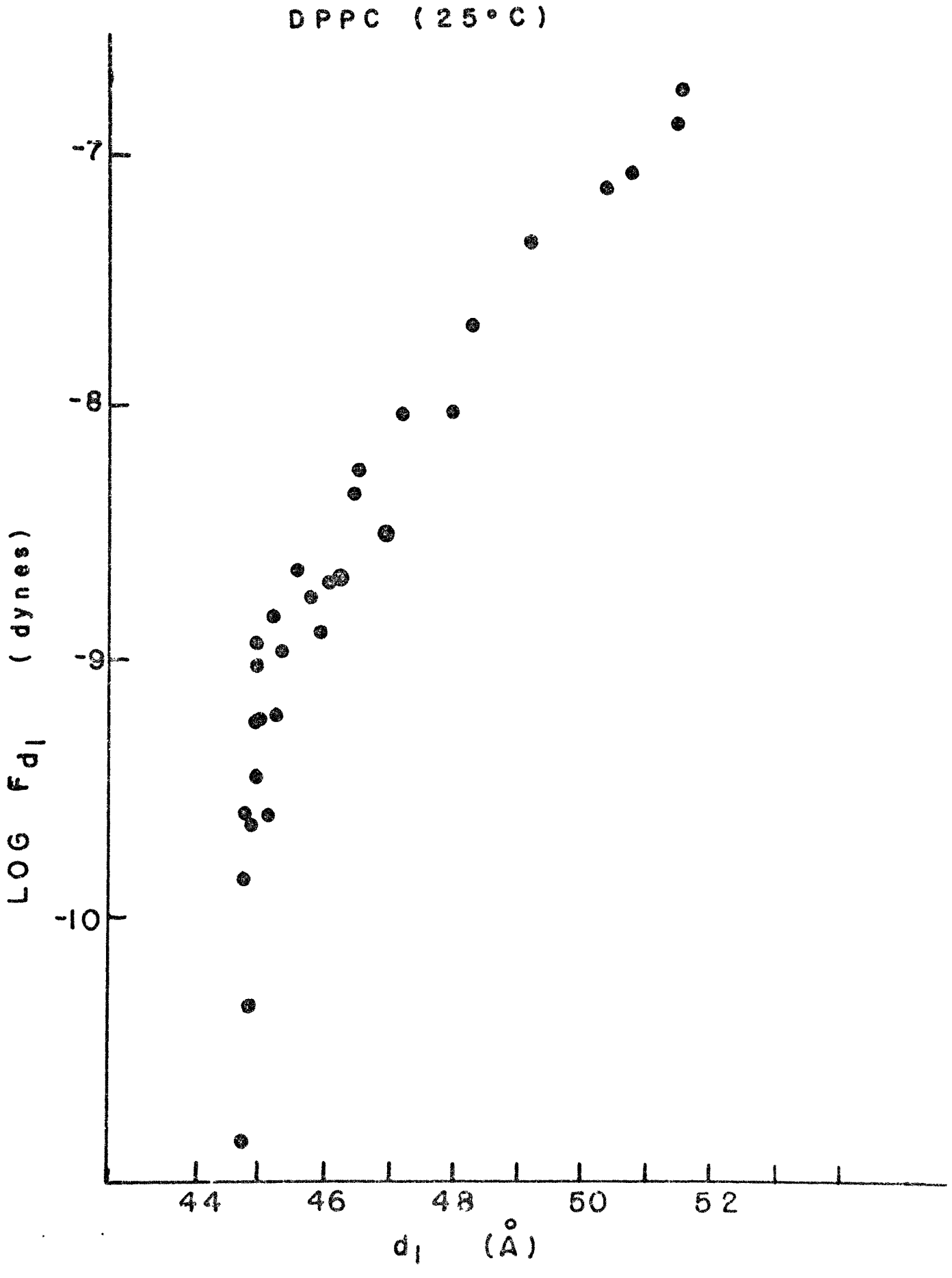
DPPC (25°C)
-7
-8
-9
-10
LOG F_{d_l} (dynes)
44
46
48
50
52
d_l (Å)

Figure 25.

Modulus of deformability Y (dynes / cm^2)
versus cross-sectional area A ($Å^2$)
for DPPC (25°C).

Data from Table X.

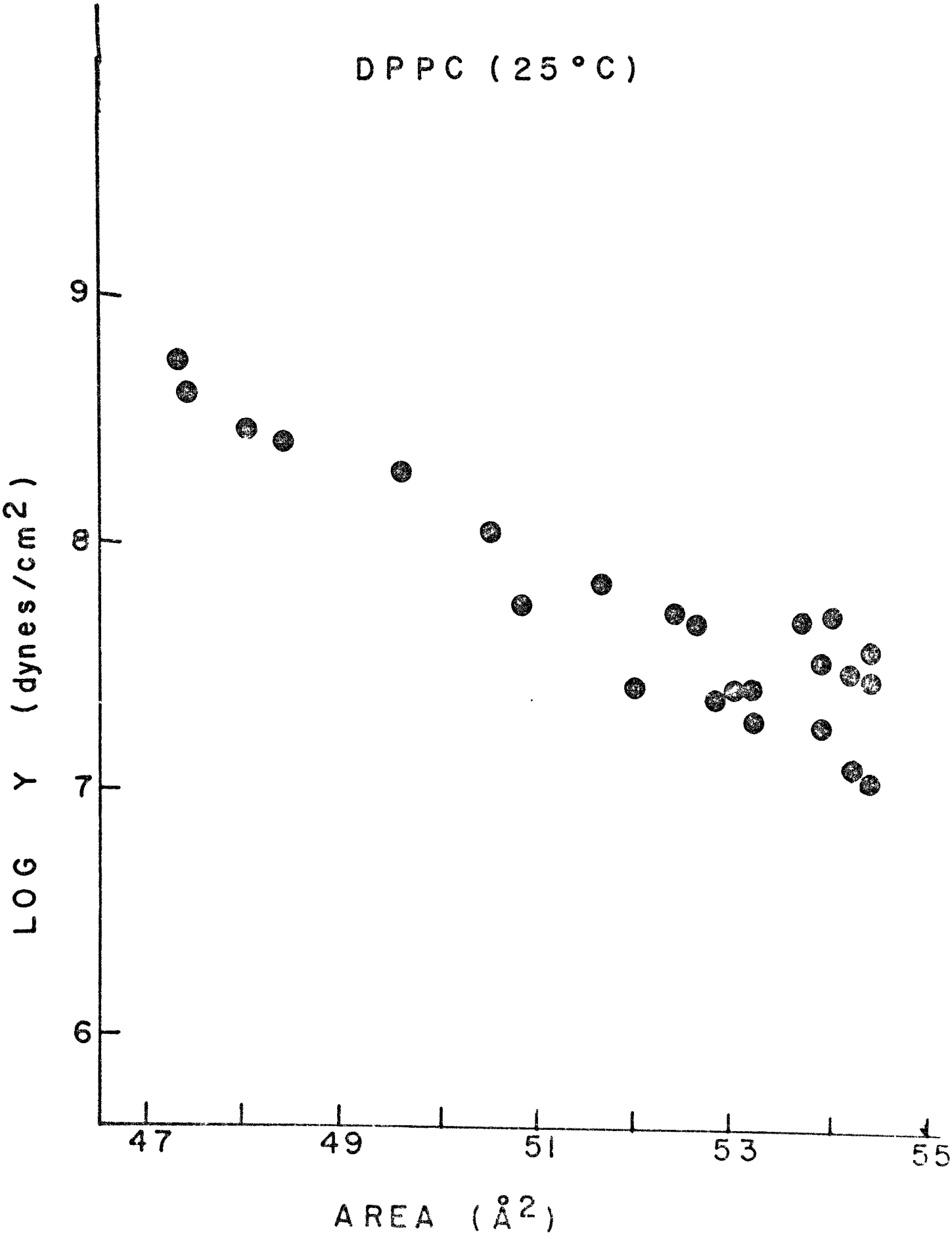
DPPC (25°C)
LOG Y (dynes/cm²)
9
8
7
6
47
49
51
53
55
AREA (Å²)

Figure 26.

Modulus of deformability Y (dynes / cm^2) versus cross-sectional area A ($Å^2$) for DPPC (25°C), DPPC (50°C), egg PE (25°C) and DPPC/CHOL 1:1 (25°C).

Data from Tables X-XIII.

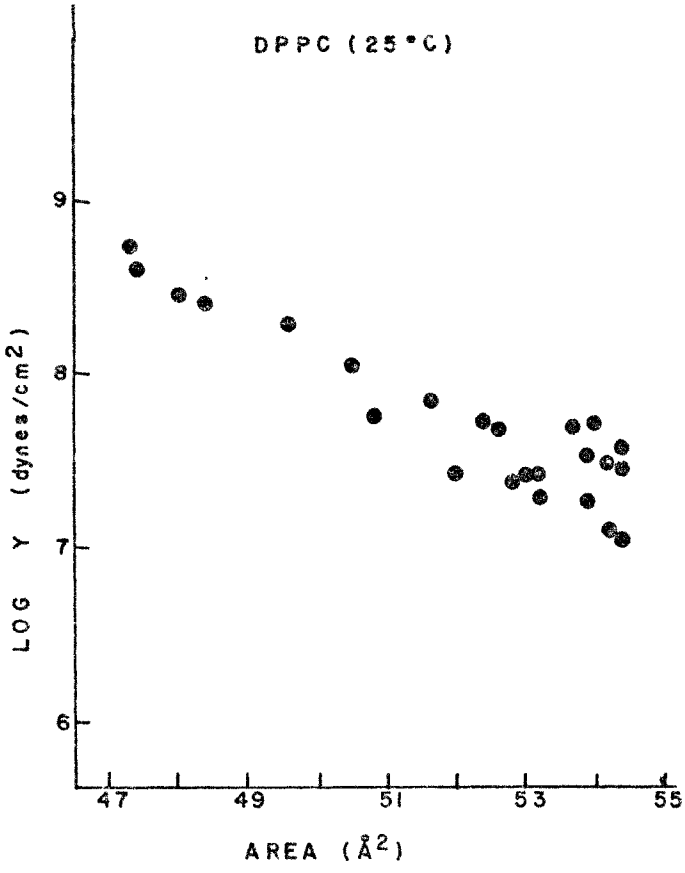
DPPC (25°C)
LOG Y (dynes/cm2)
9
8
7
6
47
49
51
53
55
AREA (Å2)

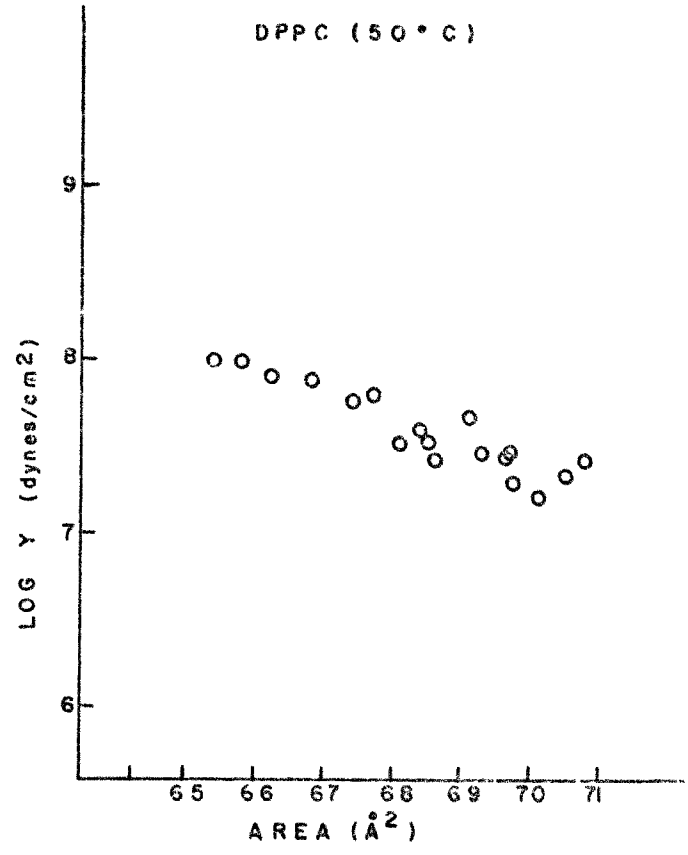
DPPC (50° C)
LOG Y (dynes/cm2)
9
8
7
6
65
66
67
68
69
70
71
AREA (Å2)

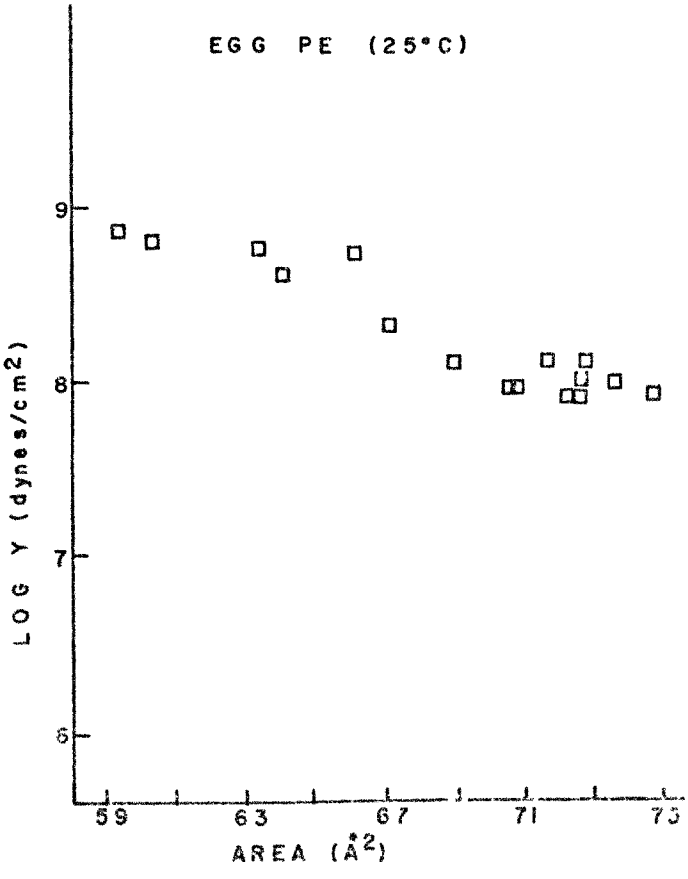
EGG PE (25°C)
LOG Y (dynes/cm2)
9
8
7
6
59
63
67
71
75
AREA (Å2)

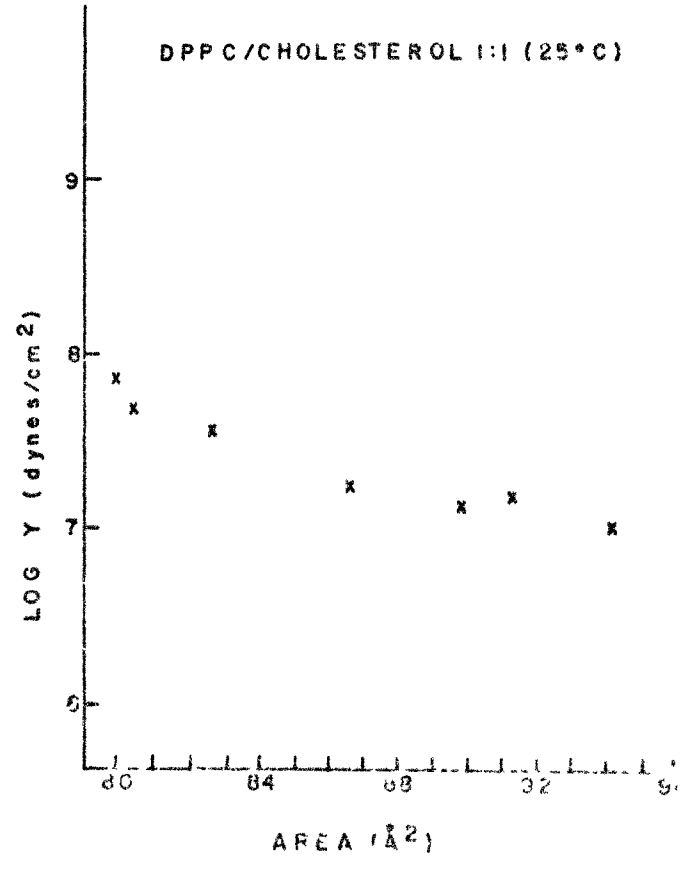
DPPC/CHOLESTEROL 1:1 (25°C)
LOG Y (dynes/cm2)
9
8
7
6
80
84
88
92
AREA (Å2)

Figure 27.

Deformation energy per molecule (kT) versus cross-sectional area A ($Å^2$) for DPPC (25°C), DPPC (50°C), egg PE (25°C) and DPPC/Cholesterol 1:1 (25°C).

Data from Tables XIV-XVII.

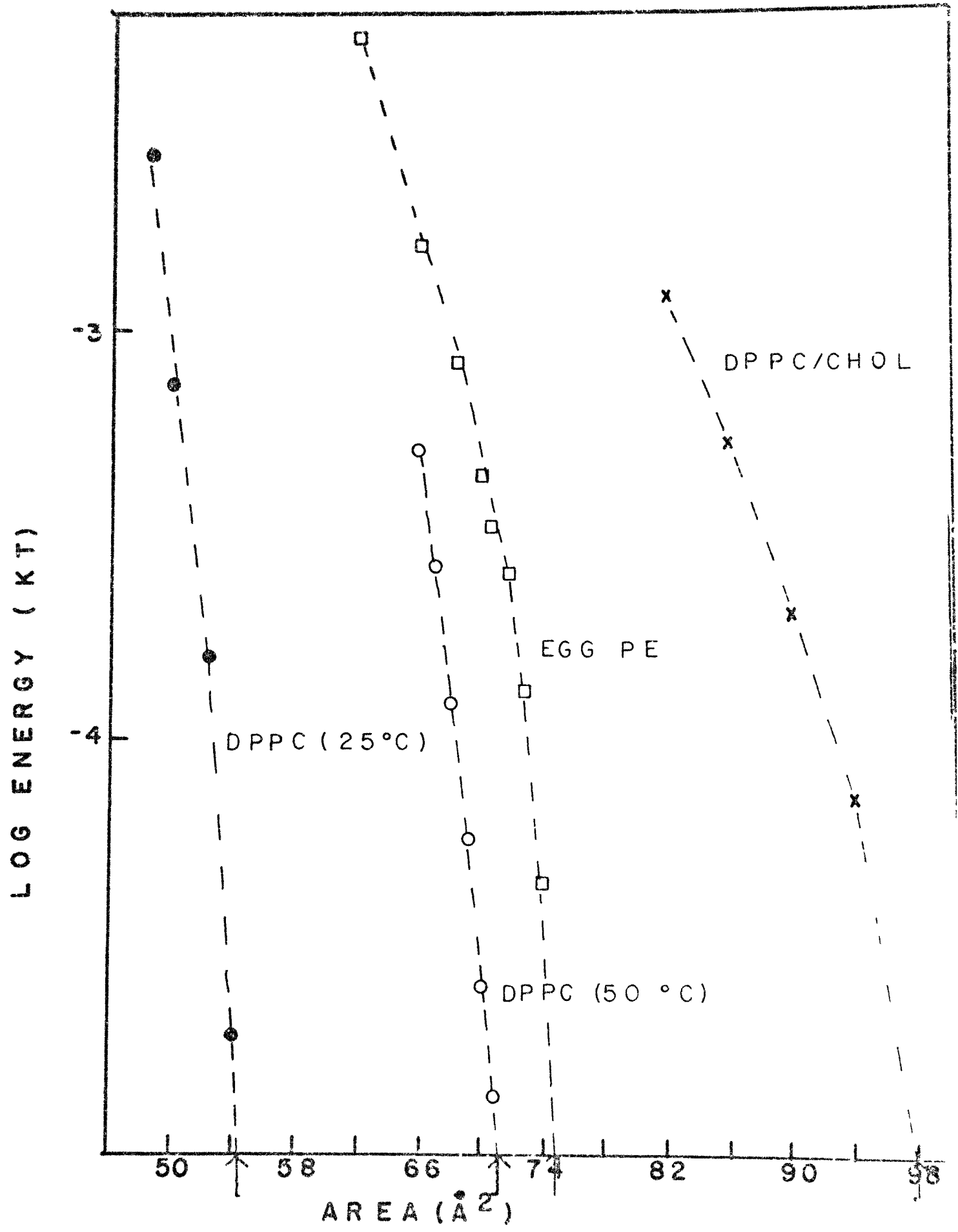
LOG ENERGY (KT)
-3
-4
DPPC/CHOL
EGG PE
DPPC (25°C)
DPPC (50 °C)
50
58
66
74
82
90
98
AREA (Å²)

Figure 28.

Deformation energy per molecule (kT) versus change in cross-sectional area from equilibrium area in water $\triangle A$ ($Å^2$) for DPPC (25°C), DPPC (50°C), egg PE (25°C) and DPPC/Cholesterol 1:1 (25°C).

Data from Tables XIV-XVII.

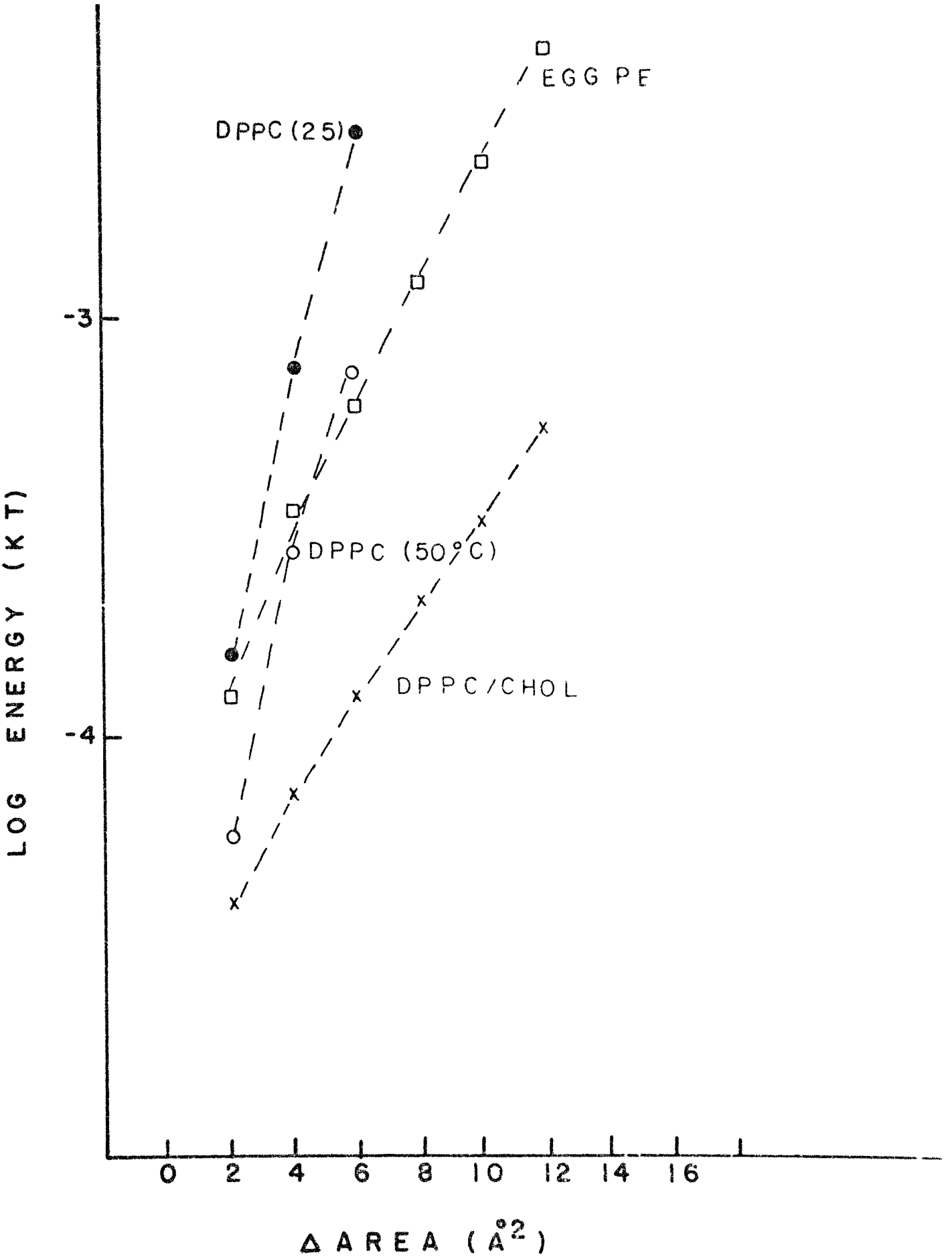
EGG PE
DPPC (25)
DPPC (50°C)
DPPC/CHOL
-3
-4
LOG ENERGY (KT)
0
2
4
6
8
10
12
14
16
Δ AREA (Å²)

GENERAL DISCUSSION

HYDRATION FORCE

The data show that for all the lipids studied here very large repulsive forces must be overcome in order for bilayers of even quite small area to make close approach. These forces are surprisingly large considering that all the lipids are zwitterionic with no net electrical charge. Indeed even in bilayers which are highly charged, electrostatic repulsion (COWLEY et al 1978) would be far outweighed by these hydration forces for small separations. F_H has not been the subject of rigorous theoretical treatment as have other forces which stabilize colloids (VERWEY and OVERBEEK 1948); it has only been described in qualitative terms as "solvation" or "hydration" effects (LENEVEU et al 1976, 1977 BARCLAY and OTEWILL 1970, 1972). It appears to be a new force that must be considered in the context of membrane phenomena.

The curves which describe the hydration forces are different for each lipid (Fig. 15). Evidently, the nature of the polar head group, the conformation of the hydrocarbon chains and the heterogeneity of these chains all have an effect on the hydration force between bilayers.

Table 3 is a summary of parameters pertaining to the hydration force for the lipids studied. Included in the table, for comparative purposes, are data obtained for egg lecithin by techniques identical to those described here (FULLER et al 1978). Comparisons of lipids which differ in these various structural ways is given below.

EFFECTS OF CONFORMATION OF THE HYDROCARBON CHAINS

There appears to be a marked effect of the conformation of the hydrocarbon chains of the lipid molecule upon the hydration forces. The length constant λ characterizes the rate at which the hydration force decreases with bilayer separation. The structural interpretation of these length

Table 3

Hydration Parameters

Lipid	λ	p Values (a)	d_w^o (Å) (b)	H(ergs) ($\times 10^{-14}$) (c)	Energy Δ 2 Å (kT) (d)	Energy Δ 6 Å (kT) (e)
DPPC (25°C)	1.98	.005	19.1	5-7	8.0×10^{-4}	2.5×10^{-3}
DPPC (50°C)	2.57	-	32.8	3-5	1.0×10^{-4}	2.0×10^{-4}
Egg PE	2.14	.005 .01	20.5	30-50	5.0×10^{-3}	2.5×10^{-2}
Egg lecithin	2.62		27.5	5-7	3.5×10^{-4}	5.0×10^{-3}
DPPC/CHOL	3.32		28.3	8-10	3.0×10^{-4}	7.0×10^{-4}

(a) Probability differences calculated using the method of BLISS (1967) (Appendix VI).

(b) Equilibrium separation in water.

(c) London-Hamaker constant (Appendix IV).

(d) Energy needed for a 2 Å change in d_w from equilibrium separation in water.

(e) Energy needed for a 6 Å change in d_w from equilibrium separation in water.

constants is unclear at the present time, however I believe that they are a reflection of water structure between bilayers. PARSEGIAN (1978) has suggested that the mathematics of a statistical comparison of slopes is unclear since scatter is associated with each parameter (ie. with both force and d_w). However standard treatment by the method of BLISS (1967) provides an estimate of significant differences between the λ's for different lipids. The length constant for the frozen DPPC curve is 1.98 which increases to 2.57 for melted DPPC. It can be said, therefore, that because of the small λ for frozen DPPC its hydration force increases more rapidly with decreasing bilayer separation than that of melted DPPC and in fact more rapidly than any of the lipids studied here. This suggests that there is a difference in the way water is structured between the bilayers of melted and frozen DPPC.

When the chains of DPPC are melted the bilayers increase their equilibrium separation in excess water from 19.1 Å to 32.8 Å. The net repulsive force F_R must therefore have increased when the chains melted. Since $F_R = F_H - F_A$, this increase may be due either to a decrease in F_A or to an increase in F_H or both. The attractive forces may be compared by examining the London-Hamaker constant H. There is an error associated with the measurement of H since equilibrium d_w is not known to an accuracy greater than $\pm$ 0.5 Å. A rigorous treatment of van der Waals forces also shows that H is not actually constant; we can, however, expect a change of only 10 % in H with bilayer separation (LENEVEU et al 1977). If we include these expected errors we can see that the range of values of H for melted and frozen DPPC overlap. The large increase in equilibrium separation in excess water from frozen to melted DPPC cannot be accounted for by a change in F_A, even using the extremes in the range for the Hamaker constants, and must therefore be due primarily to an increase in the hydration force F_H.

In order to decrease bilayer separation by either 2 or 6 Å from their

respective equilibrium separation in excess water, it requires less energy for melted DPPC than for frozen DPPC. On the other hand for bilayers to approach to the same separation it would require much more energy for melted DPPC than for frozen DPPC. This increased energy results from the greater hydration forces for melted DPPC.

EFFECT OF HEAD GROUP

Egg PE and egg lecithin are both melted at room temperature and have a heterogeneous and similar chain population (ROUSER et al 1968), but they posses different polar head groups. The length constant is significantly smaller for egg PE and again the interpretation is that the water between the bilayers is structured in different ways for these two phospholipids.

The bilayer separation in excess water is larger for egg lecithin than for egg PE. This larger separation must result from either a greater repulsion between phosphatidylcholine head groups as compared to phosphatidyl-ethanolamine groups, or may reflect a greater van der Waals attraction between egg PE bilayers. Comparison of London-Hamaker constants show that H for egg PE is significantly larger than for egg lecithin. Indeed if egg lecithin had the Hamaker constant of egg PE then the equilibrium separation in excess water would be 19 Å. Alternatively if egg PE had the Hamaker constant of egg lecithin then the attractive and repulsive forces would balance at 26 Å. The decrease in bilayer separation for egg PE could therefore be accounted for by an increase in the attractive forces. This suggests, as indicated previously (LENEVEU et al 1977), that the polar groups make an important contribution to F_A and that a more refined method of extracting coefficients characterzing van der Waals forces may be required.

EFFECT OF HETEROGENEITY OF THE CHAIN POPULATION

Melted DPPC has a homogeneous population of hydrocarbon chains while

that of egg lecithin is heterogeneous. The length constants for these two lipids are the same and this suggests that the water between the bilayers is structured in a similar way and that chain homogeneity does not affect this structure.

In excess water the equilibrium separation for melted DPPC bilayers is greater than for those of egg lecithin. The London-Hamaker constants are, however, indistinguishable and even if the extremes in the range of values for these H's were taken, the difference in equilibrium separations in excess water would not be accounted for by van der Waals forces. Therefore the larger equilibrium d_w for melted DPPC is probably due to an increase in the hydration force (F_H).

EFFECT OF CHOLESTEROL: CHAIN DISORDER BY TEMPERATURE OR CHOLESTEROL

Cholesterol in DPPC bilayers disorders the chains at 25°C and a comparison can be made between melted DPPC and the DPPC/CHOL mixture. The length constant of the DPPC/CHOL mixture is high and shows the lowest rate of change in force with bilayer separation of all the lipids. The water between these mixed lipid bilayers must be structured quite differently than for melted DPPC.

DPPC/CHOL has a smaller equilibrium separation in excess water and a larger H than does melted DPPC. If we assign to melted DPPC the London-Hamaker constant of the DPPC/CHOL mixture then the attractive and repulsive forces would balance at 28.7 Å. Alternatively if the DPPC/CHOL mixture had the H value of melted DPPC then the equilibrium separation in water would be 34.2 Å. Thus the difference in equilibrium separation in water is accounted for by a larger attractive force for DPPC/CHOL.

It requires less energy for melted DPPC than for DPPC/CHOL to change bilayer separation by either 2 or 6 Å from their respective equilibrium separations in excess water. However to bring the bilayers to the same absolute

separation requires more energy for melted DPPC than for DPPC/CHOL, this is a result of the larger attractive forces for the mixed lipid bilayers.

Overall the values for the equilibrium separation in water show two qualitatively different regions for the five lipids studied. Melted DPPC, egg lecithin and DPPC/CHOL have large separations while the equilibrium separations for frozen DPPC and egg PE are smaller. Although there are detectible differences between them, all the melted phosphatidylcholines have large equilibrium spacings, regardless of chain heterogeneity or the presence of cholesterol. When the head group is changed (egg PE) the value for d_w in excess water decreases due to an increase in the attractive force. When the chains of DPPC are frozen, the value for d_w in excess water also decreases, but this time as a result of a decrease in the hydration force.

IMPLICATIONS CONCERNING THESE INTERBILAYER REPULSIVE FORCES

The techniques described in this thesis provide a new method for the study of the microphysical properties of bilayers which may lead to a greater understanding of membrane interactions and structure. However because of the recent nature of these techniques the interpretation of results is made difficult. The large repulsive forces seen for all these lipids inevitably raise questions as to how vesicles and membranes overcome them in order to interact and/or fuse. Some worthwhile further studies might include an examination of the effects on these hydration forces of Ca^{2+}, of glycolipids, and of possible large co-operative electrostatic attraction in a system containing mixed charged lipids.

Since these lipids have very different repulsive energies at identical bilayer separations, it is interesting to ask what might happen in mixed lipid systems. Bulk segregation of lipids in mixed systems have been

reported (UNTRACT and SHIPLEY 1976) but most explanations of this behaviour invoke arguments of chain or head group packing. The results presented here indicate that differences in hydration forces may also play a role in determining when and how phase separations occur. It should be possible to predict a phase separation in mixed lipid bilayers from the repulsive hydration energies of the lipids and the change in entropy needed for this separation.

Different repulsive hydration energies for different lipids may also affect approaching cells. Only a small area of the membrane will experience interaction energies when cells or vesicles approach each other and the rest of the membrane will act as a resevoir into which lipids may freely flow. It can be envisioned that as membranes approach, those lipids which have greater hydration energies at large separations will move away from the interacting regions and into the resevoir. Thus approaching membranes may be able to influence the lipid composition in the opposing membranes.

DEFORMATION FORCE

The curves which describe the forces that deform bilayers (Figs. 20-23) are different for each lipid. Thus it appears that F_{LP} is affected by the same structural differences in the lipid as was F_R. Table 4 tabulates parameters which describe this deformation force. Comparison of lipids is given below.

EFFECT OF CONFORMATION OF THE HYDROCARBON CHAINS

Frozen DPPC was originally studied in the hope that it would be "non-deformable" so that all of the work done on this lamellar phase would go into overcoming F_R. This however was not the case, in fact frozen DPPC is quite deformable (Fig. 20) and has a value for Y at equilibrium area similar to that for melted DPPC. The explanation for this may lie in the fact that at fully swelled equilibrium in water the chains of frozen DPPC are tilted with respect to the plane of the bilayer (TARDIEU et al 1973). As water is removed the chains become progressively more perpendicular rather than being forced more closely together as are the melted chains. It thus requires about the same force to decrease A by changing the angle of tilt of frozen chains as it does to compress the fluid bilayer, near equilibrium. However as the chains become more perpendicular, frozen DPPC becomes less deformable. The rate of increase for Young's modulus is faster for frozen DPPC than for melted DPPC as are the deformation energies required for a change in area from equilibrium. Frozen DPPC is thus less deformable or "stiffer" than melted DPPC when the bilayers are compressed more than about 2 $\mathring{A}^2$ from equilibrium area in water.

EFFECT OF HEAD GROUP

Since egg PE and egg lecithin have similar heterogeneous hydrocarbon chains, the different head groups appear to affect their deformabilities. The value of Young's modulus at equilibrium area is larger for egg PE than for egg lecithin. It also requires greater energy for a 2 or 6 $\mathring{A}^2$

Table 4

Deformation Parameters

Lipid	Y^o (dynes/cm^2) (a)	A^o (Å^2) (b)	Energy Δ 2 Å^2 (kT) (c)	Energy Δ 6 Å^2 (kT) (d)
DPPC (25°C)	1-8 x 10^7	54.6	8.0 x 10^{-4}	1.0 x 10^{-2}
DPPC (50°C)	1-4 x 10^7	71.4	3.0 x 10^{-4}	6.6 x 10^{-3}
Egg PE	0.8-1.3 x 10^8	75.0	1.3 x 10^{-3}	5.9 x 10^{-3}
Egg lecithin	1-8 x 10^6	75.0	1.5 x 10^{-4}	3.7 x 10^{-3}
DPPC/CHOL	1-2 x 10^7	98.0	5.0 x 10^{-4}	1.1 x 10^{-3}

(a) Young's modulus at equilibrium area in water.

(b) Equilibrium area in excess water.

(c) Deformation energy needed for a 2 Å^2 change in area from equilibrium area in excess water.

(d) Deformation energy needed for a 6 Å^2 change in area from equilibrium area in excess water.

change in area from equilibrium for egg PE than for egg lecithin. The bilayers, therefore, become less deformable when the head groups are changed from phosphatidylcholine to phosphatidylethanolamine. Both lipids are able to sustain a large lateral pressure (compared to the other lipids) before the structural transition to crystalline chains occur (25 dynes/cm for egg lecithin, 30 dynes/cm for egg PE).

EFFECT OF HETEROGENEOUS CHAINS

Young's modulus at equilibrium and the deformation energies required for a change of 2 or 6 $Å^2$ in area from equilibrium in water are lower for egg lecithin compared to melted DPPC. Thus bilayers with heterogeneous chains are more deformable than bilayers with homogeneous chains. Melted DPPC can support only a relatively small lateral pressure (1.4 dynes/cm) before the structural transition to crystalline chains occurs.

EFFECT OF CHOLESTEROL

The lateral pressure (F_{LP}) for the DPPC/CHOL mixture is anamalously low for large changes in area (F_{LP} is less than 1 dyne/cm for a 14 $Å^2$ change in A). Both Y and the deformation energies are small and change very slowly as the bilayer is compressed. This effect may result from cholesterol acting as a "spacer" (BROW and SEELIG 1978) which pushes the head groups apart, perhaps disrupting polar group interactions. It is assumed that this behaviour does not result from cholesterol demixing from the bilayer to form a separate amorphous phase. Since cholesterol is very insoluble in water and a separate cholesterol phase that is not detectible by X-ray diffraction has not been reported, I believe this assumption to be valid. This rather surprising effect of cholesterol may have important implications for biological membranes as it provides a way to lower or even modulate surface tension as a membrane's area is changed.

IMPLICATIONS CONCERNING LATERAL PRESSURE

With all these lipids it is possible to force the bilayers to undergo a structural transition. It may in this way be possible to test directly theories concerning phase transitions in bilayers which predict changes of hydrocarbon packing and headgroup organization. These first measurements of deformabilities of bilayers may also produce information regarding the way in which molecules are incorporated into membranes. It may also be possible to test the assumption that two monolayers are a good model of a bilayer, which has been argued by some authors (EVANS and WAUGH 1977).

SUMMARY

1. Large repulsive hydration forces exist between bilayers of all the neutral lipids studied here and would preclude close approach for unpeturbed bilayers.

2. The hydration force is affected by the nature of the head group, the conformation of the acyl chains and the heterogeneity of these chains.

3. Freezing the chains of DPPC reduces the hydration force.

4. Bilayers of egg PE show a greater attractive force compared to egg lecithin.

5. The water between the bilayers lie on a continuum of chemical potentials, each lower than that of bulk water. This supports the view that the water between bilayers cannot be classified as either bound or non-bound.

6. The length constant λ is a measure of water structure between bilayers. The length constants are different for bilayers of frozen DPPC, melted DPPC, egg PE and DPPC/Cholesterol. They are the same for melted DPPC and egg lecithin.

7. The first measurements of the lateral pressure of a bilayer was made using the method of Dr. Parsegian (FULLER et al 1978).

8. Lateral pressure is also affected by the nature of the head group, the conformation of the acyl chains and the heterogeneity of these chains.

9. Introduction of cholesterol into bilayers of DPPC dramatically reduces the lateral pressure.

10. Relatively large fluctuations in the cross-sectional area (A) of a phospholipid within a bilayer can be expected, due to thermal energy.

Appendix I: List of tables corresponding to figures presented in RESULTS.

Figure	Tables
9	I, II, III IV
10	V
11	VI
12	VII
13	VIII
14	V
15	V, VI, VII VIII
16	IX
17	IX
18	Appendix VIII
19	V
20	V
21	VI
22	VII
23	VIII
24	V
25	X
26	X, XI, XII XIII
27	XIV, XV, XVI XVII
28	XIV, XV, XVI XVII

Table I: Variation of the structural parameters d, d_1, d_w and A with weight percent lipid in water for DPPC (25°C) (MW 735).

% Lipid	d (Å)	d_1 (Å)	d_w (Å)	A ($Å^2$)
90.4	57.4	51.9	5.5	47.0
84.9	58.3	49.5	8.8	49.3
80.9	59.5	48.1	11.4	50.7
78.1	60.6	47.3	13.3	51.6
75.5	62.0	46.8	15.2	52.1
71.8	62.1	44.6	17.5	54.7
70.6	63.5	44.8	18.7	54.5
65.3	63.3	-	-	-
60.8	63.0	-	-	-
54.5	63.4	-	-	-
50.2	63.9	-	-	-
49.2	63.6	-	-	-
47.5	64.1	-	-	-
45.5	63.7	-	-	-
41.0	63.5	-	-	-
40.9	63.7	-	-	-
34.4	63.6	-	-	-

Table II: Variation of the structural parameters d, d_1, d_w and A with weight percent lipid in water for DPPC (50°C) (MW 735).

% Lipid	d (Å)	d_1 (Å)	d_w (Å)	A ($Å^2$)
84.9	52.3	44.3	8.0	55.0
80.9	53.5	43.3	10.2	56.3
78.1	53.0	41.4	11.6	58.9
75.5	54.0	40.8	13.2	59.8
71.8	54.2	38.9	15.3	62.7
70.6	54.6	38.5	16.1	63.4
65.9	56.1	37.0	19.1	65.9
61.4	58.4	35.9	22.5	67.9
58.0	61.1	35.4	25.7	68.9
52.1	66.7	34.8	31.9	70.1
49.1	66.9	-	-	-
43.5	67.3	-	-	-
37.0	66.9	-	-	-
30.2	67.1	-	-	-

Table III: Variation of the structural parameters d, d_l, d_w and A with weight percent lipid in water for egg PE (25 C) (MW 727).

% Lipid	d (A)	d_l (A)	d_w (A)	A (A^2)
92.3	47.1	43.5	3.6	55.5
90.3	47.9	43.3	4.6	55.7
85.7	47.6	40.8	6.8	59.1
77.7	48.8	37.9	10.9	63.7
71.6	50.0	35.8	14.2	67.4
65.9	51.0	33.6	17.4	71.8
65.0	51.5	33.5	18.0	72.0
59.8	52.7	-	-	-
50.8	53.1	-	-	-
50.0	53.1	-	-	-
45.0	52.9	-	-	-
30.0	52.8	-	-	-

Table IV: Variation of the structural parameters d, d_l, d_w and A with weight percent lipid in water for DPPC/Cholesterol 1:1 (25 C) (MW 1096).

% Lipid	d (A)	d_l (A)	d_w (A)	A (A^2)
74.6	59.0	44.0	15.0	82.7
65.7	61.5	40.4	21.1	90.1
60.5	63.6	38.5	25.1	94.5
57.2	65.9	37.1	27.8	98.1
50.7	66.1	-	-	-
45.3	65.9	-	-	-
30.1	65.9	-	-	-

Table V: Force measurements for DPPC (25°C).

Log P (dynes / cm^2)	d (Å)	d_1 (Å)	d_w (Å)	A_2 ($Å^2$)	d_{pp} (Å)	F_{d1} (a) (dynes)	F_R (a) (dynes)	F_{LP} (dynes/cm)	F_{dpp} (a) (dynes)
8.93	56.1	51.6	4.5	47.3	7.39	-1.75E-7	4.02E-6	1.91E+1	2.45E-6
8.77	56.3	51.5	4.8	47.4	7.40	-1.30E-7	2.79E-6	1.41E+1	1.81E-6
8.47	56.8	50.8	6.0	48.0	7.45	-8.36E-8	1.41E-6	8.85	1.14E-6
8.35	57.2	50.4	6.8	48.4	7.48	-7.30E-8	1.08E-6	7.61	9.86E-7
8.01	58.3	49.2	9.1	49.6	7.57	-4.69E-8	5.07E-7	4.65	6.10E-7
7.58	59.1	48.3	10.8	50.5	7.64	-2.17E-8	1.94E-7	2.08	2.75E-7
7.19	59.4	48.0	11.4	50.8	7.66	-9.30E-9	7.83E-8	8.78E-1	1.16E-7
7.13	60.2	47.2	13.0	51.7	7.72	-9.60E-9	6.97E-8	8.76E-1	1.17E-7
6.84	61.2	46.5	14.7	52.4	7.78	-5.69E-9	3.60E-8	5.05E-1	6.80E-8
6.74	61.4	46.4	15.0	52.6	7.79	-4.65E-9	2.87E-8	4.10E-1	5.53E-8
6.62	60.7	46.9	13.8	52.0	7.75	-3.16E-9	2.15E-8	2.85E-1	3.83E-8
6.36	61.7	46.2	15.5	52.8	7.81	-2.04E-9	1.22E-8	1.79E-1	2.42E-8
6.35	62.6	45.5	17.1	53.7	7.87	-2.28E-9	1.21E-8	1.93E-1	2.63E-8
6.34	61.8	46.0	15.8	53.0	7.82	-2.00E-9	1.17E-8	1.74E-1	2.36E-8
6.28	62.1	45.8	16.3	53.2	7.84	-1.82E-9	1.02E-8	1.57E-1	2.13E-8
6.16	62.8	45.2	17.6	54.0	7.90	-1.50E-9	7.73E-9	1.26E-1	1.72E-8
6.13	62.0	45.9	16.1	53.2	7.83	-1.27E-9	7.25E-9	1.09E-1	1.48E-8
6.05	63.4	44.9	18.5	54.3	7.92	-1.24E-9	6.05E-9	1.03E-1	1.41E-8
6.03	62.9	45.3	17.6	53.9	7.89	-1.13E-9	5.84E-9	9.53E-2	1.30E-8
5.94	63.4	44.9	18.5	54.4	7.92	-9.85E-10	4.78E-9	8.13E-2	1.11E-8
5.76	62.8	45.2	17.6	53.9	7.89	-6.03E-10	3.10E-9	5.06E-2	6.92E-9
5.73	63.3	45.0	18.3	54.2	7.91	-5.98E-10	2.94E-9	4.97E-2	6.81E-9
5.52	63.5	44.9	18.6	54.4	7.93	-3,73E-10	1.80E-9	3.07E-2	4.22E-9
5.42	63.6	44.8	18.8	54.4	7.93	-5.95E-10	1.41E-9	2.44E-2	3.35E-9
5.37	63.2	45.1	18.1	54.2	7.91	-2.56E-10	1.27E-9	2.13E-2	2.92E-9
5.34	63.6	44.7	18.9	54.6	7.94	-2.52E-10	1.19E-9	2.06E-2	2.84E-9
5.31	63.7	44.8	18.9	54.4	7.93	-2.34E-10	1.11E-9	1.92E-2	2.65E-9
5.08	63.7	44.7	19.0	54.6	7.94	-1.40E-10	6.59E-10	1.14E-2	1.57E-9
4.62	63.6	44.8	18.8	54.5	7.93	-4.76E-11	2.27E-10	3.91E-3	5.38E-10
4.08	63.8	44.7	19.1	54.4	7.92	-1.41E-11	6.60E-11	1.16E-3	1.59E-10

(a) Force acting on one phospholipid molecule. E-x = 10^{-x}

Table VI: Force measurements for DPPC (50°C).

Log P (dynes / cm^2)	d (Å)	d_{l1} (Å)	d_w (Å)	$A_{Å^2}$ ($Å^2$)	d_{pp} (Å)	F_{d1} (a) (dynes)	F_R (a) (dynes)	F_{LP} (dynes/cm)	F_{dpp} (a) (dynes)
7.16	56.4	37.2	19.2	65.5	8.69	-2.44E-8	9.46E-8	1.38	2.08E-7
7.15	56.8	37.0	19.8	65.9	8.73	-2.49E-8	9.03E-8	1.39	2.11E-7
7.03	57.1	36.8	20.3	66.3	8.75	-1.94E-8	7.05E-8	1.08	1.63E-7
6.93	57.5	36.4	21.1	66.9	8.79	-1.65E-8	5.69E-8	8.97E-1	1.36E-7
6.74	58.1	36.2	21.9	67.5	8.83	-1.11E-8	3.69E-8	5.98E-1	9.16E-8
6.68	58.3	35.9	22.4	67.8	8.85	-1.08E-8	3.70E-8	5.74E-1	9.39E-8
6.40	59.1	35.6	23.5	68.5	8.89	-5.71E-9	1.73E-8	2.97E-1	4.57E-8
6.37	58.8	35.8	23.0	68.2	8.87	-5.15E-9	1.60E-8	2.70E-1	4.16E-8
6.32	60.0	35.2	24.8	69.2	8.94	-5.14E-9	1.45E-8	2.61E-1	4.04E-8
6.31	59.2	35.5	23.7	68.6	8.90	-4.71E-9	1.41E-8	2.44E-1	3.76E-8
6.18	59.4	35.5	23.9	68.7	8.91	-3.52E-9	1.04E-8	1.82E-1	2.81E-8
6.09	60.3	35.1	25.2	69.4	8.95	-3.10E-9	8.63E-9	1.56E-1	2.43E-8
6.07	60.3	35.2	25.1	69.4	8.95	-2.94E-9	8.24E-9	1.49E-1	2.31E-8
5.98	61.0	35.0	25.9	69.7	8.97	-2.46E-9	6.65E-9	1.23E-1	1.92E-8
5.96	60.9	34.9	26.0	69.8	8.98	-2.37E-9	6.36E-9	1.18E-1	1.84E-8
5.96	60.8	35.0	25.8	69.7	8.97	-2.33E-9	6.32E-9	1.17E-1	1.81E-8
5.94	60.9	35.0	25.9	69.7	8.97	-2.26E-9	6.12E-9	1.13E-1	1.76E-8
5.79	61.0	35.0	26.0	69.8	8.98	-1.60E-9	4.32E-9	8.05E-2	1.25E-8
5.55	61.4	34.8	26.6	70.0	8.99	-9.60E-10	2.51E-9	4.77E-2	7.43E-9
5.55	61.7	34.7	27.0	70.2	9.00	-9.69E-10	2.49E-9	4.79E-2	7.46E-9
5.49	62.9	34.5	28.4	70.6	9.03	-8.98E-10	2.18E-9	4.38E-2	6.88E-9
5.37	63.7	34.4	29.3	70.9	9.05	-7.12E-10	1.67E-9	3.45E-2	5.42E-9
5.34	64.8	34.3	30.5	71.2	9.06	-6.92E-10	1.55E-9	3.33E-2	5.23E-9
5.27	65.3	34.2	31.1	71.3	9.07	-6.02E-10	1.32E-9	2.88E-2	4.53E-9
5.22	65.3	34.2	31.1	71.3	9.07	-5.44E-10	1.19E-9	2.61E-2	4.10E-9
5.21	65.6	34.2	31.4	71.3	9.07	-5.27E-10	1.14E-9	2.52E-2	3.97E-9
4.93	66.6	34.2	32.4	71.4	9.08	-2.87E-10	6.08E-10	1.38E-2	2.17E-9
4.71	67.0	34.2	32.8	71.4	9.08	-1.75E-10	3.66E-10	8.41E-3	1.32E-9

(a) Force acting on one phospholipid molecule. $E\text{-}x = 10^{-x}$

Table VII: Force measurement for egg PE (25°C).

Log P (dynes / cm^2)	d (Å)	d_1 (Å)	d_w (Å)	A ($Å^2$)	d_{pp} (Å)	F_{d1} (a) (dynes)	F_R (a) (dynes)	F_{LP} (dynes/cm)	F_{dpp} (a) (dynes)
8.93	47.7	40.6	7.1	59.4	8.28	-4.42E-7	5.05E-6	3.02E+1	4.33E-6
8.79	47.9	40.0	7.9	60.3	8.34	-3.67E-7	3.71E-6	2.43E+1	3.51E-6
8.52	48.4	38.1	10.3	63.4	8.55	-2.83E-7	2.09E-6	1.70E+1	2.52E-6
8.31	48.5	37.7	10.8	64.1	8.60	-1.87E-7	1.30E-6	1.10E+1	1.64E-6
8.27	49.2	36.5	12.7	66.2	8.74	-2.14E-7	1.23E-6	1.18E+1	1.79E-6
7.79	49.3	36.2	13.1	67.1	8.80	-5.49E-8	4.13E-7	4.03	6.15E-7
7.61	50.1	35.0	15.1	69.0	8.92	-6.06E-8	2.81E-7	3.07	4.75E-7
7.10	50.3	34.8	15.5	71.7	9.10	-2.01E-8	9.02E-8	9.75E-1	1.53E-7
7.03	50.6	34.2	16.4	70.6	9.03	-1.81E-8	7.56E-8	8.78E-1	1.37E-7
7.01	50.7	34.1	16.6	70.8	9.04	-1.76E-8	7.24E-8	8.49E-1	1.32E-7
6.85	51.4	33.2	18.2	72.8	9.16	-1.41E-8	5.15E-8	6.44E-1	1.02E-7
6.77	51.4	33.3	18.1	72.6	9.16	-1.16E-8	4.27E-8	5.32E-1	8.45E-8
6.76	51.3	33.5	17.8	72.2	9.13	-1.10E-8	4.15E-8	5.12E-1	8.09E-8
6.67	51.4	33.3	18.1	72.6	9.16	-9.22E-9	3.39E-8	4.23E-1	6.71E-8
6.54	51.7	32.8	18.9	73.6	9.22	-7.35E-9	2.55E-8	3.27E-1	5.23E-8
6.29	52.1	32.5	19.6	75.0	9.30	-4.40E-9	1.41E-8	1.91E-1	3.07E-8
6.01	52.5	32.3	20.2	74.9	9.30	-2.40E-9	7.66E-9	1.03E-1	1.67E-8
5.74	52.2	32.3	19.9	74.7	9.29	-1.26E-9	4.10E-9	5.46E-2	8.79E-9
5.29	52.8	32.3	20.5	75.1	9.31	-4.66E-10	1.46E-9	1.99E-2	3.22E-9
4.76	52.8	32.3	20.5	75.1	9.31	-1.37E-10	4.32E-10	5.89E-3	9.51E-10

(a) Force acting on one phospholipid molecule. E-x = 10^{-x}

Table VIII: Force measurements for DPPC/Cholesterol 1:1 (25°C).

Log P (dynes / cm^2)	d (Å)	d_1 (Å)	d_w (Å)	A ($Å^2$)	d_{pp} (Å)	F_{d1} (a) (dynes)	F_R (a) (dynes)	F_{LP} (dynes/cm)	$F_{d_{pp}}$ (a) (dynes)
7.52	57.7	45.6	12.1	79.8	9.59	-3.50E-8	2.64E-7	2.00	3.32E-7
7.47	57.9	45.2	12.7	80.5	9.64	-3.33E-8	2.37E-7	1.87	3.12E-7
7.20	58.9	43.8	14.9	82.9	9.78	-2.23E-8	1.31E-7	1.18	2.00E-7
6.65	60.2	41.9	18.3	86.8	10.0	-8.46E-9	3.87E-8	4.08E-1	7.08E-8
6.20	62.0	39.9	22.1	91.0	10.2	-3.99E-9	1.44E-8	1.75E-1	3.10E-8
6.13	62.6	39.2	23.4	92.5	10.3	-3.68E-9	1.23E-8	1.56E-1	2.79E-8
5.55	64.2	38.1	26.2	95.4	10.5	-1.17E-9	3.42E-9	4.70E-2	8.54E-9
5.29	66.1	37.7	28.4	98.0	10.6	-7.44E-10	1.91E-9	2.81E-2	5.19E-9
4.38	66.0	37.7	28.3	98.1	10.6	-9.16E-11	2.35E-10	3.46E-3	6.38E-10

(a) Force acting on one phospholipid molecule. E-x = 10^{-x}

Table IX: Repulsive interbilayer energies for DPPC (25°C), DPPC (50°C), egg PE (25°C) and DPPC/Cholesterol 1:1 (25°C).

	Energy (ergs)			
d_w (Å)	DPPC (25°C) (a)	DPPC (50°C) (b)	Egg PE (c)	DPPC/Chol (d)
4	1.02E-13	-	-	-
6	3.68E-14	-	3.61E-13	-
8	1.31E-14	-	1.38E-13	-
10	4.49E-15	-	5.20E-14	-
12	1.46E-15	-	1.87E-14	8.54E-15
14	4.21E-16	-	6.28E-15	4.45E-15
16	9.15E-17	-	1.80E-15	2.27E-15
18	7.06E-18	3.59E-15	3.47E-16	1.11E-15
20	-	1.59E-15	9.08E-18	5.12E-16
22	-	6.91E-16	-	2.13E-16
24	-	2.87E-16	-	7.32E-17
26	-	1.11E-16	-	1.57E-17
28	-	3.67E-17	-	2.00E-19
30	-	8.58E-18	-	-
32	-	4.87E-19	-	-

(a) Obtained by integrating from 19.1. $\int_{19.1}^{\infty} 4.07 \times 10^{-5} \exp(-d_w/1.98) - (1.87 \times 10^{-5}/d_w^3) \times 10^{-8}$

(b) Obtained by integrating from 32.8. $\int_{32.8}^{\infty} 1.63 \times 10^{-4} \exp(-d_w/2.57) - (1.64 \times 10^{-5}/d_w^3) \times 10^{-8}$

(c) Obtained by integrating from 20.5. $\int_{20.5}^{\infty} 2.96 \times 10^{-4} \exp(-d_w/2.14) - (1.75 \times 10^{-4}/d_w^3) \times 10^{-8}$

(d) Obtained by integrating from 28.3. $\int_{28.3}^{\infty} 1.12 \times 10^{-5} \exp(-d_w/3.32) - (5.07 \times 10^{-5}/d_w^3) \times 10^{-8}$

Table X: Modulus of deformability (Y) for DPPC (25°C).

A (Å^2)	Δ A (Å^2)	Y (dynes/Å^2)	Log Y (dynes/cm^2)
47.3	7.3	5.53E-8	8.74
47.4	7.2	4.15E-8	8.62
48.0	6.6	2.88E-8	8.46
48.4	6.2	2.65E-8	8.42
49.6	5.0	2.06E-8	8.31
50.5	4.1	1.14E-8	8.06
50.8	3.8	5.20E-9	7.72
51.7	2.9	7.02E-9	7.85
52.0	2.6	2.50E-9	7.40
52.4	2.2	5.37E-9	7.72
52.6	2.0	4.84E-9	7.68
52.8	1.8	2.38E-9	7.36
53.0	1.6	2.66E-9	7.41
53.2	1.4	2.65E-9	7.41
53.2	1.4	1.82E-9	7.26
53.7	0.9	4.95E-9	7.69
53.9	0.7	1.77E-9	7.23
53.9	0.7	3.31E-9	7.52
54.0	0.6	5.06E-9	7.70
54.2	0.4	1.22E-9	7.08
54.2	0.4	3.00E-9	7.48
54.3	0.3	8.31E-9	7.92
54.4	0.2	2.97E-9	7.46
54.4	0.2	3.74E-9	7.57
54.4	0.2	9.89E-10	6.99

Table XI: Modulus of deformability (Y) for DPPC (50°C).

A ($Å^2$)	ΔA ($Å^2$)	Y (dynes/$Å^2$)	Log Y (dynes/cm^2)
65.5	5.9	8.9E-9	7.95
65.9	5.5	9.7E-9	7.99
66.3	5.1	8.2E-9	7.91
66.9	4.5	7.8E-9	7.89
67.5	3.9	6.0E-9	7.78
67.8	3.6	6.3E-9	7.80
68.2	3.2	3.3E-9	7.52
68.5	2.9	4.1E-9	7.61
68.6	2.8	3.5E-9	7.54
68.7	2.7	2.7E-9	7.43
69.2	2.2	4.8E-9	7.68
69.4	2.0	3.1E-9	7.49
69.4	2.0	3.0E-9	7.48
69.7	1.7	2.9E-9	7.46
69.7	1.7	2.8E-9	7.45
69.7	1.7	2.7E-9	7.43
69.8	1.6	3.0E-9	7.48
69.8	1.6	2.0E-9	7.30
70.0	1.4	1.3E-9	7.11
70.2	1.2	1.6E-9	7.20
70.6	0.8	2.2E-9	7.34
70.9	0.5	2.8E-9	7.45

Table XII: Modulus of deformability (Y) for egg PE (25°C).

A (Å^2)	ΔA (Å^2)	Y (dynes/Å^2)	Log Y (dynes/cm^2)
59.4	15.6	7.15E-8	8.85
60.3	14.7	6.19E-8	8.79
63.4	11.6	5.77E-8	8.76
64.1	10.9	4.01E-8	8.60
66.2	8.80	5.51E-8	8.74
67.1	7.90	2.11E-8	8.32
69.0	6.0	1.27E-8	8.10
70.6	4.4	8.75E-9	7.94
70.8	4.2	8.89E-9	7.94
71.2	3.80	1.27E-8	8.10
72.2	2.8	8.11E-9	7.91
72.6	2.4	9.97E-9	8.00
72.6	2.4	7.93E-9	7.90
72.8	2.2	1.37E-8	8.11
73.6	1.4	1.00E-8	8.00
74.7	0.3	8.42E-9	7.92

Table XIII: Modulus of deformability (Y) for DPPC/Cholesterol 1:1 (25°C).

A (Å^2)	ΔA (Å^2)	Y (dynes/Å^2)	Log Y (dynes/cm^2)
79.8	18.2	6.7E-9	7.83
80.5	17.5	4.6E-9	7.66
82.9	15.1	3.5E-9	7.54
86.8	11.2	1.7E-9	7.23
91.0	7.0	1.2E-9	7.08
92.5	5.5	1.4E-9	7.15
95.4	2.60	9.3E-10	6.97

Table XIV: Energy of deformation for DPPC (25°C).

A (Å^2)	Energy (ergs)(a)	Energy (kT)(a)
54	7.97E-18	1.94E-4
53	2.57E-17	6.27E-4
52	6.25E-17	1.52E-3
51	1.41E-16	3.44E-3
50	3.00E-16	7.32E-3
49	6.13E-16	1.51E-2
48	1.10E-15	2.68E-2
47.5	1.72E-15	4.20E-2

(a) Energy per molecule obtained graphically from Fig. 20.

Table XV: Energy of deformation for DPPC (50°C).

A (Å^2)	Energy (ergs)(b)	Energy (kT)(b)
71	5.92E-18	1.44E-4
70	9.96E-18	2.43E-4
69	2.33E-17	5.68E-4
68	5.29E-17	1.29E-3
67	1.10E-16	2.68E-3
66	2.09E-16	5.10E-3
65.5	2.73E-16	6.66E-3

(b) Energy per molecule obtained graphically from Fig. 21.

Table XVI: Energy of deformation for egg PE (25°C).

A (Å^2)	Energy (ergs) (a)	Energy (kT) (a)
74	1.85E-17	4.51E-4
73	5.22E-17	1.27E-3
72	1.05E-16	2.56E-3
71	1.33E-16	3.24E-3
70	1.75E-16	4.26E-3
69	2.41E-16	5.88E-3
68	3.41E-16	8.32E-3
67	4.79E-16	1.17E-2
66	6.75E-16	1.65E-2
65	9.25E-16	2.26E-2
64	1.25E-15	3.05E-2
63	1.66E-15	4.05E-2
62	2.18E-15	5.32E-2
61	2.82E-15	6.88E-2
59.5	4.00E-15	9.76E-2

(a) Energy per molecule obtained graphically from Fig. 22.

Table XVII: Energy of deformation for DPPC/Cholesterol 1:1 (25°C).

A (Å^2)	Energy (ergs) (b)	Energy (kT) (b)
94	2.85E-17	6.95E-4
92	4.83E-17	1.18E-3
90	8.13E-17	1.98E-3
88	1.34E-16	3.27E-3
86	2.15E-16	5.24E-3
84	3.36E-16	8.20E-3
82	5.27E-16	1.29E-2
80	8.04E-16	1.96E-2

(b) Energy per molecule obtained graphically from Fig. 23

Appendix II: Sample calculation to determine the change in dextran concentration when DPPC melts.

Weight ratio of lipid to total dextran solution plus lipid.	17.5 mg. / 240.0 mg.
Measured dextran concentration after lipid has equilibrated at 25°C.	22.5 %
Observed d spacing for DPPC at 25°C.	63.0 Å
Weight percent lipid in lamellar phase at 25°C (from phase diagram).	70 %
Amount of water in sample at 25°C.	7.5 mg.
Observed d spacing for DPPC at 50°C.	61.2 Å
Weight percent lipid in lamellar phase at 50°C (from phase diagram).	62 %
Amount of water in sample at 50°C.	10.7 mg.
Amount of water taken from dextran solution upon melting DPPC.	3.2 mg.
Actual dextran concentration when DPPC is melted.	23.9 %

Appendix III: Force versus percent dextran; from (LENEVEU et al 1977).

% Dextran	Log F (dynes/cm^2)	% Dextran	Log F (dynes/cm^2)
0	-	21.0	6.047
0.5	3.764	21.5	6.075
1.0	3.852	22.0	6.102
1.5	3.94	22.5	6.129
2.0	4.028	23.0	6.156
2.5	4.085	23.5	6.183
3.0	4.204	24.0	6.211
3.5	4.323	24.5	6.238
4.0	4.442	25.0	6.265
4.5	4.562	25.5	6.285
5.0	4.681	26.0	6.304
5.5	4.767	26.5	6.324
6.0	4.853	27.0	6.344
6.5	4.910	27.5	6.364
7.0	4.968	28.0	6.383
7.5	5.025	28.5	6.403
8.0	5.082	28.6	6.407
8.5	5.124	29.0	6.434
9.0	5.165	29.5	6.468
9.5	5.207	30.0	6.502
10.0	5.249	30.5	6.563
10.5	5.290	31.0	6.560
11.0	5.332	31.5	6.584
11.5	5.373	32.0	6.607
12.0	5.415	32.2	6.617
12.5	5.450	32.5	6.630
13.0	5.485	33.0	6.652
13.5	5.520	33.5	6.673
14.0	5.555	34.0	6.695
14.5	5.591	34.5	6.716
15.0	5.626	35.0	6.738
15.5	5.704	35.5	6.759
16.0	5.746	35.7	6.768
16.5	5.788	36.0	6.837
17.0	5.830	36.5	6.861
17.5	5.872	37.0	6.885
18.0	5.896	37.5	6.909
18.5	5.920	38.0	6.932
19.0	5.944	38.5	6.956
19.5	5.968	39.0	6.980
19.8	5.982	39.5	7.004
20.0	5.983	40.0	7.027
20.5	6.020	40.5	7.061

Appendix IV: Calculation of London-Hamaker constant "H" for DPPC 25°C.

$F_H = 4.07 \times 10^{-5} \exp^{(-d_w/1.98)}$

Equilibrium $d_w = 19.1$ Å

$F_H = 2.63 \times 10^{-9}$ dynes/molecule at 19.1 Å

Since $F_H = F_A$ at 19.1 Å

$F_A = 2.63 \times 10^{-9}$ dynes/molecule at 19.1 Å

Since $F_A = -H/6\pi d_w^3$

$H = -F_A\ 6\pi d_w^3$

$= 2.63 \times 10^{-9}\ 6\ (19.1)^3$

$= 3.45 \times 10^{-4}$ dynes Å/molecule

Since $A = 54.6$ Å^2 at equilibrium
then $H = 6.32 \times 10^{-14}$ ergs

Appendix V: Percentage of F_R that is F_A at 10 Å closer than equilibrium d_w.

DPPC 25°C

F_R at d_w = 9 Å	4.32×10^{-7} dynes/molecule
F_A at dw = 9 Å	2.56×10^{-8} dynes/molecule
% F_R that is F_A	5.8 %

DPPC 50°C

F_R at d_w = 22 Å	3.12×10^{-8} dynes/molecule
F_A at d_w = 22 Å	1.52×10^{-9} dynes/molecule
% F_R that is F_A	4.96 %

Egg PE

F_R at d_w = 10 Å	2.76×10^{-6} dynes/molecule
F_A at d_w = 10 Å	1.75×10^{-7} dynes/molecule
% F_R that is F_A	6.3 %

DPPC/CHOL

F_R at d_w = 18 Å	4.95×10^{-8} dynes/molecule
F_A at d_w = 18 Å	4.06×10^{-9} dynes/molecule
% F_R that is F_A	8.2 %

Appendix VI: Calculation of degree of significance between length constants.

Formula (BLISS 1967)

Term	D F	S S
Combined slope	1	$\Sigma(XY)^2 / \Sigma(X^2) = B_c^2$
Non-parallelism	h-1	$\Sigma B^2 - B_c^2$
Error	n	$\Sigma((Y^2) - B^2)$

$(X^2) = \Sigma X^2 - (\Sigma X)^2 / N$
$(XY) = \Sigma (XY) - \Sigma X \Sigma Y / N$

DPPC/CHOL:DPPC 50°C

Form	D F	S S	M S	F	P
Combined slope	1	11.733	-	680.2	-
Non-parallelism	1	0.1648	-	9.55	< 1 %
Error	30	0.5175	1.75E-2		

DPPC/CHOL:DPPC 25°C

Form	D F	S S	M S	F	P
Combined slope	1	20.028	-	514.4	-
Non-parallelism	1	0.9616	-	24.69	< 0.5 %
Error	24	0.9344	3.89E-2		

DPPC/CHOL:egg PE

Form	DF	S S	M S	F	P
Combined slope	1	11.528	-	511.2	-
Non-parallelism	1	0.5108	-	22.649	< 0.5 %
Error	19	0.4285	2.25E-2		

DPPC 50°C:egg PE

Form	D F	S S	M S	F	P
Combined slope	1	17.422	-	949.6	-
Non-parallelism	1	0.1457	-	7.941	< 1 %
Error	38	0.6972	1.83E-2		

DPPC 50°C:DPPC 25 C

Form	D F	S S	M S	F	P
Combined slope	1	26.090	-	932.48	-
Non-parallelism	1	0.4285	-	15.315	< 0.5 %
Error	43	1.2031	2.79E-2		

Egg PE:DPPC 25°C

Form	D F	S S	M S	F	P
Combined slope	1	26.621	-	764.63	-
Non-parallelism	1	0.0382	-	1.097	n.s.
Error	32	1.1141	3.48E-2		

Egg lecithin:DPPC/CHOL

Combined slope	1	27.623	-	1156.4	-
Non-parallelism	1	0.1866	-	7.8116	< 1 %
Error	32	0.7644	2.39E-2		

Appendix VI: Continued

Egg lecithin:DPPC 50°C

Term	D F	S S	M S	F	P
Combined slope	1	33.337	-	1500.5	-
Non-parallelism	1	1.5E-3	-	0.0675	n.s.
Error	51	1.1331	2.22E-2		

Egg lecithin:DPPC 25°C

Form	D F	S S	M S	F	P
Combined slope	1	41.686	-	1210.2	-
Non-parallelism	1	0.7440	-	21.60	< 0.5 %
Error	45	1.55	3.44E-2		

Egg lecithin:egg PE

Form	D F	S S	M S	F	P
Combined slope	1	33.246	-	1273.7	-
Nonparallelism	1	0.2332	-	8.934	< 0.5 %
Error	40	1.0441	2.610E-2		

Appendix VII: Calculation of equilibrium d_w if egg PE had the London-Hamaker constant of egg lecithin

F_H (for egg PE) at 26 Å	$= 1.56 \times 10^{-9}$	dynes/molecule
F_A (using the highest value of egg lecithin H) at 26 Å	$= 1.55 \times 10^{-9}$	" "
F_H (for PE) at 26.8 Å	$= 1.07 \times 10^{-9}$	" "
F_A (using the lowest value of egg lecithin H) at 26.8 Å	$= 1.08 \times 10^{-9}$	" "
F_H (for egg lecithin) at 19 Å	$= 2.94 \times 10^{-8}$	" "
F_A (using the highest value of egg PE H) at 19 Å	$= 3.0 \times 10^{-8}$	" "
F_H (for egg lecithin) at 20.3 Å	$= 1.79 \times 10^{-8}$	" "
F_A (using the lowest value of egg PE H) at 20.3 Å	$= 1.79 \times 10^{-8}$	" "

Appendix VIII: Analytical functions for separation of deformation and repulsion using METHOD I.

DPPC 25 C

$$d_w = 0.1236 + 2.0688E\text{-}2 \times V - 5.039E\text{-}6 \times V^2$$
$$A = 45.082 + 2.124E\text{-}2 \times V - 5.5566E\text{-}6 \times V^2$$
$$\ln A = 3.869 - 5.356E\text{-}2 \times \ln d_w + 4.949E\text{-}2 \times \ln d_w^2$$
$$d\, d_w/d\, V = 2.068E\text{-}2 - 5.039E\text{-}6 \times V$$
$$d\, A/d\, V = 2.124E\text{-}2 - 5.566E\text{-}6 \times V$$
$$d \ln A/d \ln d_w = -5.356E\text{-}2 + 4.949E\text{-}2 \times \ln d_w$$

DPPC 50 C

$$d_w = 2.8299 + 9.936E\text{-}3 \times V + 1.4019E\text{-}6 \times V^2$$
$$A = 46.576 + 4.035E\text{-}2 \times V - 1.6297E\text{-}5 \times V^2$$
$$\ln A = 2.6062 + 1.12586 \times \ln d_w - 0.18996 \ln d_w^2$$
$$d\, d_w/d\, V = 9.936E\text{-}3 + 1.4019E\text{-}6 \times V$$
$$d\, A/d\, V = 4.035E\text{-}2 - 1.629E\text{-}5 \times V$$
$$d \ln A/d \ln d_w = 1.1258 - 0.18996 \ln d_w$$

Egg PE

$$d_w = 0.4070 + 1.553E\text{-}2 \times V - 3.7198E\text{-}6 \times V^2$$
$$A = 51.5915 + 3.879E\text{-}2 \times V - 1.0595E\text{-}5 \times V^2$$
$$\ln A = 4.0478 - 7.9621E\text{-}2 \times \ln d_w + 8.4483E\text{-}2 \times \ln d_w^2$$
$$d\, d_w/d\, V = 1.553E\text{-}2 - 1.059E\text{-}5 \times V$$
$$d\, A/d\, V = 3.8791E\text{-}2 - 1.059E\text{-}5 \times V$$
$$d \ln A/d \ln d_w = -7.962E\text{-}2 + 8.4483\ E\text{-}2 \times \ln d_w$$

DPPC/Cholesterol

$$d_w = 0.8009 + 1.1580E\text{-}2 \times V - 1.3779E\text{-}6 \times V^2$$
$$A = 67.3913 + 2.7848E\text{-}2 \times V - 4.36812E\text{-}6 \times V^2$$
$$\ln A = 4.3907 - 0.16961 \times \ln d_w + 9.0987E\text{-}2 \times \ln d_w^2$$
$$d\, A/d\, V = 2.7848E\text{-}2 - 4.3681E\text{-}6 \times V$$
$$d\, d_w/d\, V = 1.1580E\text{-}2 - 1.3779E\text{-}6 \times V$$
$$d \ln A/d \ln d_w = 0.1696 + 9.0987E\text{-}2 \times \ln d_w$$

BIBLIOGRAPHY

BAR, R. S., DEAMER, B. G., CORNWELL, D. W., (1966). Science 153: 1010.

BARCLAY, L. M., OTTEWILL, R. H., (1970). Special Discussions of the Farady Society 1: 138.

BARCLAY, L. M., OTTEWILL, R. H., HARRINGTON, A., (1972). Kolloid-Z-u-Z Polymere 250: 655.

BERRILL, N., (1971). "Developmental Biology", McGraw-Hill, New York.

BLISS, C. I., (1967). "Statistics in Biology", McGraw-Hill, New York.

BRANTON, D., (1971). Phil. Tran. Royal Soc. B261: 133.

BROWN, M. F., SEELIG, J. C., (1978). Biochemistry 17: 181.

BRETSCHER, M. S., (1972). J. Mol. Biol. 71: 523.

BRETSCHER, M. S., RAFF, M. C., (1975). Nature 258: 43.

CHADHA, J. S., (1970). Chem. and Phys. Lipids 4: 104.

CHAPMAN, D., WILLIAMS, R. M., LADBROOKE, B. D., (1967). Chem. and Phys. Lipids 1: 445.

CHAPMAN, D., (1973). in "Biological Membranes" (D. Chapman, D. Wallach eds.) vol. 2, 91, Academic Press, London.

COWLEY, A., FULLER, N., RAND, R. P., PARSEGIAN, V. A., (1978). Biochemistry, in press.

DAVSON, H., DANIELLI, J. F., (1935). J. Cell and Comp. Phys'y. 5: 495.

EVANS, E. A., WAUGH, R., (1977). J. of Colloid and Interface Science 60: 286.

FULLER, N., RAND, R. P., PARSEGIAN, V. A., (1978). P. N. A. S., in press.

GINGELL, D., (1971). J. Theor. Biol. 30: 121.

GORTER, E., GRENDEL, F., (1925). J. Exp. Med. 41: 439.

GULIK-KRZYWICKI, T., SCHECHTER, E., LUZZATI, V., (1969a). Nature 223: 1116.

GULIK-KRZYWICKI, T., TARDIEU, A., LUZZATI, V., (1969b). Mol. Crystals and Liquid Crystals 8: 286.

JANIAK , M. J., SMALL, D. M., SHIPLEY, G. G., (1976). Biochemistry 15: 4575.

KORNBERG, R. D., McCONNELL, H. M., (1971). Biochemistry 10: 1111.

LENEVEU, D., RAND, R. P., PARSEGIAN, V. A., (1976). Nature 259: 601.

LENEVEU, D., RAND, R. P., PARSEGIAN, V. A., GINGELL, D., (1977). Biophysical J. 18: 209.

LIFSHITZ, E. M., (1956). Sov. Phys. J. E. T. P. 2: 73.

LUZZATI, V., (1968). in "Biological Membranes" (D. Chapman ed.) vol. 1, 71, Academic Press, London.

McCONNELL, H. M., (1974). Adv. Exp. Med. Biol. 51: 103.

MOSCONA, A., (1961). Sci. Am. 205: 143.

MOSCONA, A., (1968). Devel. Biol. 18: 250.

OVERTON, E., (1895). Vjschr. Natur. Ges. Zurich 40: 159.

PARSEGIAN, V. A., (1967). Science 156: 939.

PARSEGIAN, V. A., NINHAM, B. W., (1971). J. of Colloid and Interface Science 37: 332.

PARSEGIAN, V. A., GINGELL, D., (1972). J. Adhesion 4: 283.

PARSEGIAN, V. A., (1975). in "Physical Chemistry: Enriching Topics from Colloid and Surface Science" (H van Olphen, K. J. Mysesl eds.), 27, Theorex, La Jolla, California.

PARSEGIAN, V. A., (1978). Personal Communication.

RAND, R. P., LUZZATI, V., (1968). Biophysical J. 18: 125.

RAND, R. P., TINKER, D. O., FAST, P. G., (1971). Chem. and Phys. Lipids 6: 333.

RAND, R. P., CHAPMAN, D., LARSSON, K., (1975). Biophysical J. 15: 1117.

REQUENA, J., HAYDON, D. A., HLADKY, S. B., (1975). Biophys. J. 15: 77.

RIGAUD, J. L., GARY-BOBO, C. M., SANSON, A., PTAK, M., (1977). Chem. and Phys. Lipids 18: 23.

ROBERTSON, J. D., (1957). J. Physiol. 140: 58.

ROBERTSON, J. D., (1960). Prog. Biophys. and Chem. 10: 343.

ROBERTSON, J. D., (1964). in "Cellular Membranes in Development" (M. Loch ed.), Academic Press, New York.

ROBLES, E., DEN BERG, D. van, (1969). B. B. A. 187: 520.

ROUSER, G., NELSON, G. J., FLEISCHER, S., SIMON, G., (1968). in "Biological Membranes" (D. Chapman ed.) vol. 1, 5, Academic Press, London.

SANSON, A., PTAK, M., RIGAUD, J. L., GARY-BOBO, C. M., (1976). Chem. and Phys, Lipids 17: 445.

SELINGER, Z., LAPIDOT, Y., (1966). J. Lipid Res. 7: 174.

SINGER, J. D., NICHOLSON, G. L., (1972). Science 175: 720.

SJOSTRAND, F. S., (1963). Nature 199: 1262.

SMALL, D. M., (1966). J. Lipid Res. 8: 551.

SMITH, R., TANFORD, C. J., (1972). J. of Mol. Biol. 67: 75.

TARDIEU, A., LUZZATI, A., REMAN, F. C., (1973). J. Mol. Biol. 75: 711.

TAYLOR, J. A., MINGINS, J., PETHICA, B. A., TAN, B. Y., JACKSON, C. M., (1973). B. B. A. 323: 157.

TRAUBLE, J. A., SACKMAN, A., (1971). J. Am. Chem. Soc. 94: 4499.

UNTRACT, J., SHIPLEY, G. G., (1977). J. of Biol. Chem. 252: 4449.

VERWEY, E. J., OVERBEEK, J. T., (1948). "Theory of the Stability of Lyophobic Colloids", Elsevier, Amsterdam.

WEISS, L., GREEP, R. O., (1977). "Histology" 4th ed. McGraw-Hill, New York.

WHITE, S. H., (1976). Biophys. J. 14: 155.

YUE, B., JACKSON, C., TAYLOR, J., MINGINS, J., PETHICA, B., (1976). J. of the Chem. Soc. Faraday Transactions I 72: 2685.